

SYNTHESES OF POLYESTERS AND POLY(ESTER-ANHYDRIDES) FOR  
INDUSTRIAL APPLICATIONS

by

Ayşe Zeyneb Erten

B.S., Chemistry, Boğaziçi University, 2017

Submitted to the Institute for Graduate Studies in  
Science and Engineering in partial fulfillment of  
the requirements for the degree of  
Master of Science

Graduate Program in Chemistry

Boğaziçi University

2020



*Dedicated to my family*

## ACKNOWLEDGEMENTS

Firstly, I would like to thank my supervisor Assoc. Prof. A. Ersin Acar for accepting me his research group. It is a pleasure for me to express my sincerest gratitude to him for his endless support, guidance, encouragement and wise advices throughout my master studies.

I would like to thank to my thesis committee members Prof. Duygu Avcı Semiz and Prof. Metin H. Acar for giving their valuable time and reviewing my thesis.

I would also thank to all precious members of Acar Lab, namely Acarhane. They know how to live the moment despite of all the challenges they confronted. I would like to thank Banu, Didem, Ferid, Gulizar, Halenur, Kubra, Melike, and Seda for the time we spent together. They have been always kind and supportive. I would like to thank Sedef, Aysenur, and Isil for sharing their knowledge and experiences during my master years. I am pleased to express my special and deepest thanks to Sule, Refia, Goknil, and Fatma for their patience, guidance, and friendship. We spent days and nights together. All I remember is the memories that made me smile.

In addition, I would like to thank my friends Hatice Betul, Salli, and Refia (one more time) for their endless support and friendship since the first year of the university. I would like to thank Yasemin, Tugba, and Ayse for their help, friendship and always being there for me for more than 10 years. They made all the difficulties easier. I am grateful to have them in my life.

Finally, my biggest appreciations go to my beloved family. This thesis would not have been accomplished without them. Especially, I must express my gratitude to my mother Neziha for being a life mentor and a friend to me. Also, I would like to thank my father Yasin, and my brothers Seyyid and Azad for all supports and enjoyable times we had. Also, I feel so lucky to have my aunt Kebriye and my cousins Rojbin and Rukiye for giving me so much encouragement. I appreciate for their unrequited love, patience, and support.

## ABSTRACT

### SYNTHESES OF POLYESTERS AND POLY(ESTER-ANHYDRIDES) FOR INDUSTRIAL APPLICATIONS

Polyesters are one of the most important and widely used polymers in industry. Especially for powder coating application, the final properties of coating composition mainly depend on the polyester employed. These linear or branched polyesters are usually carboxylic acid terminated and thermally react with an epoxy hardener. The number of reactive end groups, the molecular weight, the viscosity, and the glass transition temperature ( $T_g$ ) of polyesters affect the curing temperature and the levelling performance of the powder coating.

For example, as the molecular weight of the polyester increases,  $T_g$  increases. This results in higher viscosity and thus poor levelling and surface quality. Therefore, in this study the aim was to synthesize poly(ester-anhydrides) that contains labile anhydride linkages. During the curing, those anhydride linkages will be broken and reacting with epoxy curing agents. In literature, poly(ester-anhydrides) are generally synthesized by acetic anhydride which limits its use in industry. In this study, aliphatic and aromatic cyclic anhydrides were examined for the synthesis of poly(ester-anhydrides) for industrial applications. They were melt mixed with carboxylic acid functional commercial polyesters that have different functionalities in order to investigate the effect of the total functionality on the poly(ester-anhydride) synthesis. Furthermore, a new polyester was synthesized and reacted with an aliphatic cyclic anhydride to gain know-how in polyesters and poly(ester-anhydride) syntheses.

According to studies, the synthesis of poly(ester-anhydrides) with succinic anhydride (SA) seems more promising than pyromellitic dianhydride (PMDA) which has limited solubility. It is most likely that, high functionality of PMDA increased both the formation and scission of the targeted anhydride linkages.

## ÖZET

### SANAYİDE UYGULANMASI İÇİN POLİESTER VE POLİESTER ANHİDRİTLERİN SENTEZİ

Poliesterler, endüstride çok kullanılan, en önemli polimerlerden biridir. Özellikle toz boya uygulamalarında, kaplama karışımının nihai özellikleri ağırlıklı olarak poliesterlere bağlıdır. Bu poliesterler, karboksilik asit içeren lineer veya dallanmış yapıda olabilirler. Kürleme esnasında asit grupları epoksi sertleştiricilerle reaksiyona girerek çapraz bağlanmayı gerçekleştirirler. Poliesterlerin reaktif uç grup sayısı, molekül ağırlığı ve camsı geçiş sıcaklıkları toz boyanın kürleme sıcaklığını ve yüzeydeki akışını etkiler.

Örneğin, poliesterin molekül ağırlığı arttıkça, camsı geçiş sıcaklığı da artar. Ancak, kaplama karışımının yüzeyde akma direncinin artmasına sebep olur ve böylece kaplamanın yüzey kalitesi bozulur. Bu sebeple poliester zincirleri arasında kırılabilir anhidrit bağları olan poliester anhidrit sentezi amaçlandı. Kürleme sırasında bu anhidrit bağları kırılacak ve artan reaktif uç grupları sebebiyle çapraz bağlanma yoğunluğunu da arttıracaktır. Literatürde poliester anhidritler genellikle endüstriyel olarak çalışılmayan asetik anhidritler ile sentezlenir. Bu çalışmada halkalı alifatik ve aromatik anhidritler, endüstride kullanılmak amacıyla, poliester anhidrit sentezi için incelendi. Farklı fonksiyonallığa sahip ticari reçineler ile eriyik hal şartlarında karıştırıldı ve toplam fonksiyonallığın poliester anhidrit sentezi üzerindeki etkisi araştırıldı. Ayrıca, poliesterler ve poliester anhidritlerin sentezi hakkında bilgi birikimi edinebilmek için yeni bir poliester sentezlendi ve alifatik halkalı bir anhidrit ile reaksiyonu kuruldu.

Yapılan çalışmalara göre süksinik anhidrit ile poliester anhidrit sentezi sınırlı çözünürlüğe sahip piromellitik dianhidrite göre daha ümit vericidir. Reaksiyona giren PMDA'nın yüksek fonksiyonallığının hem anhidrit bağlarının oluşumunu hem de kırılmasını arttırdığı düşünülmektedir.

## TABLE OF CONTENTS

ACKNOWLEDGEMENTS.....	IV
ABSTRACT.....	V
ÖZET .....	VI
TABLE OF CONTENTS.....	VII
LIST OF FIGURES .....	X
LIST OF TABLES.....	XIV
LIST OF ACRONYMS/ABBREVIATIONS.....	XVI
1. INTRODUCTION.....	1
1.1. Synthesis of Polyesters .....	2
1.1.1. General Properties of Polyesters Used in Industrial Applications.....	2
1.1.1.1. Polyesters Used in Powder Coatings.....	5
1.1.2. Melt Polymerization for Polyester Synthesis .....	6
1.2. Synthesis of Poly(ester-anhydrides) .....	8
1.3. Main Design Parameters of Powder Coatings .....	10
1.3.1. The Glass Transition Temperature ( $T_g$ ) of Polymers.....	11
1.3.1.1. Determination of Thermal Transitions.. .....	12
1.3.2. Molecular Weight of Polymers.....	12
1.3.2.1. Determination of Molecular Weight.. .....	13
1.3.3. The Relationship between $M_n$ and $T_g$ .....	14
1.3.4. Functionality of Polymers.....	15
1.3.5. End group Determination of Polymers .....	16
1.3.6. Curing of Powder Coatings .....	16
2. AIM OF THE STUDY .....	18
3. EXPERIMENTAL .....	19
3.1. Materials .....	19

3.2.	Synthesis of Poly(ester-anhydrides) from Commercial Polyesters and Cyclic Anhydrides.....	20
3.2.1.	Synthesis of Poly(ester-anhydrides) from PE-1 and SA.....	20
3.2.2.	Synthesis of Poly(ester-anhydrides) from PE-2 and SA.....	21
3.2.3.	Synthesis of Poly(ester-anhydrides) with PE-1 and PMDA.....	22
3.2.4.	Synthesis of Poly(ester-anhydrides) with PE-2 and PMDA.....	23
3.3.	Synthesis of Poly(ester-anhydrides) from the Synthesized PE-3 and SA.....	24
3.3.1.	Synthesis of PE-3 in Melt Polymerization.....	24
3.3.2.	Synthesis of Poly (ester -anhydrides) by Using PE-3 and SA.....	25
3.4.	Anhydride Determination in Poly(ester-anhydride) Chains .....	25
3.5.	Characterization .....	25
3.5.1.	<sup>1</sup> H-NMR Analysis.....	25
3.5.2.	FT-IR Analysis .....	25
3.5.3.	GPC Analysis.....	26
3.5.4.	Acid Value Determination.....	26
3.5.5.	Rheology Analysis.....	26
3.5.6.	DSC Analysis.....	26
4.	RESULTS AND DISCUSSION .....	28
4.1.	Structure Analysis of PE-1 and PE-2.....	29
4.2.	Synthesis of Poly(ester-anhydrides) from Commercial Polyesters and Cyclic ... Anhydrides.....	32
4.2.1.	Synthesis of Poly(ester-anhydrides) from PE-1 and SA.....	33
4.2.2.	Synthesis of Poly(ester-anhydrides) from PE-2 and SA.....	39
4.2.3.	Synthesis of Poly(ester-anhydrides) from PE-1 and PMDA.....	48
4.2.4.	Synthesis of Poly(ester-anhydrides) from PE-2 and PMDA.....	53
4.3.	Synthesis of Poly(ester-anhydrides) from the Synthesized PE-3 and SA.....	55
4.3.1.	Synthesis of PE-3 in Melt Polymerization.....	56

4.3.2. Synthesis of Poly(ester-anhydrides) based on PE-3 and SA .....	57
4.4. Rheological Behaviors of Polymers.....	60
5. CONCLUSION .....	64
REFERENCES .....	65
APENDIX A: SPECTROSCOPY DATA .....	68

## LIST OF FIGURES

Figure 1.1. Different polyesters synthesis methods by polycondensation reaction [3]. ....	2
Figure 1.2. Synthesis of two-step polycondensation reaction of poly(propylene succinate) [4]. .....	3
Figure 1.3. Synthesis of PET-co-PEA polyester [7]. .....	4
Figure 1.4. Structure of a) semi-crystalline polyesters compared to b) amorphous polyesters [10]. .....	6
Figure 1.5. Melt polymerization reaction set-up.....	6
Figure 1.6. Synthesis of PENIT by melt polymerization technique [11].....	7
Figure 1.7. Polyanhydride synthesis by a)melt and b)solution polymerization [12]. .....	8
Figure 1.8. Synthesis of poly(ester-anhydrides) of PLA and PCL [13].....	9
Figure 1.9. Synthesis of biodegradable poly(ester-anhydride) from diacids [14]. .....	10
Figure 1.10. Relation of volume and temperature of polymers during thermal transitions [16]. .....	11
Figure 3.1. The potential reaction mechanism of PE-1 and SA.....	20
Figure 3.2. The potential reaction mechanism of PE-2 and SA.....	21
Figure 3.3. The potential reaction mechanism of PE-1 and PMDA. ....	22
Figure 3.4. The potential reaction mechanism of PE-2 and PMDA. ....	23
Figure 3.5. The reaction mechanism of synthesis of PE-3. ....	24
Figure 4.1. Chemical structures and functionalities of the reactants used.....	28
Figure 4.2. FT-IR Spectrum of PE-1 and PE-2.....	29
Figure 4.3. <sup>1</sup> H-NMR analysis of PE-1 in CDCl <sub>3</sub> . ....	31

Figure 4.4.	DSC analysis of PE-1. ....	32
Figure 4.5.	FT-IR spectrum of PE1_SA_2 and SA. ....	33
Figure 4.6.	Possible scenarios on anhydride location a) and b) in between polyester chains, c) and d) in terminal groups of polyesters, and e) free polysuccinic anhydride formation. ....	34
Figure 4.7.	<sup>1</sup> H-NMR Analysis of PE1_SA_3 in CDCl <sub>3</sub> . ....	35
Figure 4.8.	Possible connection pathways of SA to PE-1. ....	35
Figure 4.9.	a) TMA, the proposed illustration of the location of TMA at b) beginning c) middle d) end groups of polyesters, and e) the ring closure mechanism of TMA at the end groups. ....	40
Figure 4.10.	FT-IR Analysis of PE-2 and PE2_SA_1. ....	41
Figure 4.11.	The illustration of a mixed anhydride formation a) connected to chain ends, b) in between polyesters, c) free polysuccinic anhydride, and d) succinic acid formation. ....	42
Figure 4.12.	The ortho acid catalyst cleavage of mixed anhydride linkages. ....	43
Figure 4.13.	<sup>1</sup> H-NMR analysis of PE2_6 in CDCl <sub>3</sub> . ....	44
Figure 4.14.	The possible connection pathways of SA to PE-2. ....	45
Figure 4.15.	<sup>1</sup> H-NMR analysis of PE2_1 in d <sub>8</sub> -THF. ....	45
Figure 4.16.	DSC analysis of PE2_SA_3. ....	47
Figure 4.17.	Possible connection pathways of PMDA to PE-1. ....	49
Figure 4.18.	<sup>1</sup> H-NMR analysis of PE1_PMDA_1 in CDCl <sub>3</sub> . ....	50
Figure 4.19.	FT-IR spectrum of PE2_PMDA_2. ....	53
Figure 4.20.	<sup>1</sup> H-NMR analysis of PE2_PMDA_2 in d <sub>8</sub> -THF. ....	54

Figure 4.21. <sup>1</sup> H-NMR analysis of PE3_4 in CDCl <sub>3</sub> .....	57
Figure 4.22. FT-IR spectrum of PE3_4_SA1. ....	58
Figure 4.23. <sup>1</sup> H-NMR analysis of PE3_4_SA1 in CDCl <sub>3</sub> .....	58
Figure 4.24. Temperature sweep test of PE3_3 (orange), PE3_4 (blue), and PE3_5 (claret red).....	61
Figure 4.25. Temperature sweep test of PE3_4 (blue) compared to PE3_SA1 (red) and PE3_4_SA2 (orange).....	61
Figure 4.26. Temperature sweep tests of PE-2 (black), PE2_SA_6 (green), and PE2_PMDA_2 (pink). ....	62
Figure A.1. <sup>1</sup> H-NMR Analysis of SA in CDCl <sub>3</sub> . ....	69
Figure A.2. <sup>1</sup> H-NMR Analysis of SA in d <sub>8</sub> -THF.....	69
Figure A.3. <sup>1</sup> H-NMR Analysis of PMDA in d <sub>8</sub> -THF. ....	70
Figure A.4. <sup>1</sup> H-NMR Analysis of PE-2 in CDCl <sub>3</sub> . ....	70
Figure A.5. <sup>1</sup> H-NMR Analysis of PE1_SA_5 in CDCl <sub>3</sub> .....	71
Figure A.6. <sup>1</sup> H-NMR Analysis of PE1_SA_5ppt in CDCl <sub>3</sub> . ....	71
Figure A.7. <sup>1</sup> H-NMR Analysis of PE1_SA_3_A in CDCl <sub>3</sub> .....	72
Figure A.8. <sup>1</sup> H-NMR Analysis of PE2_SA_3_A in d <sub>8</sub> -THF. ....	72
Figure A.9. <sup>1</sup> H-NMR Analysis of PE2_Pv in CDCl <sub>3</sub> . ....	73
Figure A.10. <sup>1</sup> H-NMR Analysis of PE3_5 in CDCl <sub>3</sub> .....	73
Figure A.11. FT-IR spectrum of physical mixing of PE-1 and SA. ....	74
Figure A.12. FT-IR spectrum of physical mixing of PE-2 and SA. ....	74
Figure A.13. FT-IR spectrum of PE2_Pv. ....	75

Figure A.14. FT-IR spectrum of PE2_Pv. ....	75
Figure A.15. FT-IR spectrum of PE2_PMDA1. ....	76
Figure A.16. FT-IR spectrum of PE3_4. ....	76
Figure A.17. FT-IR spectrum of PE3_4_SA_1. ....	77
Figure A.18. DSC analysis of PE-2. ....	77
Figure A.19. DSC analysis of PE2_SA_1. ....	78
Figure A.20. DSC analysis of PE1_PMDA_1. ....	78
Figure A.21. DSC analysis of PE1_PMDA_1_A. ....	79
Figure A.22. DSC analysis of PE2_PMDA_2. ....	79
Figure A.23. DSC analysis of PE3_SA_4. ....	80
Figure A.24. DSC analysis of PE3_4_SA_1. ....	80
Figure A.25. Temperature sweep test of PE-1. ....	81
Figure A.26. The temperature sweep test of PE1_SA_8, PE2_SA6, and PE2_PMDA_2. .	81
Figure A.27. The flow curves of PE3_4 (purple), PE3_4_SA1 (red), and PE-1 (black). ....	82
Figure A.28. The flow curves of PE-1 (black) and PE1_PMDA_8 (pink). ....	82
Figure A.29. Temperature sweep test of PE3_4_SA1 (red) and PE1_SA_8 (black). ....	83
Figure A.30. The flow curves of PE-2 (black) and PE2_PMDA_3 (blue). ....	83
Figure A.31. Temperature sweep tests of PE-1 (black) and PE1_PMDA_8 (pink). ....	84
Figure A.32. Temperature sweep tests of PE-2 (black) and PE2_PMDA_3 (blue). ....	84
Figure A.33. Temperature sweep tests of PE2_SA_1 (red) and PE2_SA_1 (blue). ....	85

**LIST OF TABLES**

Table 3.1.	Mole ratio and reaction conditions of PE-1 with SA. ....	20
Table 3.2.	Mole ratio and reaction conditions of PE-2 and SA.....	21
Table 3.3.	Mole ratio and reaction conditions of PE-1 with PMDA.....	22
Table 3.4.	Mole ratio and reaction conditions of PE-2 with PMDA.....	23
Table 3.5.	Mole ratio and reaction conditions of PE-3 synthesis.....	24
Table 3.6.	Mole ratio and reaction conditions of PE-3 synthesis.....	25
Table 3.7.	DSC run method 1.....	26
Table 3.8.	DSC run method 2.....	26
Table 3.9.	DSC run method 3.....	27
Table 3.10.	DSC run method 4.....	27
Table 4.1.	Structural units and chemical shifts of PE-1 units in $\text{CDCl}_3$ .....	30
Table 4.2.	General properties of commercial polyesters.....	31
Table 4.3.	The molecular weight obtained from PE1_SA reactions.....	37
Table 4.4.	Thermal behavior of PE1_SA reactions in second heating run.....	38
Table 4.5.	Acid values of synthesized samples.....	39
Table 4.6.	The molecular weight obtained from PE2_SA reactions.....	46
Table 4.7.	Thermal behavior of PE2_SA reactions in second heating run.....	47
Table 4.8.	Acid values of synthesized samples.....	48
Table 4.9.	The molecular weight obtained from PE1_PMDA reactions.....	51
Table 4.10.	Thermal behavior of PE1_PMDA reactions in second heating run.....	51

Table 4.11. Acid values of synthesized samples. ....	52
Table 4.12. The molecular weight of PE2_PMDA_3 before and after anhydride test.....	55
Table 4.13. Acid values and thermal properties of second heating cycle of PE2_PMDA reactions.....	55
Table 4.14. Molecular weights, thermal properties, and acid values of synthesized polyesters.....	56
Table 4.15. The molecular weight obtained from PE3_SA reactions. ....	59
Table 4.16. Thermal properties and acid values of PE3_4_SA reactions. ....	59

**LIST OF ACRONYMS/ABBREVIATIONS**

2MI	2-Methylimidazole
AA	Adipic acid
CHDA	cis\trans-1,4-cyclohexanedicarboxylic acid
CHDM	cis\trans-1,4-cyclohexanedimethanol
NPG	Neopentyl glycol
CDCl <sub>3</sub>	Deuterated Chloroform
C <sub>4</sub> D <sub>8</sub> O	Deuterated tetrahydrofuran
CEG	Carboxyl-end groups
DSC	Differential Scanning Calorimetry
EG	Ethylene glycol
FTIR	Fourier-transform infrared spectroscopy
GPC	Gel Permeation Chromatography
H	Hydrogen
HD	1,6-hexanediol
IPA	Isophthalic acid
$M_e$	Equivalent weight
MDF	Medium density fiberboard
$M_n$	Number average molecular weight
$M_w$	Weight average molecular weight

NMR	Nuclear Magnetic Resonance
PBT	Poly (butylene terephthalate)
PCCD	Poly (1,4-cyclohexylidencyclohexane- 1,4-dicarboxylate)
PCL	Poly ( $\epsilon$ - caprolactone)
PDI	Polydispersity index
PEA	Poly (ethylene adipate)
PEN	Poly (ethylene naphthalate)
PET	Poly (ethylene terephthalate)
PLA	Poly lactide
PTT	Poly (trimethylene terephthalate)
SA	Succinic anhydride
TAB	Tetrabutylammonium Bromide
$T_g$	Glass transition temperature
THF	Tetrahydrofuran
TMA	Trimellitic anhydride
TMP	Trimethylol propane
$T_m$	Crystalline melting temperature
TPA	Terephthalic acid
PMDA	Pyromellitic dianhydride
VOC	Volatile organic compounds
$G'$	Storage modulus

$G''$	Loss modulus
$f$	Functionality
$\eta$	Viscosity

## 1. INTRODUCTION

Polyesters are one of the major families of polymers thanks to wide variety of monomers and properties, which offer biodegradability, biocompatibility, high durability, film and fiber forming ability, and low-cost production. Therefore, there are many application areas including automotive industry, food packaging, bottles, fibers, coating systems and biomedical applications [1].

Polyesters are typically obtained by step-growth polymerization of diacids or derivatives and diols. Rate of esterification and physical property of the final resin mainly depend on the monomer structure and composition, polymer morphology, and stoichiometry, catalyst, and reaction temperature.

Polyesters can be divided as thermosetting and thermoplastic where the latter usually contains reactive hydroxyl and carboxyl end groups. For powder coating applications, in order to achieve better adhesion, impact resistance, and exterior durability; relatively low molecular weight and branched thermosetting polyesters are preferred. The carboxyl terminated thermosetting polyesters are crosslinked with epoxy resins during a curing process which is non-reversible (Section 1.3.6).

In powder coating industry,  $T_g$  of carboxyl terminated polyesters employed for the crosslinking generally are around 50-55 °C which often requires high molecular weighted polyesters. However, for low temperature cured coating systems, high molecular weight polyesters are not desired since they cannot melt and diffuse adequately on the applied surface. In addition, the increased molecular weight, results in decreased concentration of reactive end-groups and thus lower crosslinking density. In other words, one has to compromise between the  $T_g$  requirement and crosslink density.

In this study it is aimed to increase  $T_g$  of polyesters by using poly (ester-anhydrides) as a powder coating resin. Thanks to improved number of reactive end groups by introducing labile anhydride linkages, it is expected to increase crosslink density and viscosity of final resin.

## 1.1. Synthesis of Polyesters

There are several polycondensation reaction methods to synthesize polyesters by two or more functional monomers. They can be obtained typically by direct esterification of dicarboxylic acids and transesterification of methyl esters with diols or their derivatives (Figure 1.1). The polymerization reaction may proceed through ester-hydroxyl, ester-carboxyl, ester-ester, and anhydride-hydroxyl interchange reactions at temperatures above 160 °C.

Depending on the monomers and processing techniques, different vacuum and temperature profiles are needed for the elimination of small by-products such as water and methanol when the melt process is used. In addition, polyesters can be synthesized by ring-opening polymerization of cyclic esters (*e.g.* lactones and lactides) [2].

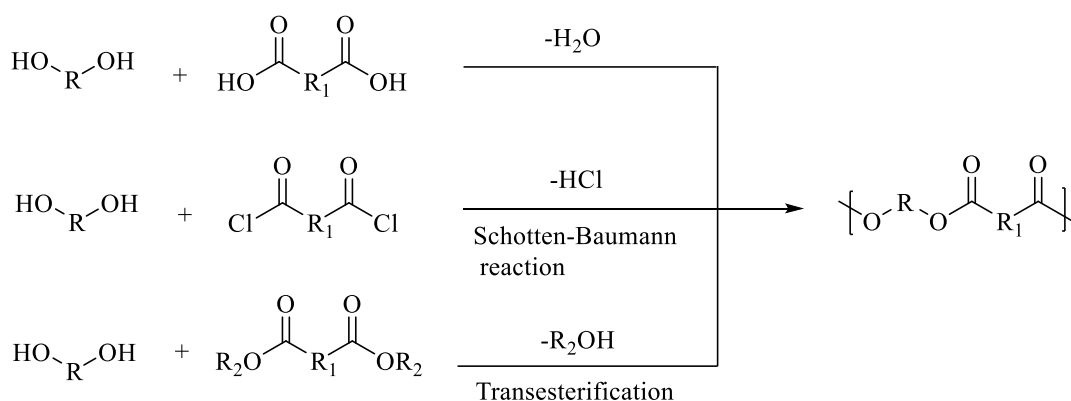


Figure 1.1. Different polyesters synthesis methods by polycondensation reaction [3].

### 1.1.1. General Properties of Polyesters Used in Industrial Applications

Polyesters are present in most of the polymer class that is commercially important in industry. Polyesters that are used in engineering thermoplastics are mainly composed of polyethylene terephthalate (PET) as fiber, film, and solid-state resin. Other thermoplastic or thermosetting polyester resins and elastomers that may be composed of fully aliphatic, aromatic, and aliphatic-aromatic structures provide various properties and application areas in industry.

In general, aliphatic polyesters are easily degradable under acid, alkaline or enzymatic catalysis. They may be semi-crystalline polymers or viscous fluids with a low melting point, which is not suitable commercially for coating applications. Depending on the application low molecular weighted aliphatic polyesters may be used as plasticizers for polymer mixtures. On the other hand, aliphatic polyesters that have low molecular weight *i.e.* polybutylene adipate and polycaprolactone, can be used as macromonomers for synthesis of polyurethane foam in packaging, furniture, and automotive industries. For example, in Figure 1.2, a bio-based aliphatic polyester polyol is synthesized with polycondensation polymerization of succinic acid and 1,3-propanediol as an alternative to petrochemical-based polyester polyols [4].

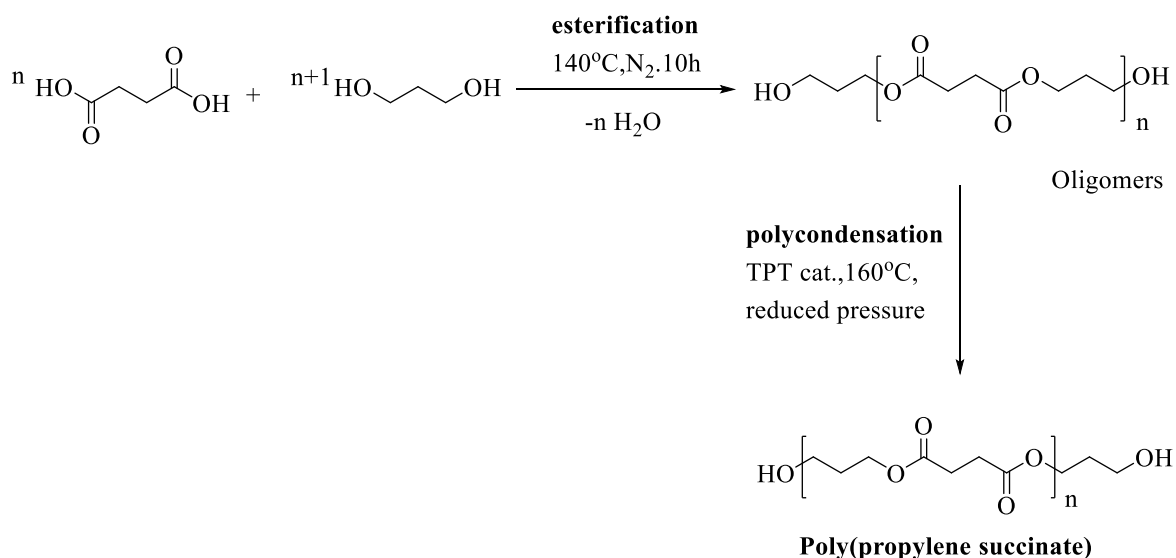


Figure 1.2. Synthesis of two-step polycondensation reaction of poly(propylene succinate) [4].

For biomedical applications, there are several commercially available aliphatic polyesters. The homo- and copolymers of lactide, glycolide, 3-hydroxybutyrate, and  $\epsilon$ -caprolactone are dominating mainly in drug delivery systems, or prosthetics [5]. These biobased polyesters have bioresorbable and biodegradable backbone, which generates non-toxic byproducts that are also biocompatible and hydrolysable by human and animal body with no need for an extra surgeon operation.



1.1.1.1. Polyesters Used in Powder Coatings. There are several well-known raw materials used to synthesize thermosetting semi-crystalline and amorphous polyesters in powder coatings. Isophthalic acid (IPA), terephthalic acid (TPA), adipic acid (AA), cis\trans-1,4-cyclohexanedicarboxylic acid (CHDA), difunctional or multifunctional alcohols such as neopentyl glycol (NPG), ethylene glycol (EG), trimethylol propane (TMP), cis\trans-1,4-cyclohexanedimethanol (CHDM), 1,6-hexanediol (HD), and glycerol are among them. In addition, aromatic anhydrides (e.g. PMDA and TMA) are also used to increase branching of polymer network. The end group of polyesters (functionality) is determined by monomer stoichiometry.

For powder coating applications, molecular weight, viscosity and  $T_g$  of polyester resins are crucial factors for the curing process, storage stability and outdoor weatherability of polyesters. The polyesters have relatively low molecular weight and contain branching monomer units to obtain amorphous resin which will crosslink during the curing processes. These thermosetting commercial resins are mainly composed of NPG and TPA monomers which promise good outdoor weatherability and high  $T_g$  for storage stability [2]. Aromatic diacids such as IPA and TPA are mainly used as building blocks in order to improve  $T_g$  of coating binders. However, aromatic diacids may cause yellowing in coating compositions [9]. Therefore, aliphatic diacids or diols are used instead since they are less susceptible to the photo-oxidation/degradation. The ratio between mole percentage of aliphatic and aromatic units determine the thermal properties of the polyester resin.

In the example below, Figure 1.4, the powder coating resin is prepared by introducing a semi-crystalline polymer into an amorphous polyester in order to tune the levelling performance of coating. Levelling performance is known as film forming behavior of polymers which determines surface appearance and the flow. Both polyesters are synthesized in similar compositions except the former polymer is synthesized with 1,6-hexanediol (HD) and the latter with neopentyl glycol (NPG) as diol monomer. It is aimed to decrease melt viscosity of polyester and improve its flow on surface before curing process by use of a semi-crystalline polymer that has rapid drop in viscosity at its melting point. Thus the mixture of both resins result in smoother and higher gloss coating surface with less orange peel look [10].

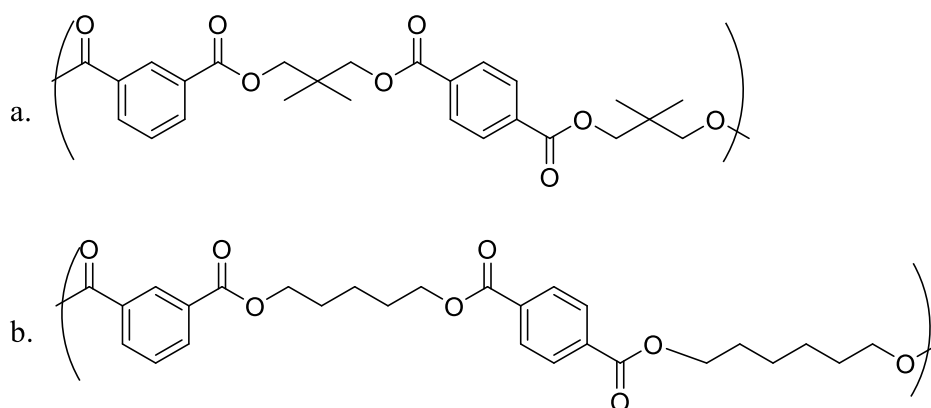


Figure 1.4. Structure of a) semi-crystalline polyesters compared to b) amorphous polyesters [10].

### 1.1.2. Melt Polymerization for Polyester Synthesis

Commercial polyesters are commonly synthesized by the melt polymerization technique. Solvent free reactants are heated above their melting point in a glass or stainless-steel reactor under nitrogen atmosphere. The reaction progress can be followed by measuring the torque by of the mechanical stirrer (Figure 1.5).



Figure 1.5. Melt polymerization reaction set-up.

Esterification is a reversible process. The melt viscosity increases as high degree of polymerization is achieved and the final stage of the polymerization is diffusion controlled. In order to prevent the ester hydrolysis and increase the molecular weight, according to Le Chatelier principle, by-products must be collected to shift the equilibrium towards products. An inert gas may be purged, or vacuum may be applied to favor the removal. Unlike solution polymerization, additional purification step is not necessary if a high degree of polymerization is achieved.

For example, in Figure 1.6, one-stage synthesis of PENIT copolyester with melt polymerization is shown. Molten mixture is stirred under  $N_2$ . Esterification step is completed by heating the mixture from 200 °C to 240 °C over several hours until the whole water is collected from the reactor. Vacuum is applied to achieve polycondensation of oligomers at the end of the reaction [11].

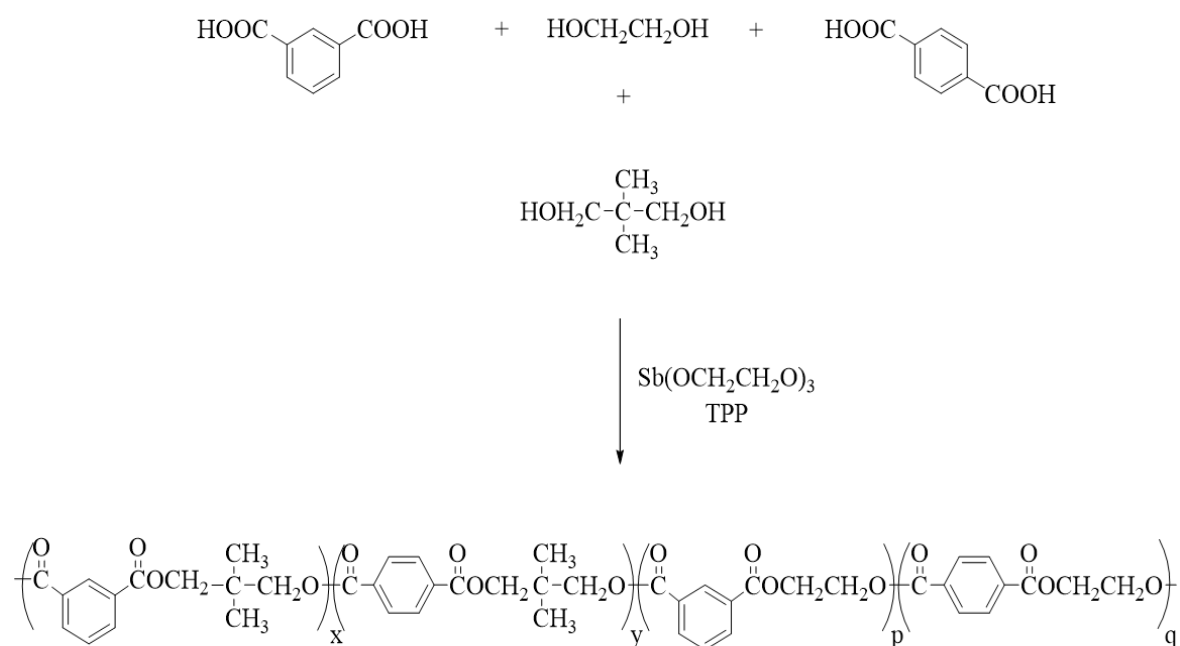


Figure 1.6. Synthesis of PENIT by melt polymerization technique [11].



behavior of polymers and hydrolysis rate of anhydride linkages can be monitored by the drop of the molecular weight [13].

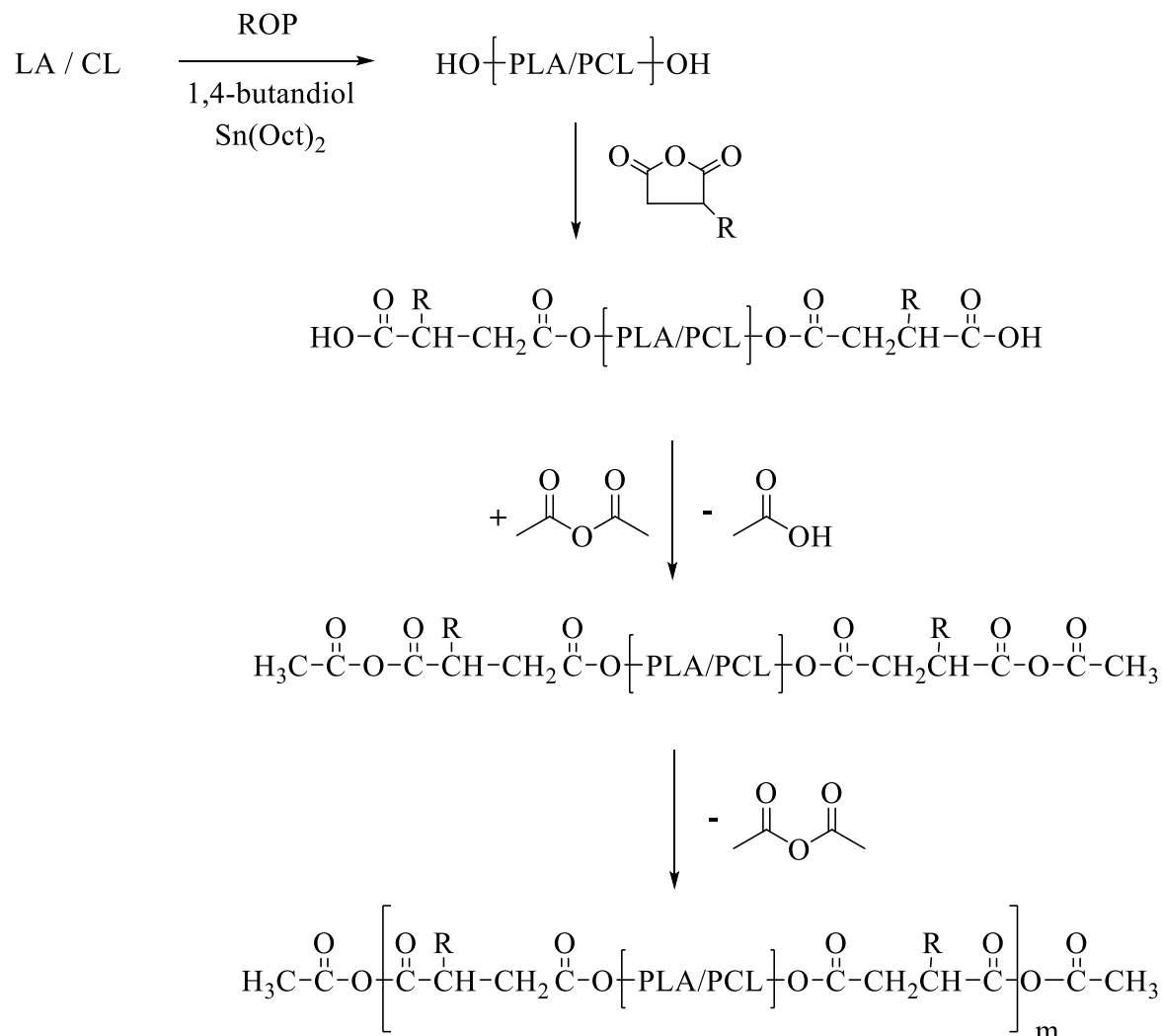


Figure 1.8. Synthesis of poly(ester-anhydrides) of PLA and PCL [13].

The synthesis of a poly(ester-anhydride), that is based on copolymerization of aliphatic and aromatic diacids, is shown in Figure 1.9. At first, p-Hydroxy benzoic acid's terminal hydroxyl group is converted to carboxylic acid by cyclic anhydrides. After refluxing with acetic anhydride resultant compound is melt polymerized under high vacuum [14].

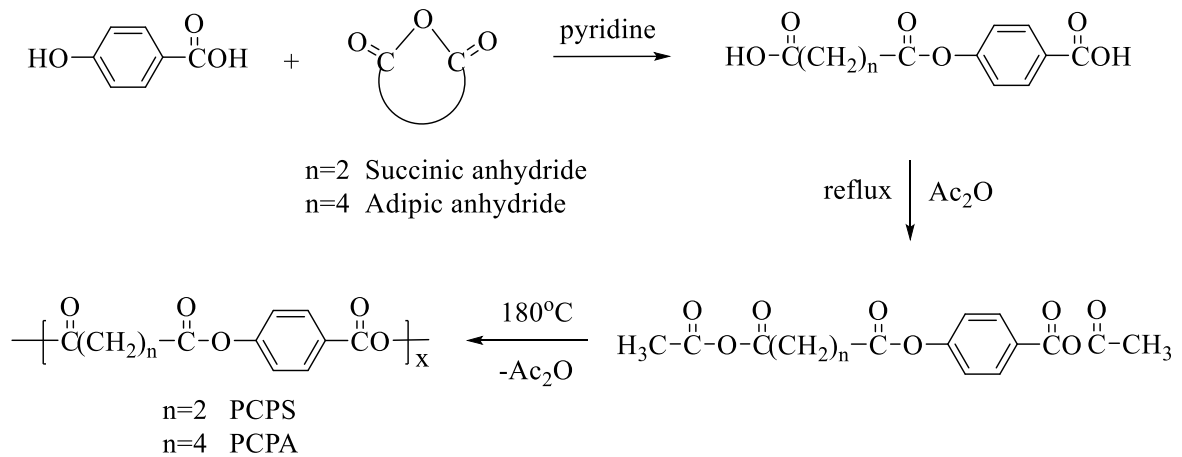


Figure 1.9. Synthesis of biodegradable poly(ester-anhydride) from diacids [14].

### 1.3. Main Design Parameters of Powder Coatings

Powder coating is a widely used method in industry for surface coating applications. It is an energy saving, cost-effective and environmentally friendly process. The main advantage of powder coating is that all components are solid. Therefore, there is no volatile organic compounds (VOC) release. Unlike conventional solvent-borne coatings, the drying process is not necessarily, and the film formation is obtained in molten phase. As a result, long-lasting, durable, decorative, and protective finishes are achieved.

A reactive polyester resin (binder), curing agent, fillers and pigments are main components of powder coating. Ingredients are melt mixed and homogenized in extruder below the curing temperature. The extrusion temperature, which is generally 100 °C should be lower than the curing temperature [15]. The coating composition is then ground and filtered after cooling. Coating is applied by an electrostatic gun. Electrostatically charged powders are sprayed on substrate to form uniform layer and then cured by heat [2]. Resin viscosity and curing rate determine the levelling performance of the coating [10].

Powder coating can be applied to various surfaces like metal, glass, and fiberboard. The curing temperature depends on the curing system of the resin and the preparation process of the coating. The curing temperature may differ between 130-200 °C [8]. However, these temperatures limit the powder coating application for materials that cannot tolerate. As an

example, in order to prevent deformation of heat sensitive surfaces *e.g.* wood, medium density fiberboard (MDF), and plastics, the curing temperature is desired to be lower than 120°C. Although powder coating is cost-effective for long-term coating applications, it needs large amount of investment.

The final coating performance is mainly depending on the polyester resin. Therefore, it is beneficial to address main design parameters of polyesters used in powder coatings.

### 1.3.1. The Glass Transition Temperature ( $T_g$ ) of Polymers

The degree of order and arrangement of polymer chains determine the polymer morphology. While amorphous polymers have randomly coiled structure, crystalline polymers have long range order.

The temperature interval where the transition from stiff, brittle to a rubbery phase occurs is called the glass transition temperature ( $T_g$ ).  $T_g$  has second-order transition characteristics and there is no discontinuity during the transition as seen in Figure 1.10. In contrast, crystalline polymers have an abrupt change in volume at the phase transition, which is called the melting temperature ( $T_m$ ). Semi-crystalline polymers have both amorphous and crystalline regions and exhibit both thermal transitions  $T_g$  and  $T_m$  [16].

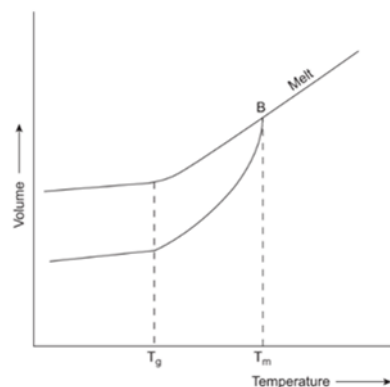


Figure 1.10. Relation of volume and temperature of polymers during thermal transitions [16].

There are several factors that affect  $T_g$  of polymers. When an amorphous polymer is heated, segmental motions between polymer chains increases significantly. As the mobility of polymer chains increases  $T_g$  value will decrease. Therefore, any plasticizers or pendant groups connected to the backbone, which increase rotational motion and free volume between chains, will cause a decrease in  $T_g$ . On the other hand, increase in molecular weight, chain stiffness, intermolecular forces, molecular symmetry, and crosslinkers will increase  $T_g$  [17].

$T_g$  determines physical and chemical stability and the rheological behavior during storage and film formation of the powder coating composition [18]. The base resin should have  $T_g$  higher than 50°C since the other components of coating formulation may act as plasticizer and lower  $T_g$ . During the curing process of powder coatings, the  $T_g$  of powder-coated composition increases as the degree of crosslinking increases. Final powder coating mixture should have  $T_g$  values around 50-60 °C to overcome agglomeration problems during storage [8].

1.3.1.1. Determination of Thermal Transitions. Thermal transitions in polymers is determined by the Differential Scanning Calorimeter (DSC) method. The instrument measures heat flow difference between a reference and a polymer sample as a function of time or temperature. Absorbed or evolved heat amount is calculated through heating and cooling cycles[19]. Under isothermal or non-isothermal conditions the kinetic parameters of the curing reactions powder coating is analyzed by DSC [20].

### **1.3.2. Molecular Weight of Polymers**

Polymers are made of mixture of uneven chain lengths. Molecular weight determines resins` physical and mechanical properties such as thermal behavior, chemical resistance, melt viscosity, tensile strength, and weatherability.

Each polymer chain has a different polymerization degree which yield different sizes of chains. In general, molecular weight distribution is typically identified by number-average molecular weight ( $M_n$ ) and weight-average molecular weight ( $M_w$ ).

Number-average molecular weight ( $M_n$ ) is defined as total weight of polymer chains divided by the number of chains;

$$\overline{M}_n = \frac{W}{\sum_{i=1}^{\infty} N_i} = \frac{\sum_{i=1}^{\infty} N_i M_i}{\sum_{i=1}^{\infty} N_i} \quad (1.1)$$

where  $N_i$  is the number of molecules which have  $M_i$  molecular weight and  $W$  is total weight[17]. Whereas weight-average molecular weight ( $M_w$ ) is determined by particle mass and is always larger than  $M_n$ ;

$$\overline{M}_w = \frac{\sum_{i=1}^{\infty} N_i M_i^2}{\sum_{i=1}^{\infty} N_i M_i} \quad (1.2)$$

Also, broadness of molecular weight distribution is calculated by the ratio of  $M_w$  to  $M_n$  named as polydispersity index (PDI).

$$PDI = \frac{\overline{M}_w}{\overline{M}_n} \quad (1.3)$$

The lower the PDI value, the better control over polyester synthesis reactions. Controlling molecular weight and molecular weight distribution also reduce VOC emissions during the curing process of coating [21,2].

1.3.2.1. Determination of Molecular Weight. Molecular weight of polymers can be measured by several methods. Apart from solution viscosity, light scattering, osmometry, and end group analysis, gel permeation chromatography (GPC) is one of the widely used methods [22].

There are different types of columns which can separate low, medium, or high molecular weighted polymers in GPC. Polymer samples are prepared according to a specific concentration before they pass into the columns. These columns are usually made of small crosslinked polystyrene beads with different pore diameters.

Samples diffuse from these pores at different rate based on their hydrodynamic volume. Molecular weight distribution of samples is measured by the polymer amount that reaches the detector as a function of time. Since smaller polymers can fit and be trapped in

beads, their diffusion is slowed down. Therefore, their retention time are longer. In contrast, large polymers do not penetrate beads so they have shorter retention time [19].

### 1.3.3. The Relationship between $M_n$ and $T_g$

Chain end segments of a polymer has higher mobility than internal segments that is restricted from both sides. Therefore, chain ends provide free volume for molecular motion. According to the Flory-Fox equation, number-average molecular weight ( $M_n$ ) and glass transition temperature ( $T_g$ ) are related to each other [17].

$$T_g = T_g^\infty - \frac{k}{M_n} \quad (1.4)$$

$T_g^\infty$  is the  $T_g$  at infinite molecular weight and  $k$  is the constant which depends on free volume in a polymer. If there is a decrease in  $M_n$  value, the number of chain ends will increase in the polymer mixture. This means, there will be more free volume which will result in a decrease in  $T_g$  [17]. As seen in Figure 1.11, higher molecular weight improves  $T_g$  values of amorphous or semi-crystalline polymers up to a limiting value.

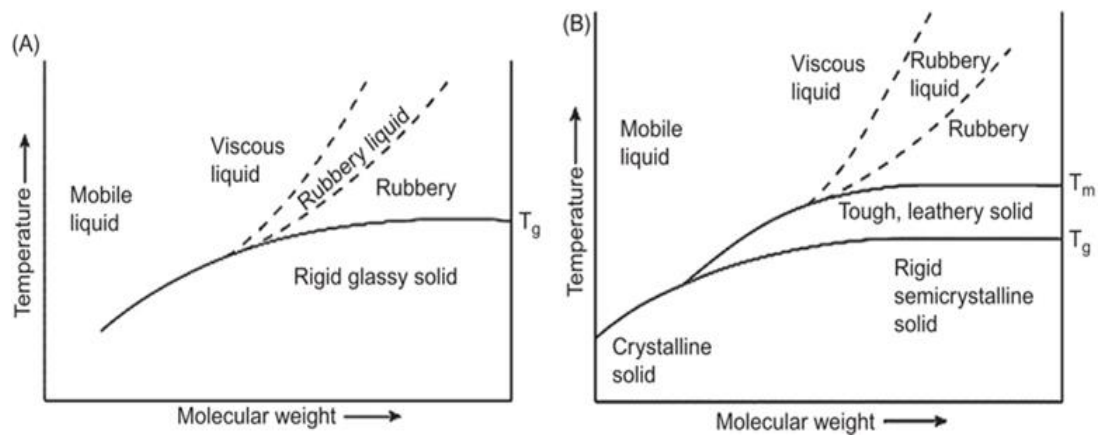


Figure 1.11. Effect of molecular weight on properties of A) amorphous and B) semi-crystalline polymer [23].

### 1.3.4. Functionality of Polymers

Functionality is defined as the total number of reactive functional groups at the polymer chain ends. Monomers and polymers are classified based on their number of functional units (*e.g.* difunctional for linear chains).

Tri-dimensional polymer structures can be obtained by addition of monomers that have functionality more than two, such as polyols and multi-acid anhydrides added during the polymerization. In addition, coupling of several multifunctional oligomers may also enable branching or crosslinking of polyesters [17].

Functionality affect viscosity and the curing properties of polyesters especially for thermosetting coating compositions. It is the limiting factor for crosslinking density. During the curing process high functionality will result in fast increase in viscosity and stem the film formation of the coating composition [18].

$M_n$  of polymer samples can be derived by functionality as shown below;

$$\overline{M}_n = \frac{f \cdot w \cdot e}{a} \quad (1.5)$$

where  $w$  is the weight of the polymer sample,  $f$  is the functionality of polymer,  $e$  is equivalent weight of titrant which is 56 g eq<sup>-1</sup> for 1 N KOH, and  $a$  is the amount of titrant used in g [24].

The relationship between molecular weight and functionality results in equivalent weight of the polymer,  $M_e$ . It is defined as the mass of polymer per mole of end groups calculated as follows [24].

$$M_e = \frac{\overline{M}_n}{f} \quad (1.6)$$



In the same way of acid-epoxy resins, acid anhydride-epoxy curing is also well-known curing system. The crosslinking density is higher and it is less sensitive to stoichiometric deviations during the curing process [18].

## 2. AIM OF THE STUDY

Previously, the synthesis of poly(ester-anhydrides) based on the polycondensation of cycloaliphatic polyesters, poly(1,4-cyclohexylidencyclohexane-1,4-dicarboxylate), (PCCD), with acetic anhydride was studied for powder coatings in our laboratory [27]. However, the release of acetic acid during the formation of anhydride linkages limits its application in industry. In this thesis, it is aimed to synthesize poly(ester-anhydrides) by the reaction of commercial polyesters with cyclic anhydrides in melt. One synthesized and two commercial polyesters were used as polyester precursor for the potential synthesis of poly(ester-anhydrides). The main goal is to obtain poly(ester-anhydrides) that may be used as a reactive component in acid/epoxy based powder coating formulations.

### 3. EXPERIMENTAL

In this thesis, two different cyclic anhydrides (succinic anhydride and pyromellitic dianhydride) were reacted with different polyesters. The effect of the functionality of monomers and polymers was examined on the poly(ester-anhydride) synthesis in melt.

Industrially available carboxyl terminated commercial resins were used as polyester precursors. In Section 4.1, the general properties of commercial polyesters are summarized which will be named as PE-1 and PE-2. Both commercial polyesters were supplied by Pulver Kimya Tic.A.S. In addition, PE-3 was synthesized and reacted with succinic anhydride in order to understand the reaction difference between the commercial polyester PE-1 and PE-3.

All reactions were conducted under nitrogen atmosphere in melt. It is well known that it is crucial to minimize oxygen content in the reaction medium, which will induce thermo-oxidative degradation. Succinic anhydride was sublimed on the top of the glass reactor even at low temperatures, which interfere in the stoichiometry of the reactants. Therefore, a heating tape was used to overcome sublimation problem.

ESM4450 48 x 48 1/16 DIN Universal Input PID Process Controller with Smart I/O Module System was used to heat the glass reactor in silicon oil. Reactions were handled and terminated by observation of the torque value of the reaction mixture. The stirring rate of Heidolph overhead stirrer was set to 50 rpm. Before the resin analysis, they were stored several days in vacuum.

#### 3.1. Materials

Pyromellitic dianhydride (PMDA) was obtained from TCI. Succinic anhydride (SA), 2-methylimidazole (2-MI), tetrabutylammonium bromide (TAB), terephthalic acid (TPA), isophthalic acid (IPA), adipic acid (AA), ethylene glycol (EG), dibutyltin(IV) oxide, diisobutyl amine were obtained from Aldrich.

### 3.2. Synthesis of Poly(ester-anhydrides) from Commercial Polyesters and Cyclic Anhydrides

#### 3.2.1. Synthesis of Poly(ester-anhydrides) from PE-1 and SA

Di-functional carboxyl terminated polyester (10.0 g, 0.0056 mole) was reacted with different mole ratio of succinic anhydride as shown in Table 3.1. The reactions were conducted without catalyst. Vacuum was applied in order to initiate polycondensation reaction. The potential reaction mechanism is illustrated in Figure 3.1.

Table 3.1. Mole ratio and reaction conditions of PE-1 with SA.

Sample Name	PE-1: SA (mole ratio)	Temp (°C)	Vacuum(mbar)	Total Time (hour)
PE1_SA_1	1.00: 1.00	120→140	-	2.0
PE1_SA_2	1.00: 1.00	120→140	500→10 (3 h)	5.5
PE1_SA_3	1.00: 0.50	120→140	500→5 (1.5 h)	4.0
PE1_SA_4	1.00: 0.50	180→210	500→5 (1.5 h)	3.0
PE1_SA_5	1.00: 0.50	180→210	500→75 (2 h)	6.0
PE1_SA_6	1.00: 1.00	160	-	1.5
PE1_SA_7	1.00: 1.00	180	-	1.5
PE1_SA_8	1.00: 1.00	220	-	1.0
PE1_SA_9	1.00: 1.00	230	-	1.5
PE1_SA_10	1.00: 1.00	235	-	1.5

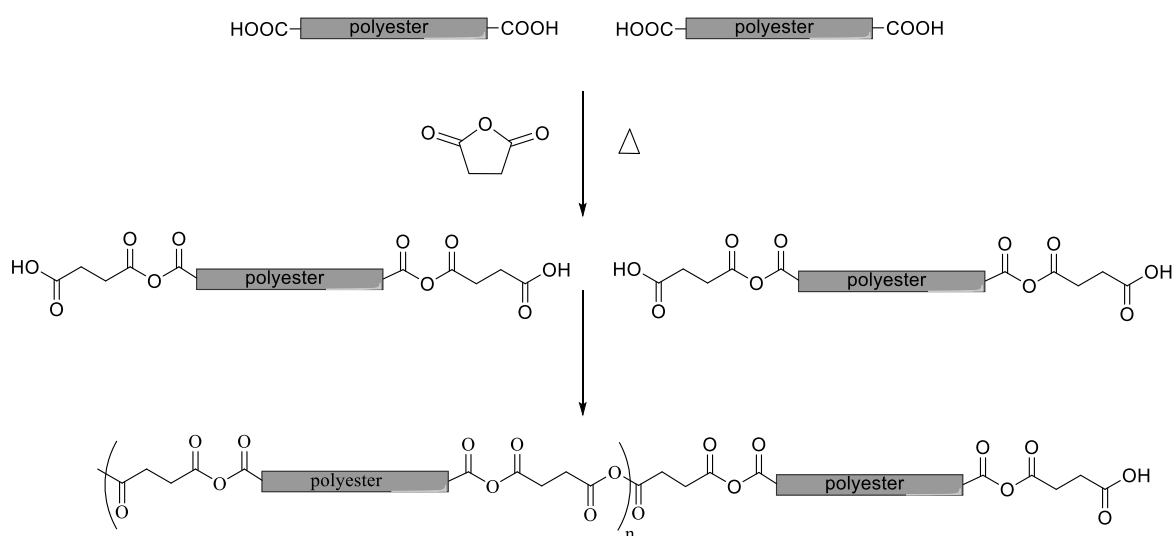


Figure 3.1. The potential reaction mechanism of PE-1 and SA.

### 3.2.2. Synthesis of Poly(ester-anhydrides) from PE-2 and SA

Tetra-functional polyester, PE-2 (10.0 g, 0.0125 mole), was melt mixed with the same ratio of succinic anhydride (5.0 g, 0.0470 mole) at different temperatures as seen in Table 3.2. Tetrabutylammonium bromine (TAB) and 2-methyl imidazole (2MI), were used as catalysts at 1% mole ratio (0.000125 mole, w.r.t. PE-2). No by-product formation was observed. The potential reaction mechanism is illustrated in Figure 3.2.

Table 3.2. Mole ratio and reaction conditions of PE-2 and SA.

Sample Name	PE-2: SA (mole ratio)	Catalyst	Temp (°C)	Vacuum (mbar)	Total Time (hour)
PE2_R	-	-	120→135	-	1.5
PE2_Rv	-	-	120→230	500→3(3h)	5.0
PE2_SA_1	1.00: 1.00	TAB	120→135	-	1.5
PE2_SA_2	1.00: 1.00	2MI	120→135	-	1.5
PE2_SA_3	1.00: 1.00	-	120→135		1.5
PE2_SA_4	1.00: 1.00	-	120→135	500→8(2h)	5.0
PE2_SA_5	1.00: 1.00	-	160	-	1.5
PE2_SA_6	1.00: 1.00	-	220		1.0

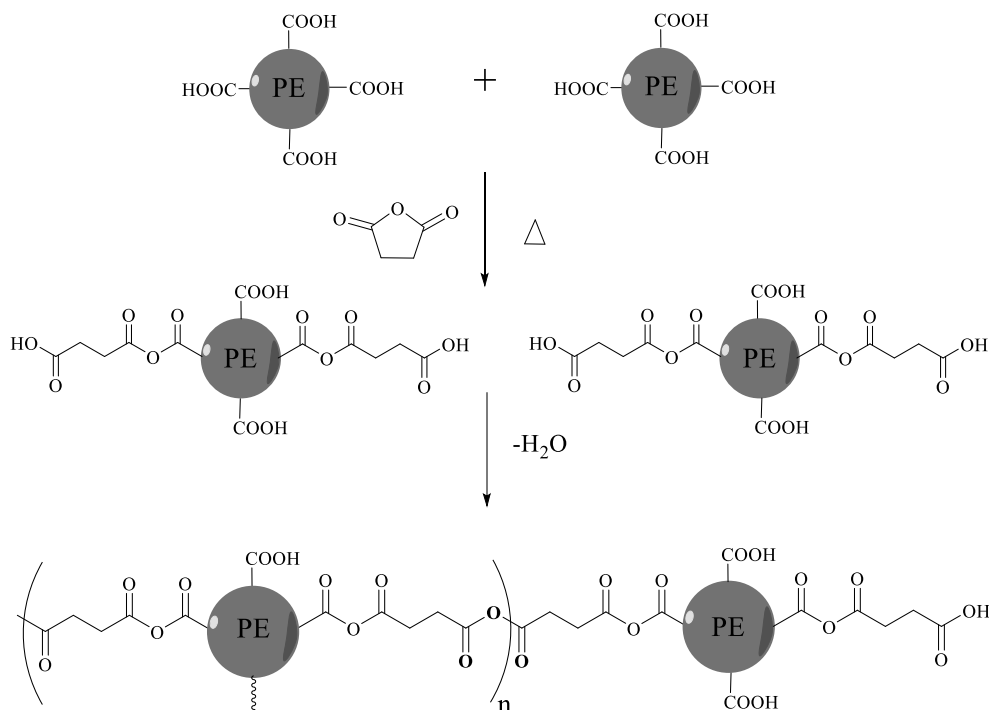


Figure 3.2. The potential reaction mechanism of PE-2 and SA.

### 3.2.3. Synthesis of Poly(ester-anhydrides) with PE-1 and PMDA

Di-functional polyester, PE-1 (10.0 g, 0.0056 mole), and two functional pyromellitic dianhydride were reacted at different mole ratios and temperature conditions as shown in Table 3.3. There were no sublimation and by-product formation during the process. The potential reaction mechanism is illustrated in Figure 3.3. There was no sublimation of the aromatic anhydride during the reaction.

Table 3.3. Mole ratio and reaction conditions of PE-1 with PMDA.

Sample Name	PE-1: PMDA (mole ratio)	Temp (°C)	Vacuum(mbar)	Total Time (hour)
PE1_PMDA_1	1.00 :1.00	140→180	500→10 (1h 15 min)	3.0
PE1_PMDA_2	1.00 :1.00	160	-	1.5
PE1_PMDA_2_1	1.00 :1.00	160	-	5.0
PE1_PMDA_3	1.00 :2.00	160	-	1.5
PE1_PMDA_4	1.00 :1.00	180	-	1.5
PE1_PMDA_5	1.00 :1.00	180	500→25 (3.5 h)	5.0
PE1_PMDA_6	1.00 :0.20	180	-	1.5
PE1_PMDA_7	1.00 :0.40	180	-	1.5
PE1_PMDA_8	1.00 :0.01	260	-	15 min

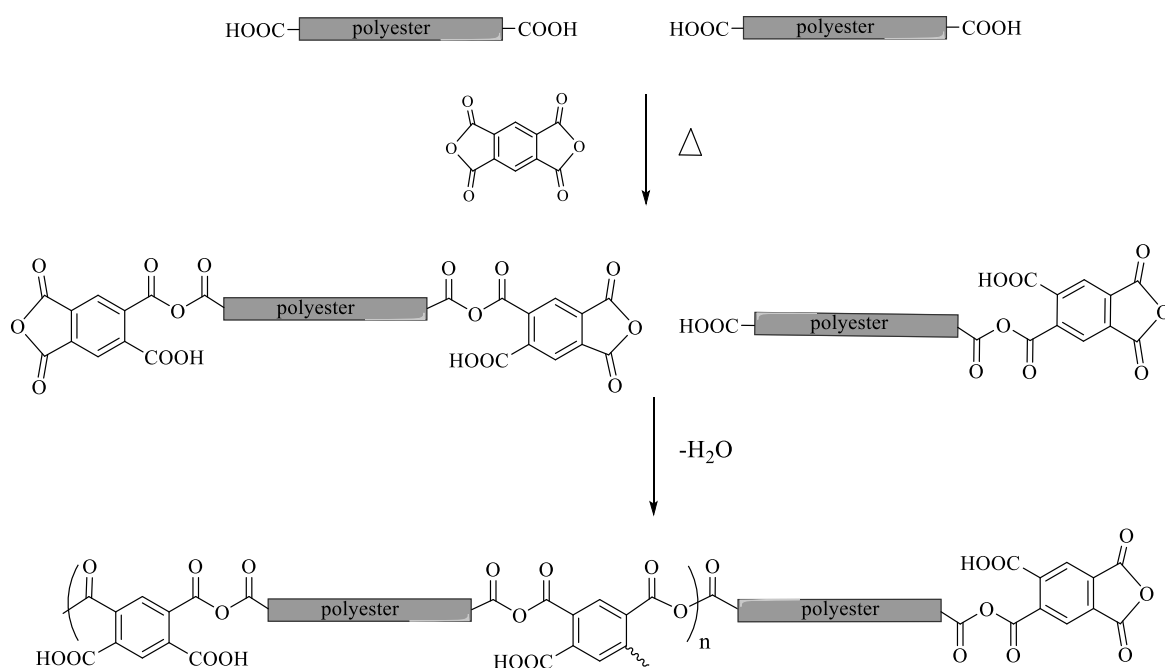


Figure 3.3. The potential reaction mechanism of PE-1 and PMDA.

### 3.2.4. Synthesis of Poly(ester-anhydrides) with PE-2 and PMDA

Tetra-functional polyester, PE-2 (15.0 g, 0.0187 mole) and two functional pyromellitic dianhydride were mixed at different mole ratio and temperature conditions, as depicted in Table 3.4. Vacuum was not applied during reactions. There was no sublimation of the aromatic anhydride during the reaction. The potential reaction mechanism is illustrated in Figure 3.4.

Table 3.4. Mole ratio and reaction conditions of PE-2 with PMDA.

Sample Name	PE-2: PMDA (mole ratio)	Temp (°C)	Vacuum(mbar)	Total Time (hour)
PE2_PMDA_1	1.00:1.00	120→160	-	1.5
PE2_PMDA_2	1.00:1.00	180→220	-	2.0
PE2_PMDA_3	1.00:0.01	260	-	15 min

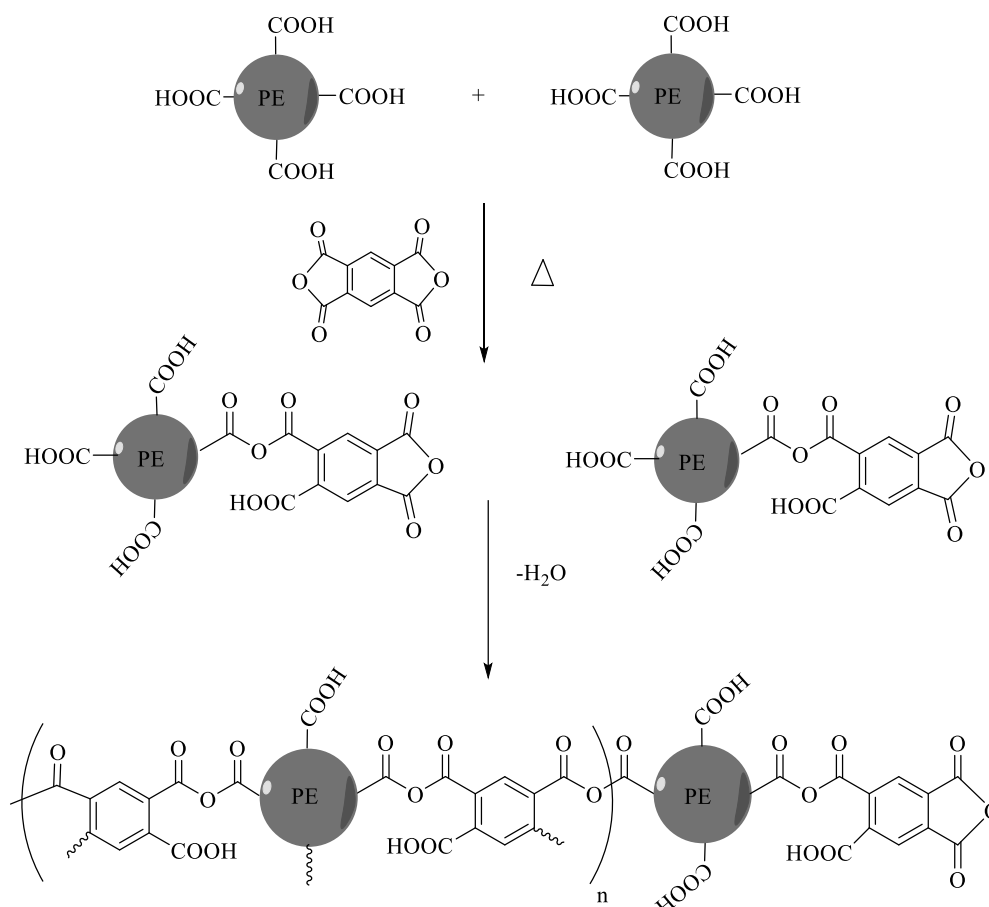


Figure 3.4. The potential reaction mechanism of PE-2 and PMDA.

### 3.3. Synthesis of Poly(ester-anhydrides) from the Synthesized PE-3 and SA

#### 3.3.1. Synthesis of PE-3 in Melt Polymerization

A carboxyl terminated linear polyester (PE-3) was synthesized using diacids and diols. Terephthalic acid (TPA), isophthalic acid (IPA), adipic acid (AA), neopentyl glycol (NPG), and ethylene glycol (EG) were mixed in a mole ratio where the alcohol to acid ratio was set to 1.02:1 under nitrogen atmosphere. Dibutyltin(IV) oxide was used as catalyst in different mole ratios. The reaction mechanism is illustrated in Figure 3.5. The reaction temperature was increased progressively from 150 °C to 260 °C. Monomer addition was done in two-steps. After the esterification was completed, vacuum was applied in order to initiate the polycondensation reaction. Water was collected as by-product.

Table 3.5. Mole ratio and reaction conditions of PE-3 synthesis.

Sample Name	Alcohol: Acid ratio (mole ratio)	Catalyst %	Vacuum (mbar)	Total Time(hours)
PE3_1	1.02 :1.00	1:1000	500→2(1h)	9h40min
PE3_2	1.02 :1.00	5:1000	500→3(1h)	6
PE3_3	1.00: 1.00	5:1000	500→2(1h)	10h15min
PE3_4	1.02: 1.00	1:1000	500→2(1h)	12
PE3_5	1.03: 1.00	1:1000	500→1(1h)	10

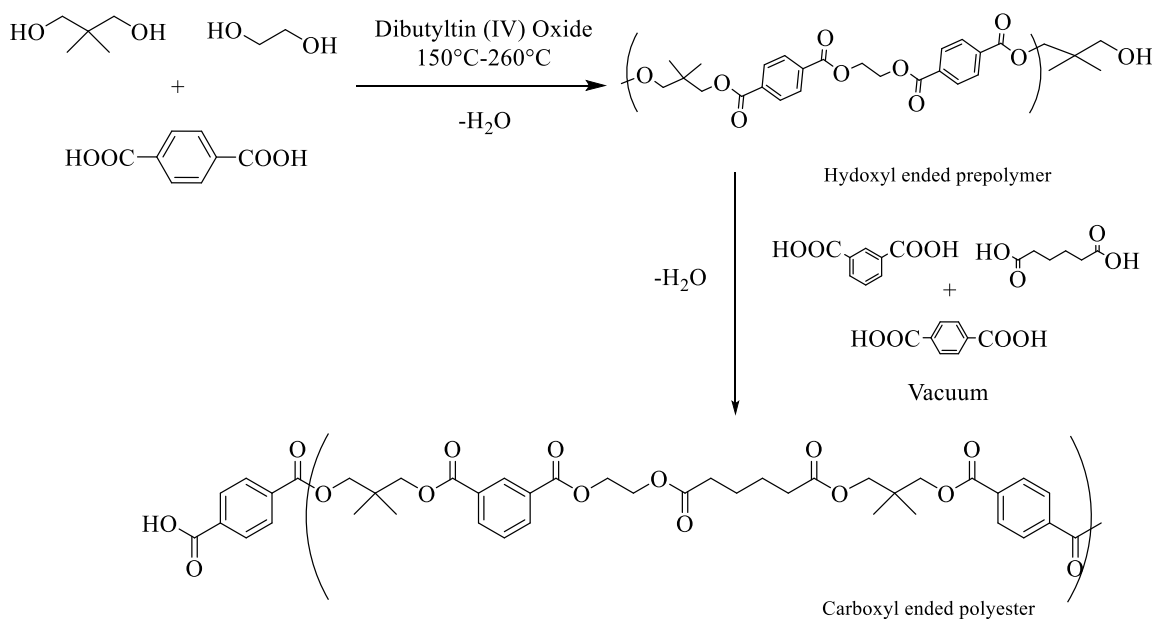


Figure 3.5. The reaction mechanism of synthesis of PE-3.

### 3.3.2. Synthesis of Poly (ester -anhydrides) by Using PE-3 and SA

The di-functional carboxyl terminated polyester (PE3\_4, 4.00 g, 0.0017 mole) was mixed with succinic anhydride (0.35 g, 0.0033 mole) in the same mol ratio as shown in Figure 3.6. Catalyst was not added to the reaction mixture. The proposed reaction mechanism is the same as the one shown in Section 3.2.1.

Table 3.6. Mole ratio and reaction conditions of PE-3 synthesis.

Sample Name	PE3_4: SA (mole ratio)	Temp (°C)	Vacuum(mbar)	Total Time (hour)
PE3_4_SA1	1.00: 1.00	160→220	500→0.2(1h 40min)	4.0
PE3_4_SA2	1.00: 1.00	160→220	500→2(1h)	6.5

### 3.4. Anhydride Determination in Poly(ester-anhydride) Chains

The anhydride linkages were detected by the anhydride test. 1 g of sample was dissolved in EtOAc and THF mixture. 1N NaOH is added until pH of solution approaches to 8-9. Several drops of diisobutylamine is added in order to break labile anhydride linkages. Lastly, 1N of HCl should be added to adjust the pH of mixture to 6-7. The organic layer of mixture is extracted by several water addition. The collected sample is dried in rotary evaporator and kept 1 day in vacuum before GPC analysis.

## 3.5. Characterization

### 3.5.1. <sup>1</sup>H-NMR Analysis

Varian Gemini 400 MHz spectrometer was used in CDCl<sub>3</sub> and C<sub>4</sub>D<sub>8</sub>O for <sup>1</sup>H-NMR analysis.

### 3.5.2. FT-IR Analysis

Nicolet 380 FT-IR spectrometer was used for analysis.

### 3.5.3. GPC Analysis

Viscotek VE2001 GPC instrument was used for molecular weight determination. The column temperature was 35°C. THF is used as a solvent and samples were filtered with 0.45µm filter. The concentration of samples was set to 4 mg/ml. The flow rate was set to 0.5 mL/min.

### 3.5.4. Acid Value Determination

Mettler Toledo T50 instrument was used for acid value determination. An appropriate amount of sample was dissolved in 50 ml benzyl alcohol and stirred for 10 min. The solution was titrated with 1 N KOH. The Analysis was done at Pulver Kimya Tic.A.S.

### 3.5.5. Rheology Analysis

Anton Paar MCR302 rheometer with 20 mm parallel plate was used. The temperature sweep test was done at temperatures ranging from 20°C to 200°C. The Analysis was done at Pulver Kimya Tic.A.S.

### 3.5.6. DSC Analysis

Exstar SII DSC 7020 instrument was used for thermal analysis. Analysis was done with heating and cooling rate of 10°C/min. The methods were given below:

Table 3.7. DSC run method 1.

Initial T(°C)	Final T(°C)	Hold Time (min)
-20	200	1
200	-20	2
-20	200	1

Table 3.8. DSC run method 2.

Initial T(°C)	Final T(°C)	Hold Time (min)
-20	190	1
190	-20	2
-20	190	1

Table 3.9. DSC run method 3.

Initial T(°C)	Final T(°C)	Hold Time (min)
-20	250	1
250	-20	2
-20	250	1

Table 3.10. DSC run method 4.

Initial T(°C)	Final T(°C)	Hold Time (min)
0	250	1
250	0	2
0	250	1

## 4. RESULTS AND DISCUSSION

Anhydrides are often unstable and prone to hydrolysis. The stability of the anhydride linkages between polymer chains are expected to be higher than monomeric anhydrides due to the potential hydrophobicity of the polymer backbone. In this thesis, cyclic anhydrides were examined as alternatives to acetic anhydride that is commonly used in poly(ester-anhydride) syntheses by the melt processes. In addition, the possibility of formation of anhydride linkages between carboxyl terminated polyesters was expected to be dependent on the total functionality of the reactants (Figure 4.1). Therefore, two commercial polyesters with different functionalities were used.

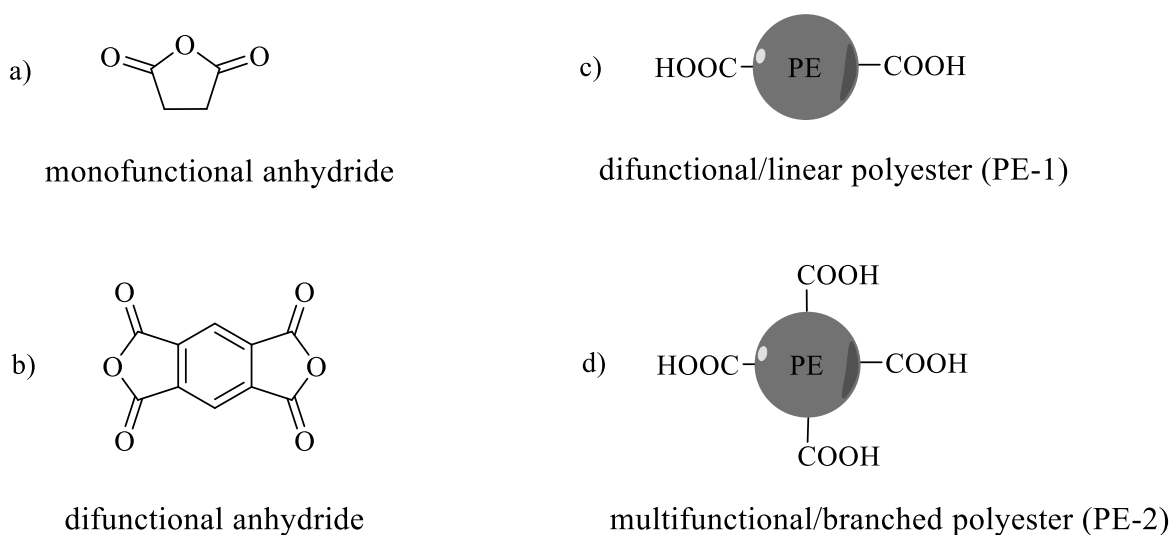


Figure 4.1. Chemical structures and functionalities of the reactants used.

In this study, succinic anhydride (SA) and pyromellitic dianhydride (PMDA) were used (Figure 4.1). Succinic anhydride is cycloaliphatic and has a single anhydride. Pyromellitic dianhydride is aromatic and has two anhydrides per molecule. PMDA is a known chain extender used to couple hydroxyl terminated polymers [28]. The chain extension occurs by the polyaddition of reactive end groups and the chain extender.

Two commercial polyesters PE-1 and PE-2 are both amorphous and have very similar monomer compositions. The former has two functionalities (carboxylic acid

terminated at both end groups) whereas the latter has approximately four (branched carboxylic acid terminated). The carboxylic acid groups are aromatic in nature. It is known that aromatic-aromatic anhydride linkages are more stable than the aliphatic-aliphatic anhydride linkages therefore it was expected that the aromatic carboxylic acid terminated polyesters would serve better the syntheses of the targeted polyester anhydrides.

A new polyester, PE-3, was synthesized in our laboratory and reacted with succinic anhydride in order to find out the difference and the effect of the composition of resins on poly(ester-anhydrides) syntheses. In addition, the exact ingredients of commercial of PE-1 and PE-2 are not known, they may contain catalyst and other additive. Thus, by synthesizing PE-3 a better known and controlled polymer was obtained.

#### 4.1. Structure Analysis of PE-1 and PE-2

The structural analyses of the polyesters were done by FT-IR and NMR. Both polyesters had similar characteristic bands of polyesters as shown in Figure 4.2.

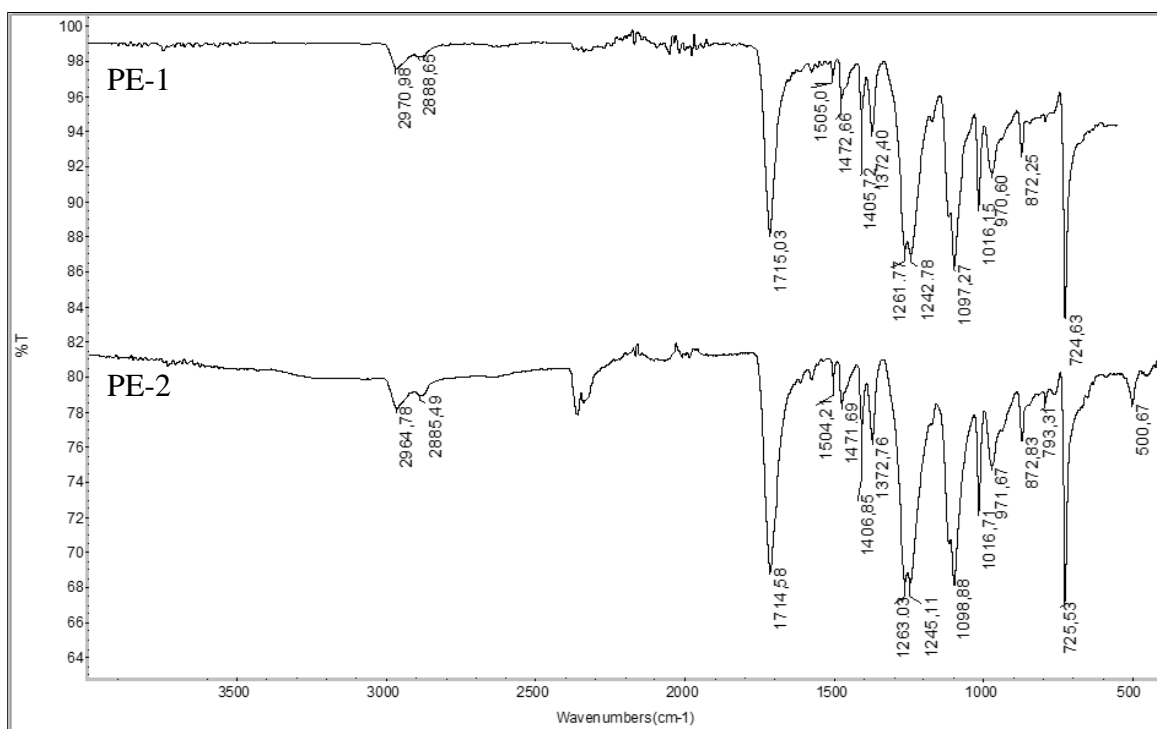
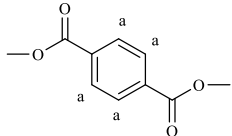
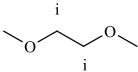
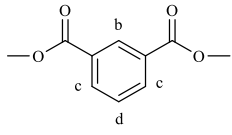
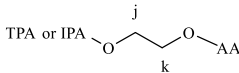
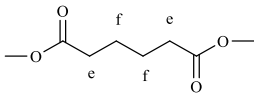
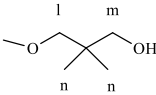
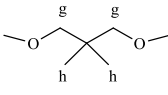
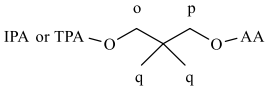


Figure 4.2. FT-IR Spectrum of PE-1 and PE-2.

In the example of PE-1, the hydroxyl stretching vibration of -COOH was observed as a broad peak above  $3000\text{ cm}^{-1}$ . The absorption bands around  $2964\text{ cm}^{-1}$  and  $2885\text{ cm}^{-1}$  were C-H stretching (symmetric and asymmetric) of the methylene groups. The intense C=O stretching vibration of the ester groups was observed at  $1715\text{ cm}^{-1}$ . The absorption bands at  $1262\text{ cm}^{-1}$ ,  $1243\text{ cm}^{-1}$ ,  $1097\text{ cm}^{-1}$ , and  $1016\text{ cm}^{-1}$  were assigned as C-O stretching vibrations of the ester groups. At  $1505\text{ cm}^{-1}$ ,  $1473\text{ cm}^{-1}$ ,  $1406\text{ cm}^{-1}$ , and  $725\text{ cm}^{-1}$  C-H stretching of the 1,4 aromatic groups were observed. At  $1372\text{ cm}^{-1}$  C-H bending was observed.

Table 4.1. Structural units and chemical shifts of PE-1 units in  $\text{CDCl}_3$ .

Structural Unit	Chemical Shifts (ppm)	Structural Unit	Chemical Shifts (ppm)
	a. 8.09		i. 4.70
	b. 8.67 c. 8.20-8.22 d. 7.52		j. 4.51 k. 4.41
	e. 2.43 f. 1.65		l. 4.20 m. 3.41 n. 1.02
	g. 4.26 h. 1.17		o. 4.14 p. 3.98 q. 1.06

The monomer composition of PE-1 and PE-2 were similar. The peak assignments for the  $^1\text{H-NMR}$  of PE-1 are given in table 4.3. Both terephthalic and isophthalic acid were connected to diols. The peak corresponding to the aromatic protons of the terephthalic acid repeat units (peak a) were at 8.09 ppm and those coming from the isophthalic acid repeat units (peak b, c, and d) were at 8.67, 8.20-8.22, and 7.52 ppm, respectively. The peaks at 2.43 and 1.65 ppm belong to the aliphatic methylene groups of adipic acid repeat units. The absorption of the methylene groups (peak g) of neopentyl glycol was at 4.26 and ethylene glycol (peak i) was at 4.70 which were connected to aromatic units by ester linkages. The peak at 1.17 ppm belongs to methyl groups (peak h) of neopentyl glycol repeating groups. Further detail of proton peaks was shown in Table 4.1.

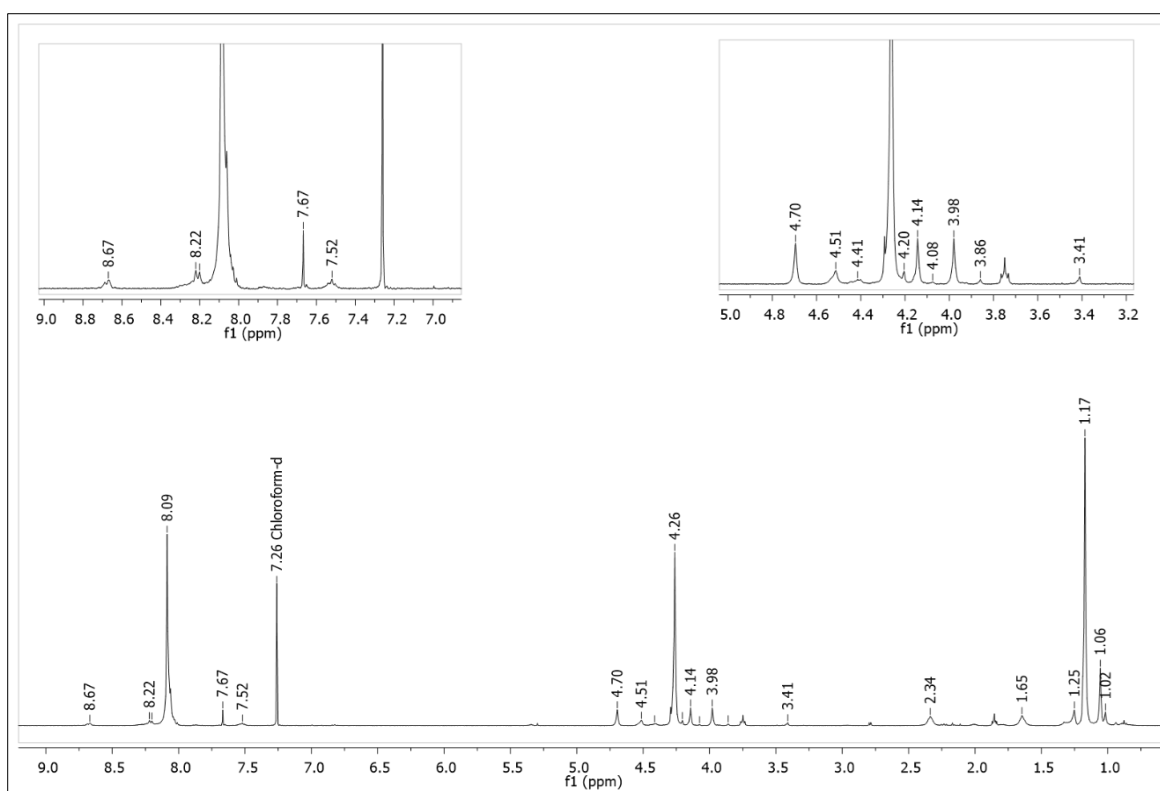


Figure 4.3.  $^1\text{H-NMR}$  analysis of PE-1 in  $\text{CDCl}_3$ .

As previously mentioned in Section 1.4.3, the carboxylic acid protons were not visible in  $^1\text{H-NMR}$ . Although both polyesters were carboxyl terminated, hydroxyl bearing methylene proton peaks (at 3.41 ppm) with low integral values could be observed. The main difference between PE-1 and PE-2 is that the latter contains peaks corresponding to aromatic peaks (3 H atoms at 8.48 ppm, 8.39 ppm, and 7.84 ppm) coming from the ester derivative of trimellitic anhydride which was employed most probably to induce the multi-functionality (around four). PE-2 contains diethylene glycol (at 4.52 ppm and 3.89 ppm) monomer units instead of ethylene glycol units in PE-1.

Table 4.2. General properties of commercial polyesters.

Polyester	Functionality	Acid Value (mg KOH/g)	$T_g$ ( $^{\circ}\text{C}$ )	$M_n$ (g/mol)	$M_w$	PDI
PE-1	2	31	51	3831	11643	3.04
PE-2	4	71	44	3273	5337	1.63

Thermal analysis of polyesters, PE-1 (in Figure 4.4) and PE-2 were done by DSC (method 3). Polyesters were heated from  $-20^{\circ}\text{C}$  to  $250^{\circ}\text{C}$  at a rate of  $10^{\circ}\text{C}/\text{min}$ . They were cooled at the same rate to eliminate history of samples. According to the results, an enthalpy of relaxation was observed in the first heating run, which overlapped with  $T_g$ . This is most probably the result of different thermal histories. Therefore,  $T_g$  values were calculated in the second heating run.

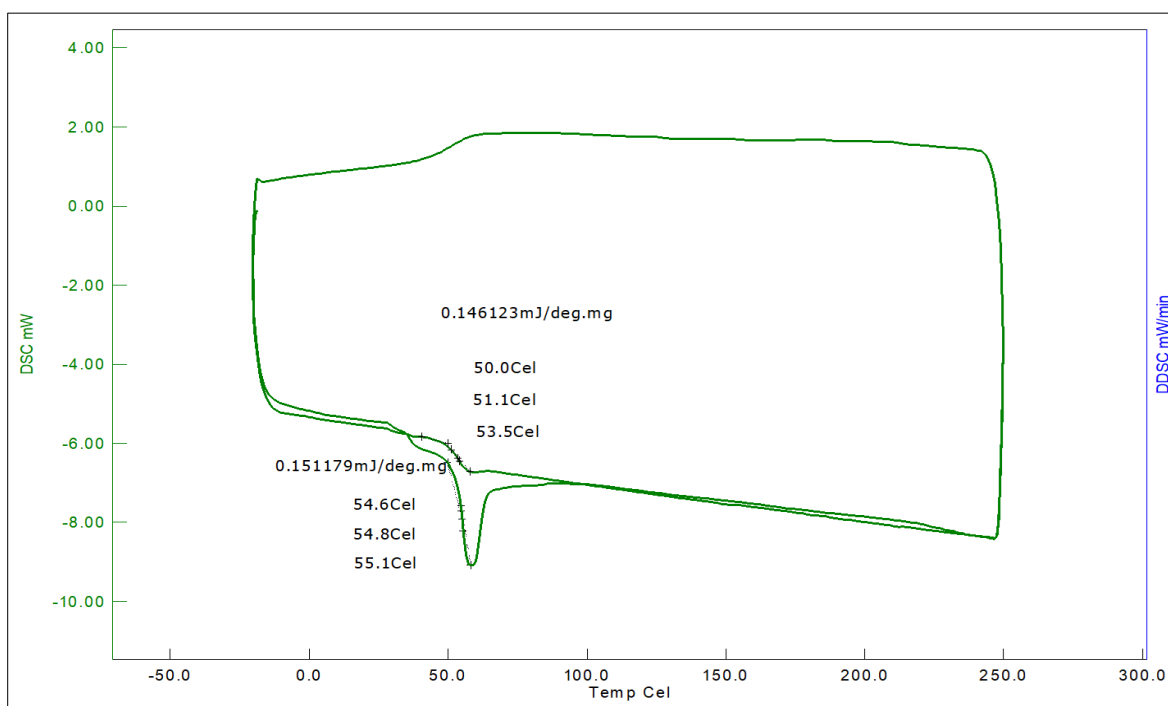


Figure 4.4. DSC analysis of PE-1.

## 4.2. Synthesis of Poly(ester-anhydrides) from Commercial Polyesters and Cyclic Anhydrides

In this section, experiments will be presented according to number of functionality of reactants in four categories:

- (i) the reaction of monofunctional SA with difunctional PE-1.
- (ii) the reaction of monofunctional SA and four functional PE-2.
- (iii) the reaction of difunctional PMDA with difunctional PE-1.
- (iv) the reaction of difunctional PMDA with four functional PE-2.

Reactions were carried out in melt and the product, potential poly(ester-anhydrides), were first characterized by FT-IR and  $^1\text{H-NMR}$ , then, the molecular weights before and after the anhydride test (which cleaves the anhydride linkages by aminolysis) were compared in order to confirm the formation of poly(ester-anhydrides).

#### 4.2.1. Synthesis of Poly(ester-anhydrides) from PE-1 and SA

The difunctional linear polyester was melt mixed with succinic anhydride at different temperatures. Above  $230\text{ }^\circ\text{C}$ , SA started to degrade, and coloration occurred. Therefore, in order to prevent such degradation and preserve the anhydride linkages between carboxyl ended chains, reactions were conducted at minimal temperatures ( $120\text{ }^\circ\text{C}$  to  $140\text{ }^\circ\text{C}$ ). Reaction temperature was increased progressively as indicated in Table 3.1 where a yellowing was observed at temperatures higher than  $180\text{ }^\circ\text{C}$ . Both hard and brittle resins were obtained.

According to the FT-IR of final resins, Figure 4.5, the molecular structure of the polyester was preserved. There were new symmetric and asymmetric anhydride  $\text{C}=\text{O}$  absorption peaks at  $1786\text{ cm}^{-1}$  and  $1869\text{ cm}^{-1}$ . The succinic anhydride has anhydride  $\text{C}=\text{O}$  absorption peaks at  $1774\text{ cm}^{-1}$  and  $1858\text{ cm}^{-1}$ . Thus, new anhydride linkages were detected.

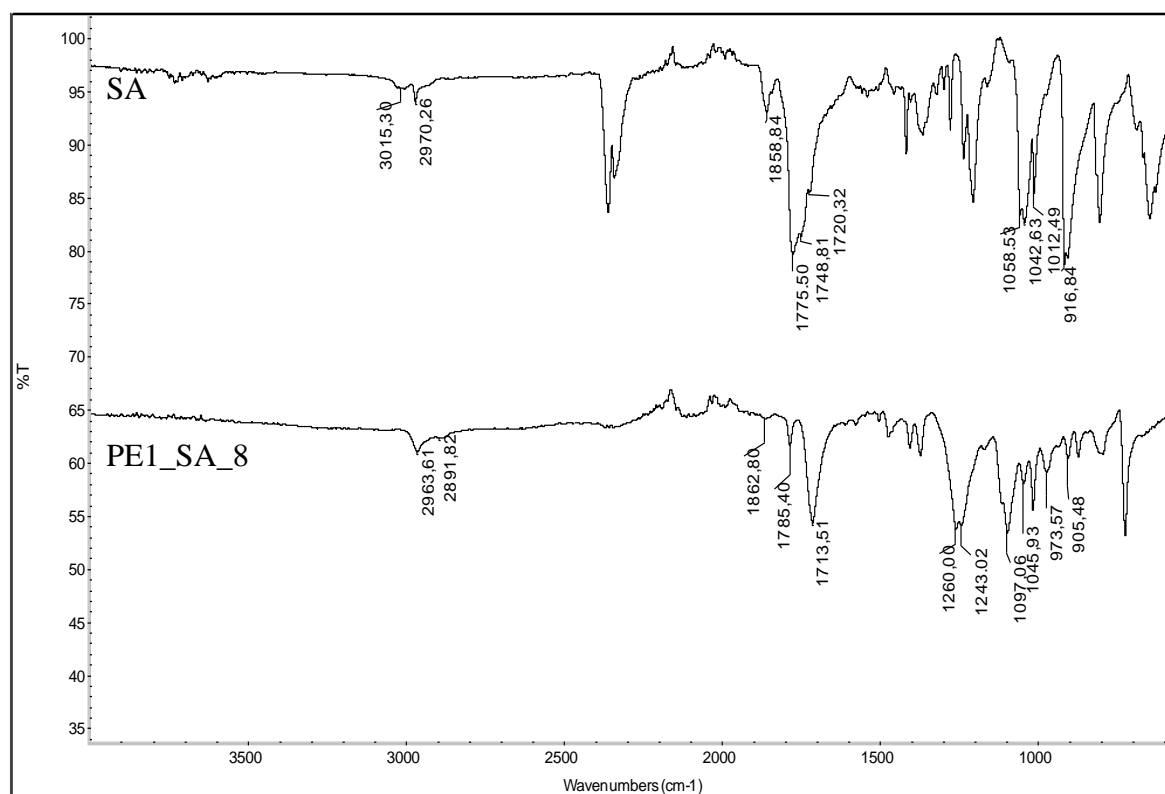


Figure 4.5. FT-IR spectrum of PE1\_SA\_2 and SA.

In Figure 4.6, the possible locations of different potential anhydride linkages that may be formed are illustrated. First, the anhydride absorption peaks maybe due to the formation of a new anhydride linkage which was obtained by coupling of aromatic carboxyl terminated polyester chains (option a in Figure 4.6). Second, the shifting may result from the possible formation of new linear mixed anhydride linkages between several succinic anhydrides (polysuccinic anhydride) either connected to the polyester chain ends (option c and d) or free (e). It would not be possible to differentiate the latter three option by GPC result (anhydride test) since the cleavage of the anhydrides would not result in a significant molecular weight drop.

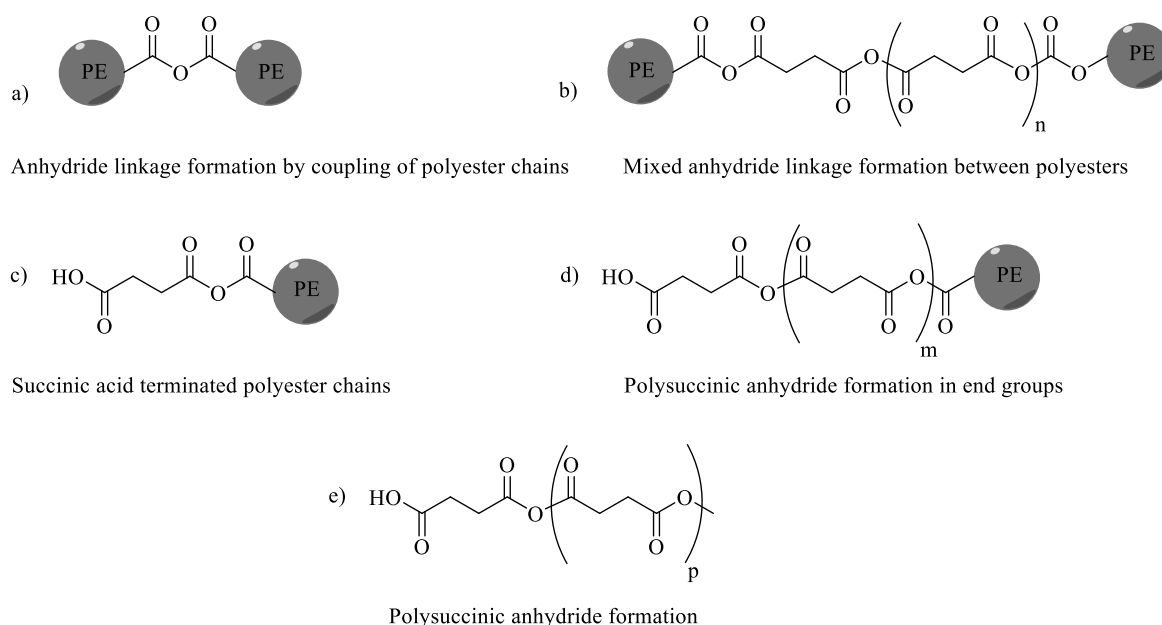


Figure 4.6. Possible scenarios on anhydride location a) and b) in between polyester chains, c) and d) in terminal groups of polyesters, and e) free polysuccinic anhydride formation.

After reaction with SA, three different peaks at 3.00 ppm, 2.71 ppm, and 2.67 ppm were found in  $^1\text{H-NMR}$ , which all belong to the methylene peaks of SA but with different connectivity (Figure 4.7). There was always some residual unreacted succinic anhydride in the polymer as detected at 3.00 ppm. It is estimated that methylene groups of SA which were interconnected through anhydride and ester linkages appeared at 2.71 ppm and 2.67 ppm

respectively (Figure 4.8). These methylene peaks were assigned after detailed experiments and research as will be presented below.

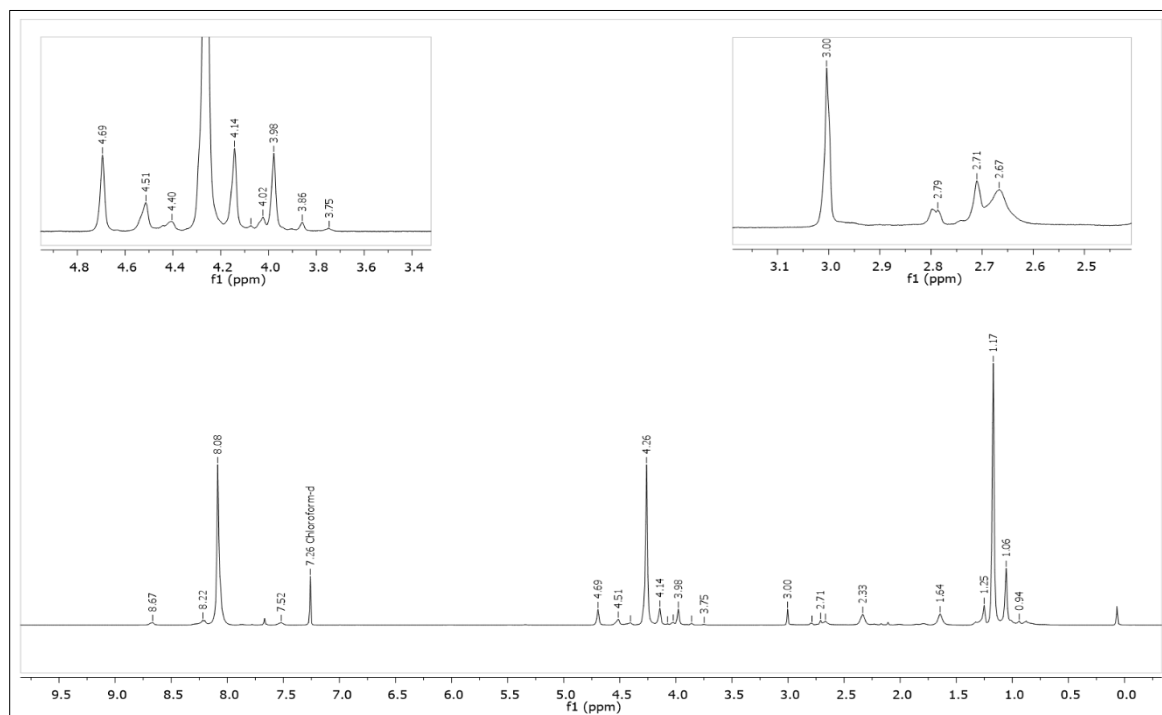


Figure 4.7.  $^1\text{H-NMR}$  Analysis of PE1\_SA\_3 in  $\text{CDCl}_3$ .

First of all, it was thought that there were four possible connection pathways of SA into to polyesters as shown in Figure 4.8.

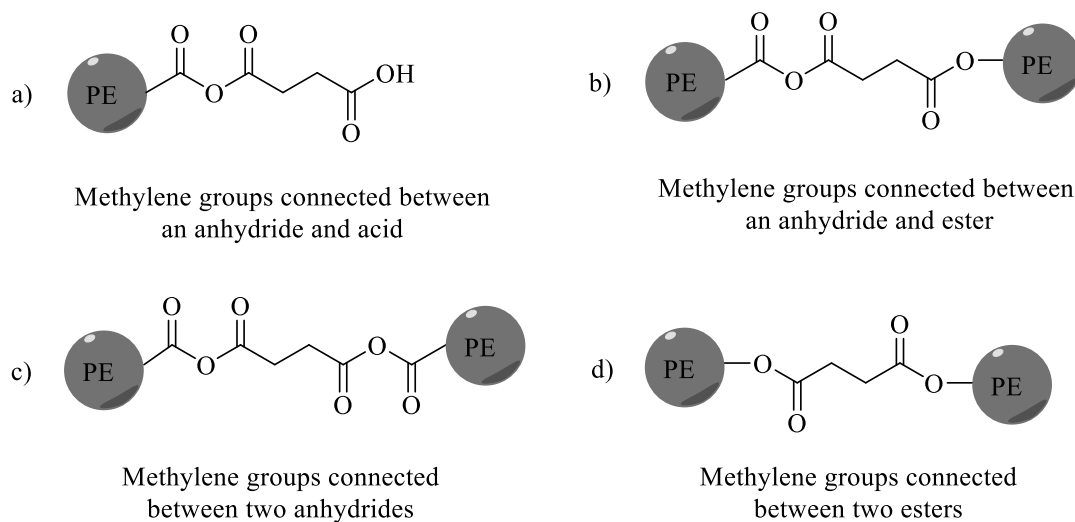


Figure 4.8. Possible connection pathways of SA to PE-1.

Secondly, to differentiate the methylene peaks of the residual SA from that of the incorporated SA (*i.e.* as polyanhydrides), <sup>1</sup>H-NMR analyses of samples (PE1\_SA\_4 and PE1\_SA\_5) after purification and anhydride test were done. For the purification, the samples were dissolved in DCM and precipitated into MeOH/H<sub>2</sub>O mixture. After precipitation and anhydride test, the peak at 2.71 ppm were diminished significantly but some succinic methylene protons were still detectable at 2.67 ppm which should correspond to the esterified succinic units. Thus, it can be concluded that anhydrides of succinic acid existed in an acyclic manner at the chain ends (option d in Figure 4.8).

Although PE-1 is acid terminated, hydroxyl end groups were detected in <sup>1</sup>H-NMR. At the end of the melt reaction, integral values of the methylene protons of terminal NPG connected to an ester unit (Table 4.1, peak l) and hydroxyl end (Table 4.1, peak m) were diminished and new polyester peak at 4.02 ppm (Figure 4.7) was observed. In other words, hydroxyls of terminal NPG were involved in esterification reactions with SA. The methylene groups of these SA units incorporated to the chain as part of the ester were detected at 2.67 ppm.

If two polyester units are linked by an anhydride, a decrease in the molecular weight after the anhydride test should be observed since the test is designed to cleave anhydride bonds. As shown in Table 4.3, the expected decreases were observed in PE1\_SA\_3, PE1\_SA\_8 and PE1\_SA\_9. The experiments were carried out using polymers with different monomer composition, and different temperature/vacuum profiles. It can be said that, at high temperature and shorter reaction time, higher molecular weight poly(ester-anhydrides) are obtained (PE1\_SA\_8).

It is important to mention that in some samples although the molecular weight of final resins increased (PE1\_SA4 and PE1\_SA\_7), no drop in molecular weight thus no anhydride linkage was detected by the anhydride test, which most likely indicates a molecular weight increase due to ester bond formation through transesterification reactions.

Table 4.3. The molecular weight obtained from PE1\_SA reactions.

Sample Name	$M_n$ (g/mol)	$M_w$ (g/mol)	PDI	$M_n$ (g/mol) Anhydride Test	$M_w$ (g/mol) Anhydride Test	PDI Anhydride Test
PE-1	3831	11643	3.04	-	-	-
PE1_SA_1	3445	12018	3.49	-	-	-
PE1_SA_2	3814	10791	2.83	3720	10712	2.88
PE1_SA_3	4619	12098	2.62	2924	11588	3.96
PE1_SA_4	4291	9334	2.18	9790	12238	1.25
PE1_SA_5	2388	8537	2.68	-	-	-
PE1_SA_6	5122	11119	2.17	4648	13710	2.95
PE1_SA_7	4475	12313	2.75	4327	12261	2.83
PE1_SA_8	5567	13730	2.45	3636	10947	3.01
PE1_SA_9	4363	9551	2.19	2586	8664	3.35
PE1_SA_10	4106	9333	2.27	3763	9256	2.46

Increasing the reaction time and applying vacuum decreased  $M_n$  and thus  $T_g$  values (e.g. PE1\_SA\_1&2 and 4&5). The anhydride formation and chain scission reactions may occur at the same time and competitive rates especially in an acidic medium. However, since the anhydride bonds are less stable, they may be cleaved at prolonged reaction times and the net observed result may reflect the one only coming from the scission reactions. In other words, one cannot omit the temporary formation of anhydrides just by looking to the results.

The DSC analysis was done with method 1. The  $T_g$  of final resins were less than  $T_g$  of the polyester precursor, PE-1 ( $T_g = 51$  °C). In Table 4.4, the highest  $T_g$  was obtained where the ratio of PE-1 and SA was set to 1.00:0.50. To understand the source of  $T_g$  decrease, PE1\_SA\_4 and PE1\_SA\_5 were purified by precipitation to remove any unreacted SA which could act as plasticizer. Indeed,  $T_g$  increased to the  $T_g$  of the precursor resin after the purification process. It can be deduced that unreacted SA worked as plasticizers.

As seen in Table 4.4, after  $T_g$ , an exotherm, which is known as cold crystallization or annealing, was observed. Although PE-1 is an amorphous polymer, for reactions of PE1 and SA, after  $T_g$  there was a  $T_m$  between 137 to 156 °C. These meltings were not observed when the mole concentration of SA was low (PE1\_SA\_4 and PE1\_SA\_5). It is possible that these  $T_c$  and  $T_m$  values correspond to some sort of polysuccinic anhydride crystallites/domains in the polymer composition since they do not correspond to that of SA or its acid form.

Table 4.4. Thermal behavior of PE1\_SA reactions in second heating run.

Sample Name	$T_g$ (°C)	$T_c$ (°C)	$T_m$ (°C)
PE-1	51	-	-
PE1_SA_1	35	75	155
PE1_SA_2	29	75	144
PE1_SA_3	38	-	-
PE1_SA_4	44	-	-
PE1_SA_4_ppt	50	-	-
PE1_SA_5	41	-	-
PE1_SA_5_ppt	51	-	-
PE1_SA_6	37	-	156
PE1_SA_7	31	68	147
PE1_SA_8	34	85	137
PE1_SA_9	33	-	137
PE1_SA_10	33	-	-

High acid values were obtained after reaction with SA as seen in Table 4.5. To check whether there will be any change in the structure in SA (ring opening), blank SA was heated at 160 °C for 4.5h under nitrogen atmosphere. There was no shifting observed for carbonyl peaks in FT-IR and <sup>1</sup>H-NMR analysis. According to DSC analysis, only one  $T_m$  appeared in the first heating cycle, which corresponds the melting point of succinic anhydride (120°C). SA was sublimed and collected on the top of the DSC sampling furnace. There was no crystallization peak during cooling and no  $T_m$  formation in the second heating cycle. According to this blank experiment, it was estimated that, carboxyl groups of polyesters may initiate the formation of short polysuccinic anhydride chains.

In addition, no significant shifting was observed when both components PE-1 and SA were physically mixed at room temperature and analyzed with FT-IR. According to DSC result of physically mixed compounds, at first heating run the  $T_g$ , which belonged to PE-1(53°C), and  $T_m$ , (120 °C) which belonged to SA, were observed. During second heating run, only  $T_g$  was detected at a lower value, 31°C. Sublimation of SA was observed in DSC sampling furnace. It can be said that remained SA melted in the polymer composition and decreased  $T_g$ .

Table 4.5. Acid values of synthesized samples.

Sample Name	Acid Value (mg KOH/g)	Sample Name	Acid Value (mg KOH/g)
PE1_SA_1	81.0	PE1_SA_6	28.0
PE1_SA_2	88.4	PE1_SA_7	7.9
PE1_SA_3	66.8	PE1_SA_8	14.3
PE1_SA_4	50.4	PE1_SA_9	91.5
PE1_SA_5	64.4	PE1_SA_10	95.3

To sum up, the shifting in symmetric and asymmetric anhydride absorption stretching were observed in FT-IR. Beside poly(ester-anhydride) formation, the possibility of formation of mixed anhydride linkages in chain ends and free polysuccinic anhydride seems likely. Poly(ester-anhydride) synthesis was confirmed for several experiments by the anhydride test. Although a  $T_g$  increase was expected, the residual unreacted SA seems to lower the  $T_g$ .

#### 4.2.2. Synthesis of Poly(ester-anhydrides) from PE-2 and SA

A multifunctional polyester (approximately four terminal aromatic carboxylic acid), PE-2, was melt mixed with succinic anhydride in order to compare the reactivity of PE-2 and the previously employed difunctional linear polyester (PE-1). At temperatures higher than 100°C, the molten mixture of PE-2 and SA was colored (light pink to brown) and transparent which then became opaque at the final cooling step. The final resins were waxy and flexible at first but became harder in time with further cooling. Discoloration and gas evolution were observed at high temperatures. Therefore, reactions were conducted at low temperatures.

First, blank experiments of PE-2 ( $M_n$ :3273 g/mol,  $M_w$ :5337 g/mol, PDI: 1.63) were done by using PE-2 only (PE2\_R and PE2\_Rv) where the samples were heated alone with and without applying a vacuum to understand the behavior of the starting polyester under the experimental conditions. There was no significant change in FT-IR of PE2\_R. At high temperature and under vacuum, for PE2\_Rv, a new anhydride absorption peak observed at 1783  $\text{cm}^{-1}$  in FT-IR result.

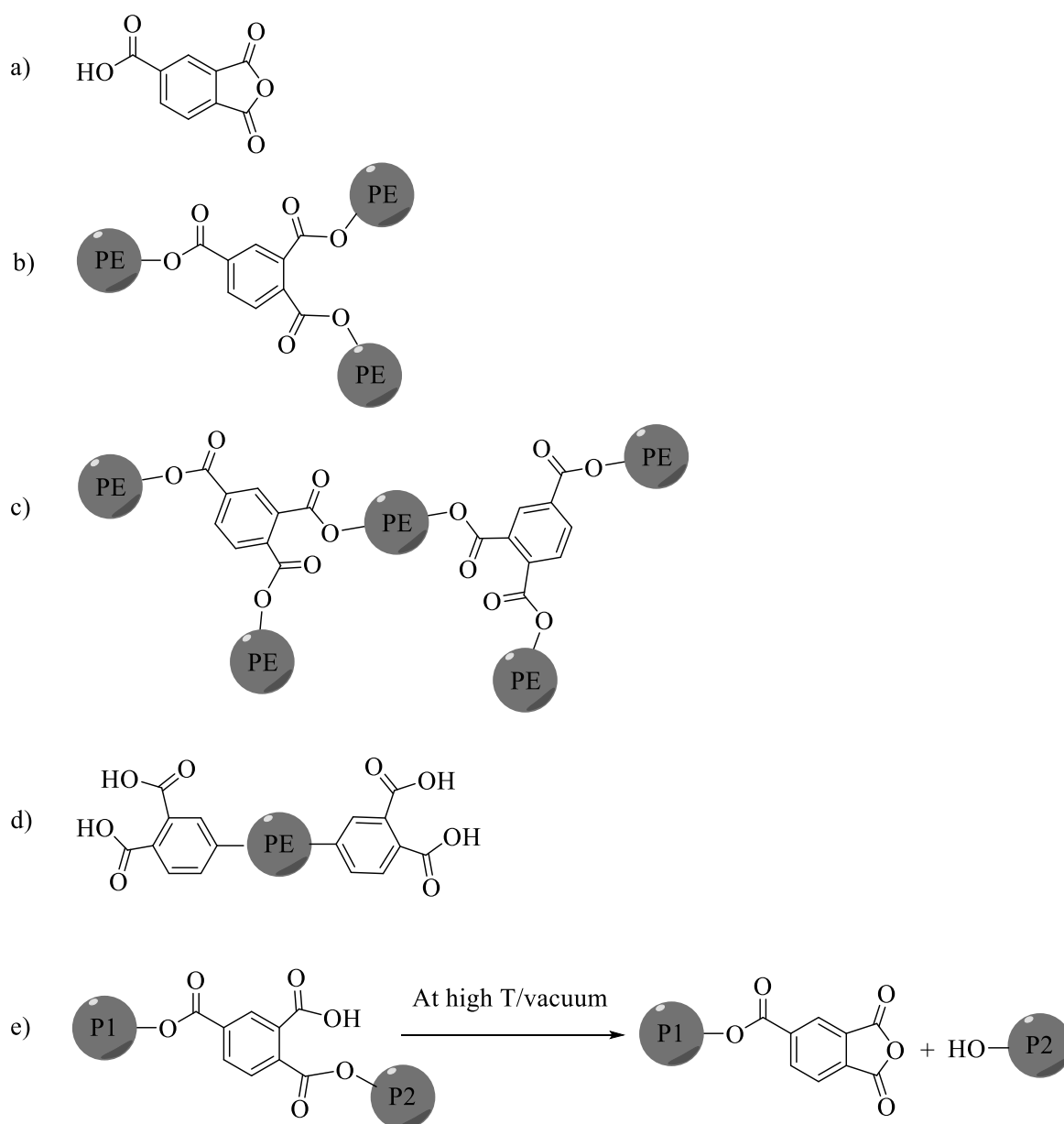


Figure 4.9. a) TMA, the proposed illustration of the location of TMA at b) beginning c) middle d) end groups of polyesters, and e) the ring closure mechanism of TMA at the end groups.

It may be thought that high temperature and vacuum may have promoted the synthesis of poly(ester-anhydride), that is indicative of coupling of polyester's carboxyl end groups, but there was a decrease in molecular weight ( $M_n$ : 2992 g/mol,  $M_w$ : 9429 g/mol, PDI: 3.15) and an increase in polydispersity index as well (Table 4.5). The possible locations of TMA in polyester chains is illustrated in Figure 4.9. It may be assumed that ortho carboxyl

group in a TMA unit that is present at polyester chains may ring close to form cyclic anhydrides while cleaving an existing ortho-ester. This would lower the molecular weight and increase PDI. However similar results may be obtained by carboxylic acid induced competitive anhydride formation and chain scission reactions as discussed above.

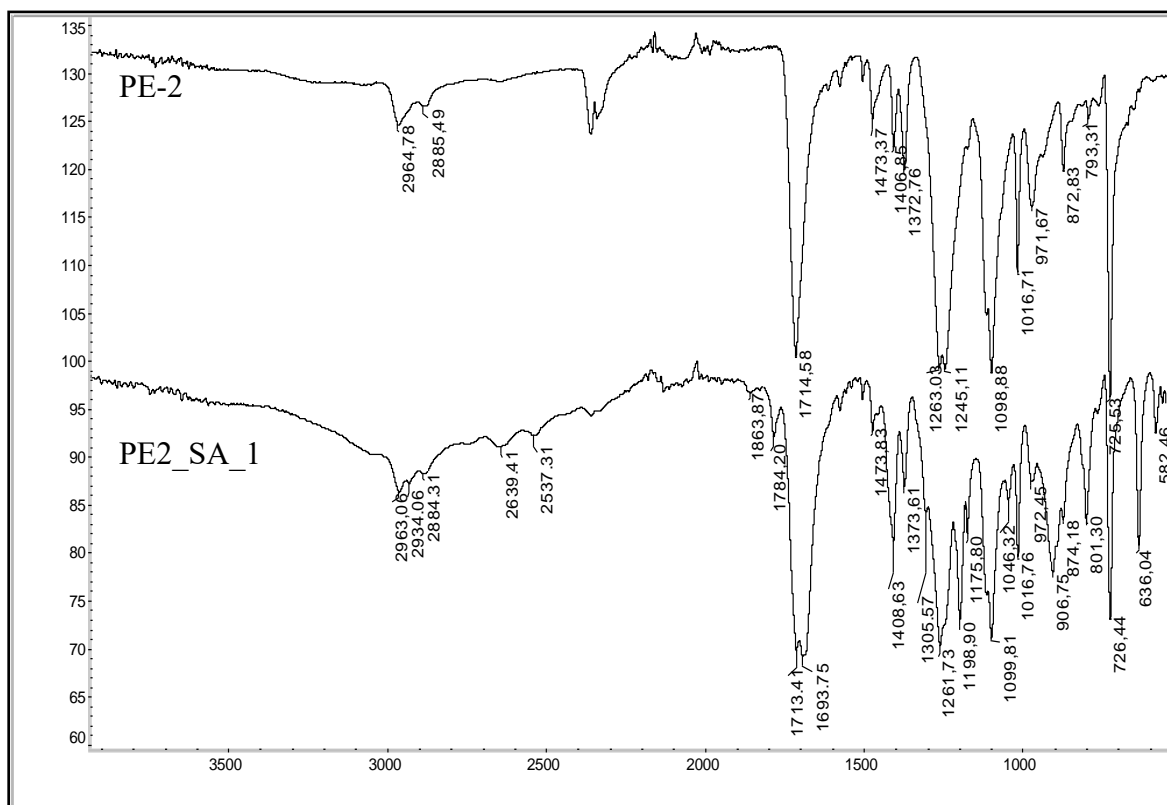
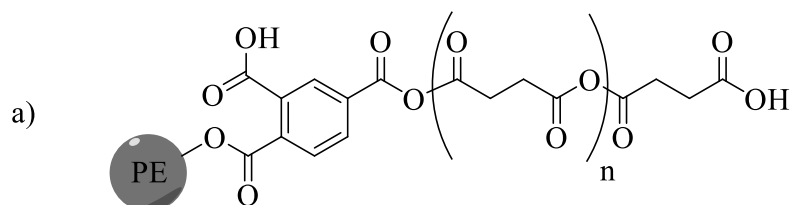


Figure 4.10. FT-IR Analysis of PE-2 and PE2\_SA\_1.

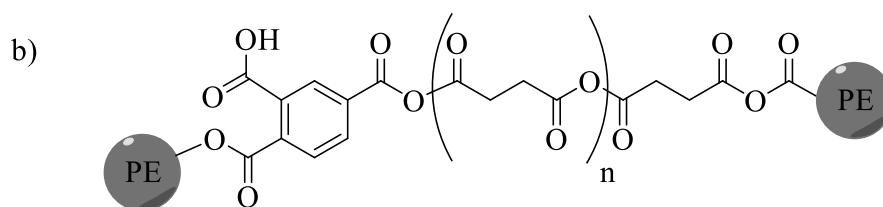
According to FT-IR of PE2\_SA reactions, Figure 4.10, similar to PE1 and SA reactions as previously mentioned in Section 4.2.1, there were new carbonyl absorption peaks at  $1784\text{ cm}^{-1}$  and  $1864\text{ cm}^{-1}$ , which may indicate the presence of mixed anhydride linkages. Some sort of oligomerization between succinic anhydrides is also possible as illustrated in Figure 4.11.

Unlike PE-1 with SA reactions, the color of final resins changed from light pink to dark brown. The coloration was thought to indicate the formation of intense acid ends in the medium. As seen in Figure 4.10, the carbonyl group stretching that may be attributed succinic acid (or conjugated acid) was observed at  $1693\text{ cm}^{-1}$ . Succinic acid has carbonyl absorption peak at  $1692\text{ cm}^{-1}$  [29]. Two adjacent C-H stretching absorption peaks were

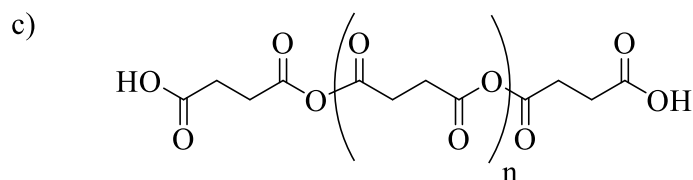
detected at  $2640\text{ cm}^{-1}$  and  $2537\text{ cm}^{-1}$  and were attributed to the  $\text{-C-H}$  stretching of the succinic acid. One can deduce that, as shown in Figure 4.11, in addition to mixed anhydride formation in the polymer composition (either in between chains or connected to end groups), succinic acid formation was also observed in the reaction of SA with PE-2.



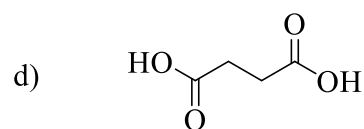
Mixed anhydride formation connected to chain ends of polyesters



Mixed anhydride formation in between chain ends of polyesters



Polysuccinic anhydride formation



Succinic acid formation

Figure 4.11. The illustration of a mixed anhydride formation a) connected to chain ends, b) in between polyesters, c) free polysuccinic anhydride, and d) succinic acid formation.

It is interesting that the formation of succinic acid was not observed in the experiments with PE-1, but with PE-2. First, it was assumed that additives or the catalyst,

used in synthesis of PE-2, may be promoting the succinic acid formation. Secondly, different from PE-1, PE-2 is multifunctional and has high acid value (71 mg KOH/g). In addition to the formation of mixed anhydride linkages, the cleavage under acidic conditions could also trigger the succinic acid formation as illustrated in Figure 4.12. The formation of cyclic anhydrides and cleavage by carboxyl terminated units may occur simultaneously. Because of the acid catalyst degradation of these linear mixed anhydride linkages high amount of succinic acid formation may be observed at the end of reactions.

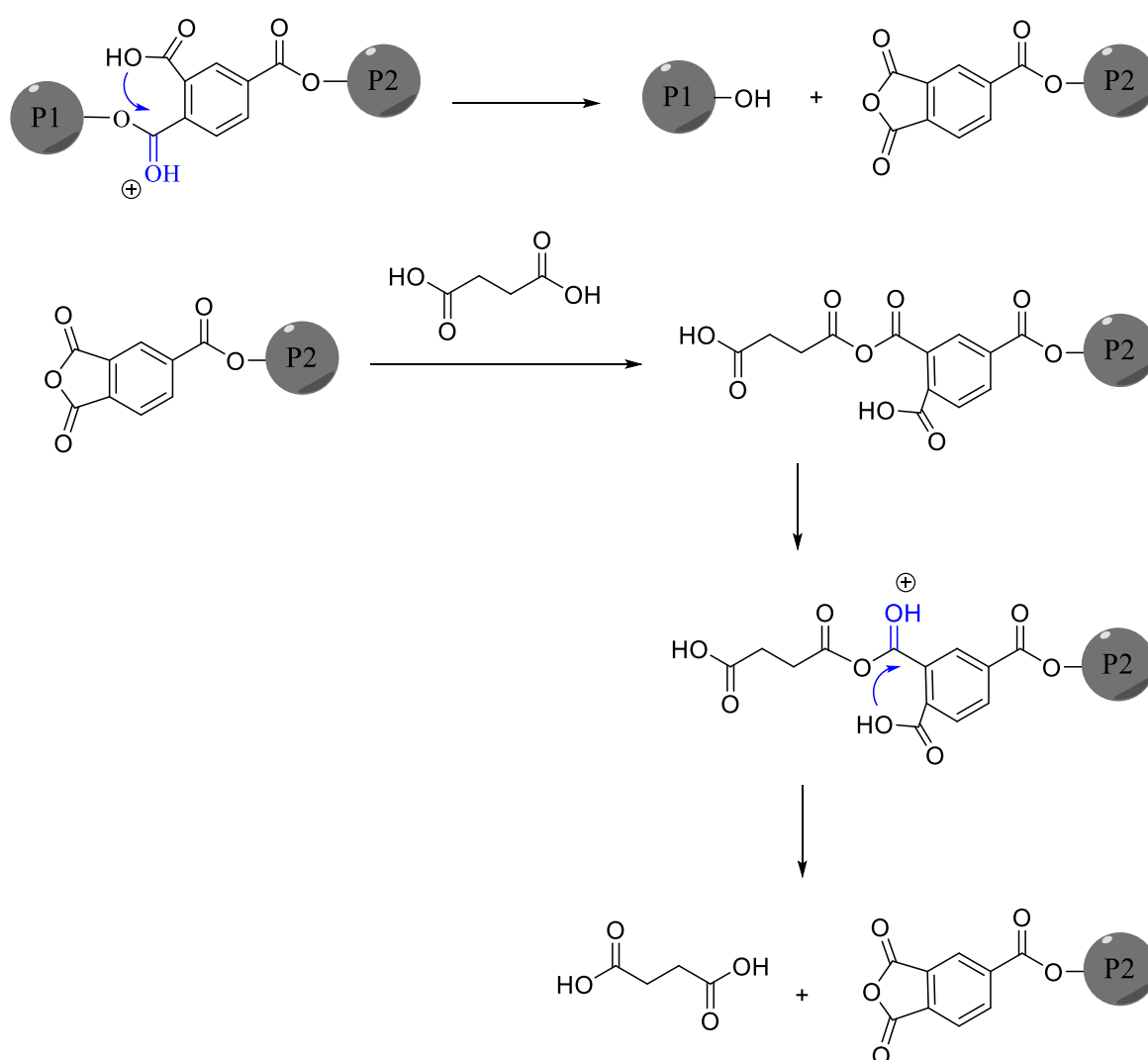


Figure 4.12. The ortho acid catalyst cleavage of mixed anhydride linkages.

As seen in Figure 4.13, different from PE-1 with SA reactions, there were several changes in the structure of the aromatic regions of PE-2. Peaks at 8.48 ppm, 8.39 ppm, and

7.84 ppm, which were assigned as H atoms of TMA groups in PE-2, were diminished. The integral of methyl groups belongs to neopentyl glycol, which was assumed to be connected to TMA (1.11 ppm), was also lowered. In other words, ortho-ester cleavage occurred between TMA and NPG units. The released hydroxyl terminated chains involved in direct or transesterification reactions.

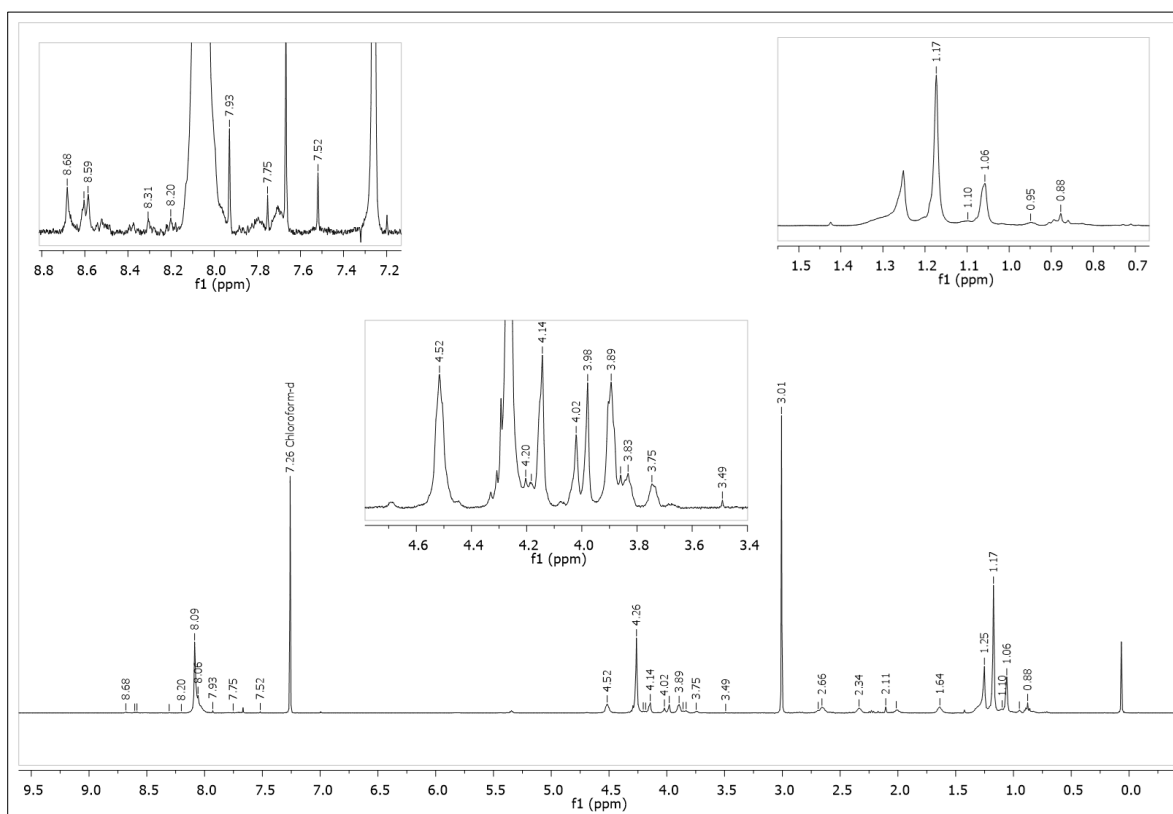


Figure 4.13.  $^1\text{H-NMR}$  analysis of PE2\_6 in  $\text{CDCl}_3$ .

In  $^1\text{H-NMR}$ , the shifting in methylene groups of SA which were connected to ester and anhydride units was observed at 2.53 ppm, and 2.48 ppm respectively. The possible connection pathways of SA into PE-2 were shown in Figure 4.14. The methylene groups of succinic anhydrides (2.88 ppm, singlet) was expected to be more deshielded than the methylene groups of succinic acid in  $^1\text{H-NMR}$  in Figure 4.15. According to NMR analysis of PE2\_SA reactions, beside of unreacted succinic anhydride monomer peaks, there were high amount of linear methylene groups (or can be thought as succinic acid units) observed at 2.48 ppm (singlet). The integral value of peaks at 2.88 ppm and 2.48 ppm were diminished

after anhydride test. The multiplet hydrogen peaks at 2.53 ppm with small integral value was attributed to esterified succinic units (option c in Figure 4.14).

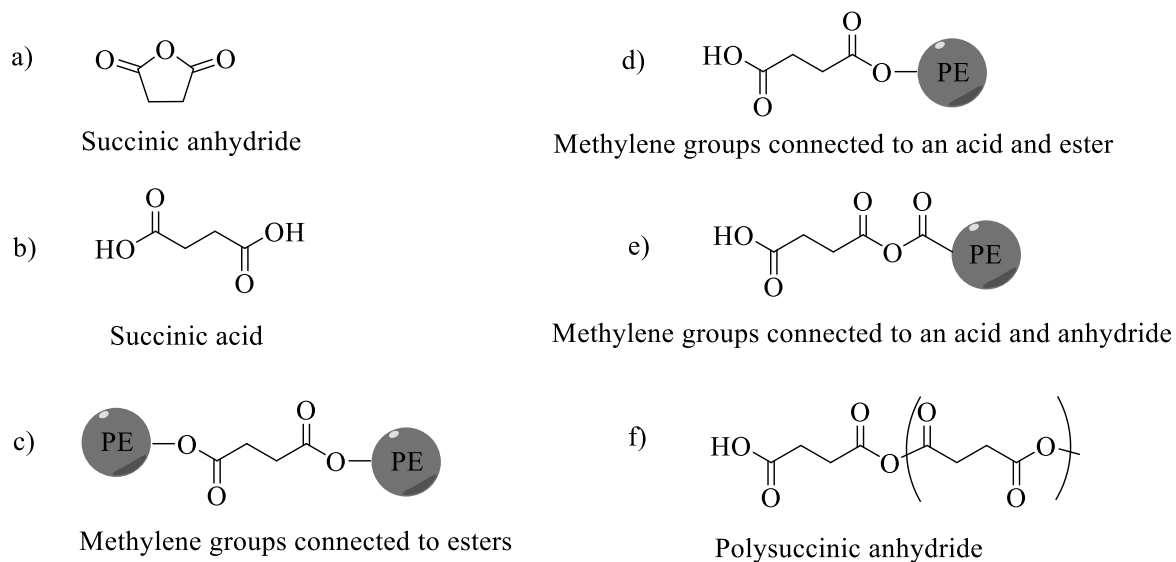


Figure 4.14. The possible connection pathways of SA to PE-2.

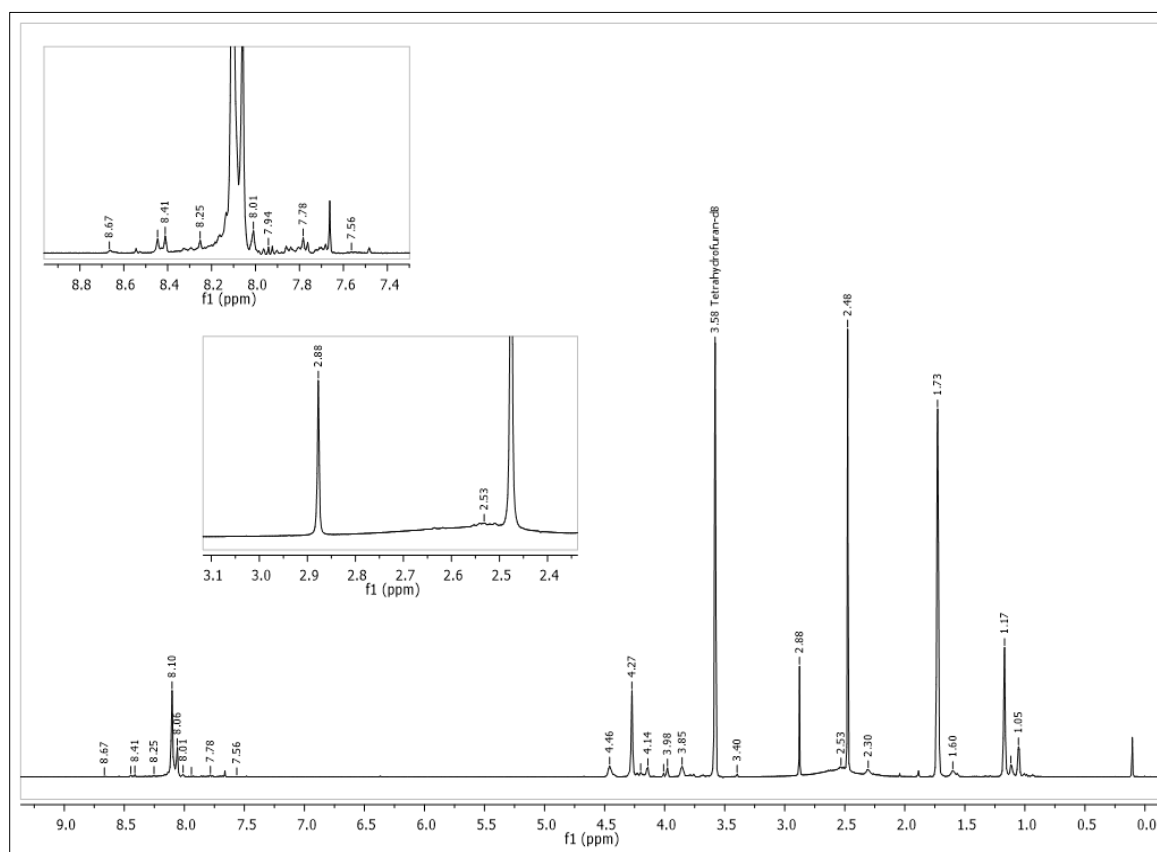


Figure 4.15.  $^1\text{H-NMR}$  analysis of PE2\_1 in  $d_8\text{-THF}$ .

The molecular weights of the resins were measured (Table 4.6).  $M_n$  's in these reactions did not increase much and were similar to that of the starting PE-2 ( $M_n$ : 3273 g/mol,  $M_w$ : 5337 g/mol, PDI: 1.63). After the anhydride test, as expected no significant decrease in  $M_n$  was observed. However, there was an increase in  $M_w$  and PDI. The acid value of PE-2 (71 mg KOH/g) is higher than PE-1 (31 mg KOH/g). It was thought that as the functionality of polyester increased (higher concentration of carboxylic end groups), the possibility of degradation of anhydride linkages also increased similar to the polyester degradation. It is well known that even in polyesters, which are far more stable than the anhydrides, a higher acid number, means a higher degradation rate. In addition to high acid number, high reaction temperature induced the degradation and decreased  $M_n$  of polyesters (PE2\_SA\_3 at 120-135°C,  $M_n$ : 3111 g/mol and PE2\_SA\_6 at 220°C,  $M_n$ : 2468 g/mol).

The molecular weight of samples before and after anhydride test is shown in Table 4.6. It can be deduced that poly(ester-anhydride) synthesis was not achieved by the reaction of SA with PE-2.

Table 4.6. The molecular weight obtained from PE2\_SA reactions.

Sample Name	$M_n$ (g/mol)	$M_w$ (g/mol)	PDI	$M_n$ (g/mol) Anhydride Test	$M_w$ (g/mol) Anhydride Test	PDI Anhydride Test
PE-2	3273	5337	1.64	-	-	-
PE2_R	3119	5958	1.91	-	-	-
PE2_Rv	2992	9429	3.15	-	-	-
PE2_SA_1	3238	9350	2.89	3341	7095	2.12
PE2_SA_2	3000	9120	3.04	3398	6814	2.01
PE2_SA_3	3111	9411	3.02	3264	5438	1.66
PE2_SA_4	3489	9541	2.73	-	-	-
PE2_SA_5	3359	9907	2.96	3441	5891	1.71
PE2_SA_6	2468	7372	2.99	2445	6889	2.82

The thermal behavior of resultant polyesters was analyzed by DSC using method 2.  $T_g$  of the synthesized polymers were lower than  $T_g$  of PE-2 (44°C). These low  $T_g$  values of final resins, in Table 4.7, may explained by plasticizing effect of both succinic acid, succinic anhydride, or mixed anhydride linkage formation in the polymer composition.

Table 4.7. Thermal behavior of PE2\_SA reactions in second heating run.

Sample Name	$T_g$ (°C)	$T_c$ (°C)	$T_m$ (°C)
PE2_R	39	-	-
PE2_R_v	45	-	-
PE2_SA_1	5	-	168
PE2_SA_2	-	55	96 and 157
PE2_SA_3	4	59	91 and 145
PE2_SA_4	29	-	174
PE2_SA_5	15	-	103 and 141
PE2_SA_6	18 and 42	-	171
PE-2	44	-	-

For the reactions of PE-2 with SA, unlike reactions of PE-1 with SA, a distinct crystallization temperature appeared during the cooling cycle at temperatures between 57 °C to 151 °C. For example, as seen in Figure 4.16,  $T_c$  was found at 100°C during cooling cycle (20.6 mJ/mg). A cold crystallization was observed after  $T_g$  at 59°C. Two melting temperatures were obtained in the first heating run and again in the second heating run at 91 °C and 147 °C with enthalpy of 7.39 mJ/mg and 17.3 mJ/mg.  $T_m$  of SA is 120°C whereas  $T_m$  of succinic acid is 190°C. It can be deduced that there were different crystallinities melted in polymer composition which may indicate the presence of polysuccinic anhydrides. The presence of the latter proposed structure needs further proof.

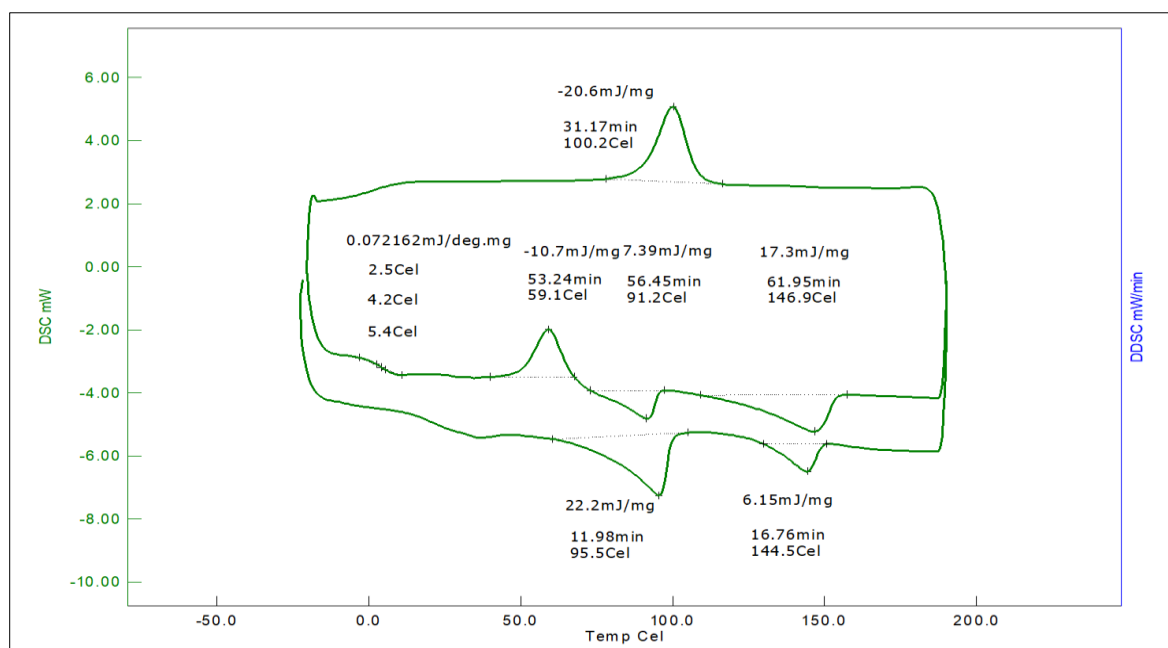


Figure 4.16. DSC analysis of PE2\_SA\_3.

Table 4.8. Acid values of synthesized samples.

Sample Name	Acid Value (mg KOH/g)	Sample Name	Acid Value (mg KOH/g)
PE2_R	43.9	PE2_SA_3	4.2
PE2_Rv	70.9	PE2_SA_4	8.0
PE2_SA_1	9.8	PE2_SA_5	5.9
PE2_SA_2	7.3	PE2_SA_6	10.7

The acid values of all resins were lower than the precursor PE-2 (Table 4.8). The decrease in the acid values of resins may be explained by the lowering of the concentration of carboxyl end groups by oligomerization of succinic anhydride monomers. However, during titration with KOH, those mixed anhydride linkages were expected to be broken and increase acid value. It is possible that the polymer was not entirely dissolved during analysis.

It was thought that the high acid values of PE-2 which also required higher amount of SA, affected the poly(ester-anhydride) syntheses adversely by introducing too much acidic character. The acid value are as follows; PE-2 is 71 mg KOH/g and PE-1 is 31 mg KOH/g. In conclusion, poly(ester-anhydride) synthesis was not achieved for the reactions of SA with PE-2. At high amount of SA and high acid values of PE-2, although some poly(ester-anhydride) formation could be formed they were most likely suppressed by the ortho acid catalyzed chain scission reactions.

#### 4.2.3. Synthesis of Poly(ester-anhydrides) from PE-1 and PMDA

PE-1 and PMDA were melt mixed to understand the effect of using a di-functional anhydride to the poly(ester-anhydride) synthesis. Depending on how anhydrides are opened, (acyclic anhydride formation, hydrolysis, alcoholysis, *etc.*) PMDA may introduce multifunctionality that may go up to four, therefore, some branching through anhydride linkages were expected. The aromatic ring of PMDA could introduce more rigid (aromatic-aromatic anhydride) linkages compared to succinic anhydride (aliphatic-aliphatic anhydride). Although the melting point of PMDA is 283 °C, it dissolved in the polymer melt above 180 °C. The appearance of the reactive mixture was opaque below 160 °C, which then became transparent at higher temperatures where some yellowing was observed.

New anhydride absorption peaks appeared at 1791 cm<sup>-1</sup> and 1854 cm<sup>-1</sup> in FT-IR. The PMDA starting material has the two characteristic symmetric and asymmetric anhydride

stretching vibrations at  $1764\text{ cm}^{-1}$  and  $1841\text{ cm}^{-1}$ . The new peaks in carbonyl stretching may come from several plausible structures which all contains different forms of anhydride linkages as illustrated in Figure 4.17. PMDA may connect to terminal group of the polyesters by an anhydride or ester linkage (option a and b). The new peaks may also arise from coupling of carboxyl terminated polyesters by mixed anhydride linkages (option c) or by both ester and anhydride linkages (option d).

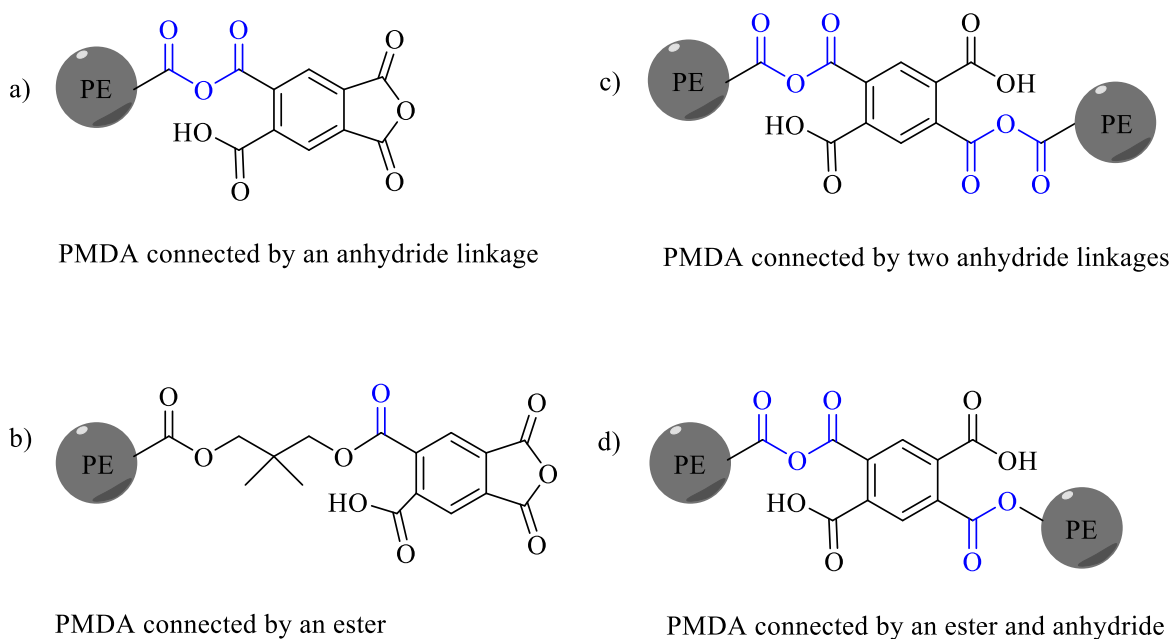


Figure 4.17. Possible connection pathways of PMDA to PE-1.

Apart from PE1\_PMDA\_1 (Table 4.9), final resins were not soluble in  $\text{CDCl}_3$  for NMR analysis (Figure 4.18). Results indicated that the residual  $-\text{CH}_2\text{-OH}$  end of polyester (3.41 ppm) was involved in esterification reaction. A small integral of a new methyl group connected to NPG was detected at 1.13 ppm. In other words, a small amount of PMDA was involved in esterification reaction with PE-1 and connected to NPG end group of PE-1 (option b in Figure 4.16). A new aromatic H atom peak was found out at 8.64 ppm which was estimated to belong to the protons of PMDA. However, H atoms of PMDA that are connected either to an ester, acid, or anhydride could not be distinguished.

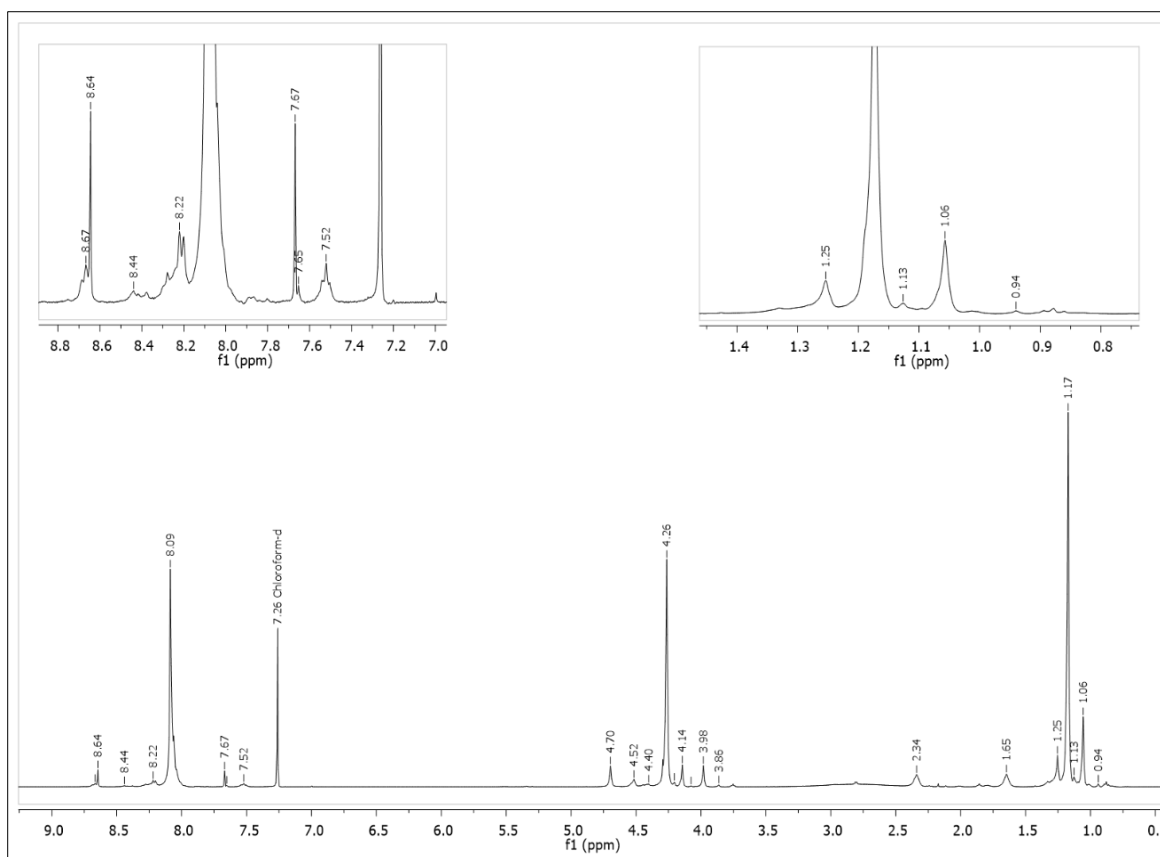


Figure 4.18.  $^1\text{H-NMR}$  analysis of PE1\_PMDA\_1 in  $\text{CDCl}_3$ .

In initial experiments (Table 4.9), the molecular weights of the final resins did not increase significantly except for PE1\_PMDA\_1 (from  $M_n=3831$  to  $5728\text{g/mol}$ ) whose molecular weight then dropped to  $4028\text{ g/mol}$  after the anhydride test. In addition, as expected, an increase in  $T_g$  was observed after the anhydride formation (PE-1:  $51^\circ\text{C}$ , PE1\_PMDA\_1:  $55^\circ\text{C}$ ), but interestingly no decrease in  $T_g$  was detected after the anhydride test ( $56^\circ\text{C}$ ). We believe that this is due to the reactions (crosslinking) of residual PMDA left in the polymer sample. This experiment was run in a temperature range of  $140\text{-}180^\circ\text{C}$ . Therefore, additional experiments were carried out to optimize the anhydride formation in a temperature range of  $160^\circ\text{C}$  to  $180^\circ\text{C}$ .

Table 4.9. The molecular weight obtained from PE1\_PMDA reactions.

Sample Name	$M_n$ (g/mol)	$M_w$ (g/mol)	PDI	$M_n$ (g/mol) Anhydride Test	$M_w$ (g/mol) Anhydride Test	PDI Anhydride Test
PE-1	3831	11643	3.04	-	-	-
PE1_PMDA_1	5728	13808	2.41	4028	13750	3.40
PE1_PMDA_2	4378	15543	3.55	-	-	-
PE1_PMDA_2_1	3421	10249	2.99	-	-	-
PE1_PMDA_3	4192	13420	3.20	4613	16752	3.63
PE1_PMDA_4	3158	11330	3.58	3197	12603	3.94
PE1_PMDA_5	3833	13015	3.39	-	-	-
PE1_PMDA_6	3132	12553	4.01	3010	22769	7.56
PE1_PMDA_7	2250	9218	4.10	-	-	-
PE1_PMDA_8	4031	12731	3.15	3756	13611	3.62

The molecular weight observed for PE1\_PMDA\_4/6/7 experiments were lower than PE-1 ( $M_n$ : 3831 g/mol,  $M_w$ : 11643 g/mol, PDI= 3.04), but  $T_g$  of these resins were higher than PE-1. The DSC analysis was done with method 4 (Table 4.10). In the first heating cycles of resins, the glass transition temperature of samples was lower than 51 °C and the melting temperatures were around 205-212 °C. There was no crystalline region detected in the second heating runs. It was assumed that  $T_g$  increase in the second heating run, was the result of the crosslinking reactions induced by the aromatic anhydrides of residual PMDA with PE-1. For example, as the weight percent of PMDA was increased from 0.8% (PE1\_PMDA8) to 11% (PE1\_PMDA\_4),  $T_g$  increased from 54 °C to 59°C (Table 4.10).

Table 4.10. Thermal behavior of PE1\_PMDA reactions in second heating run.

Sample Name	PMDA w%	$T_g$ (°C)
PE1_PMDA_1	11	56
PE1_PMDA_2	11	59
PE1_PMDA_2_1	11	58
PE1_PMDA_3	20	56
PE1_PMDA_4	11	59
PE1_PMDA_5	11	58
PE1_PMDA_6	2	55
PE1_PMDA_7	5	59
PE1_PMDA_8	0.8	54
PE-1	-	51

It was found that results from the initial experiments (Table 4.9) indicated mostly a molecular weight decrease rather than an increase. To check whether or not this was a time dependent result, a control experiment was carried out where during the reaction (PE1\_PMDA\_2), a sample was taken after 1.5 hours, and the reaction was proceeded for an extra 3.5 hours. Indeed, the molecular weight of the resin decreased from 4378 to 3421 g/mol as expected.

In addition, the polymers obtained had higher acid values than the starting polyester (Table 4.11). This could be the result of the polyester hydrolysis, which produces carboxylic acid end group or residual PMDA left as anhydride or the corresponding multi-carboxylic acid. To check this, the mole ratio of PMDA was changed, however, no direct relationship between molecular weight and PMDA content could be established. The increase or decrease in acid values were inconsistent. Further experiments to elucidate the mechanism which led to high acid numbers were then abandoned. The low solubility of the unreacted PMDA and its acid equivalent, rendered both the GPC analysis of these resins and the acid value measurements extremely difficult and not reliable. The limited solubility of PMDA, rendered the purification of these samples extremely difficult and non-reproducible, in general.

Table 4.11. Acid values of synthesized samples.

Sample Name	Acid Value (mgKOH/g)	Sample Name	Acid Value (mgKOH/g)
PE1_PMDA_1	22.0	PE1_PMDA_5	92.1
PE1_PMDA_2	96.9	PE1_PMDA_6	46.0
PE1_PMDA_2_1	13.9	PE1_PMDA_7	59.3
PE1_PMDA_3	24.6	PE1_PMDA_8	48.5
PE1_PMDA_4	14.0	PE-1	31

To conclude, although poly(ester-anhydride) synthesis was achieved at first, the optimization process was not successful. It needs more work to optimize parameters, *e.g.* working temperatures, PMDA ratio and reaction time. Since the project was targeting an industrial process, the results were found not robust enough to carry on such pathway for the moment.

#### 4.2.4. Synthesis of Poly(ester-anhydrides) from PE-2 and PMDA

Two functional PMDA and four functional PE-2 were melt mixed. Due to the higher amount of functionality of PE-2, compared to PE-1 which was difunctional, a more branched polymer network was expected to be formed by either the targeted anhydride linkages or possible transesterification side reactions. PE2\_PMDA\_1 was conducted at low temperatures (120-160°C) at first. The color of final resin was white. It seemed like PMDA did not efficiently dissolve in PE-2. Thus, the temperature was increased to 220°C (PE2\_PMDA\_2) to increase the solubility. Indeed, the polymer mixture had a more homogenous appearance, but the color of the polymer melt changed to brown. To limit the color change but increase the solubility of PMDA, the experiment, PE2\_PMDA\_3 was conducted at higher temperature (260°C) but shorter reaction time.

The resulting polymers were analyzed by FT-IR and NMR. In FT-IR as previously mentioned, there were new peaks that belonged to the symmetric and asymmetric stretching of anhydride carbonyls at 1775  $\text{cm}^{-1}$  and 1853  $\text{cm}^{-1}$  (Figure 4.19). The source of these new anhydride peaks can be explained as described in Figure 4.17.

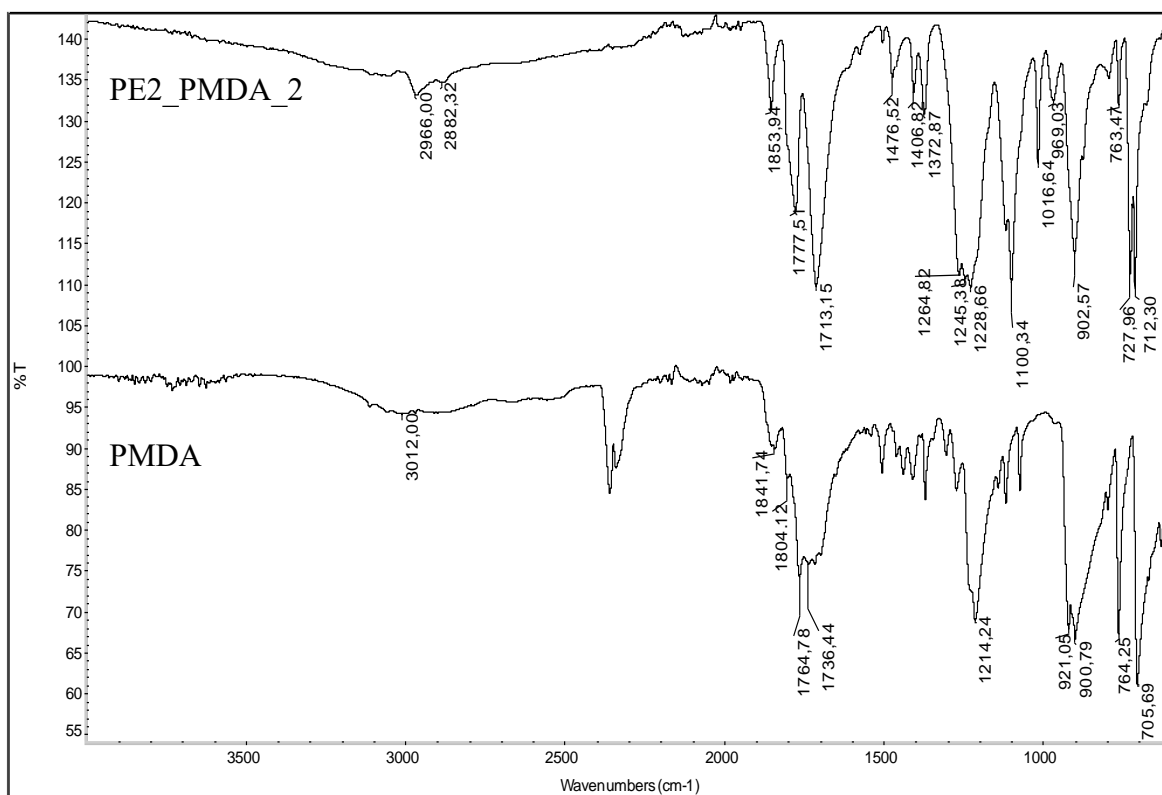


Figure 4.19. FT-IR spectrum of PE2\_PMDA\_2.

There was no significant change in the polymer backbone when compared to PE-2 (Figure 4.20). The integral peaks between 1.17 and 1.06 ppm were attributed to methyl groups of NPG. After the reaction with PMDA, integral value of 1.11 ppm was increased (from 36.4 to 66.1). Therefore, it can be said that more NPG were connected to aromatic groups by direct or transesterification with PMDA. Two peaks at 8.31 ppm and 8.01 ppm were attributed to H atoms of PMDA.

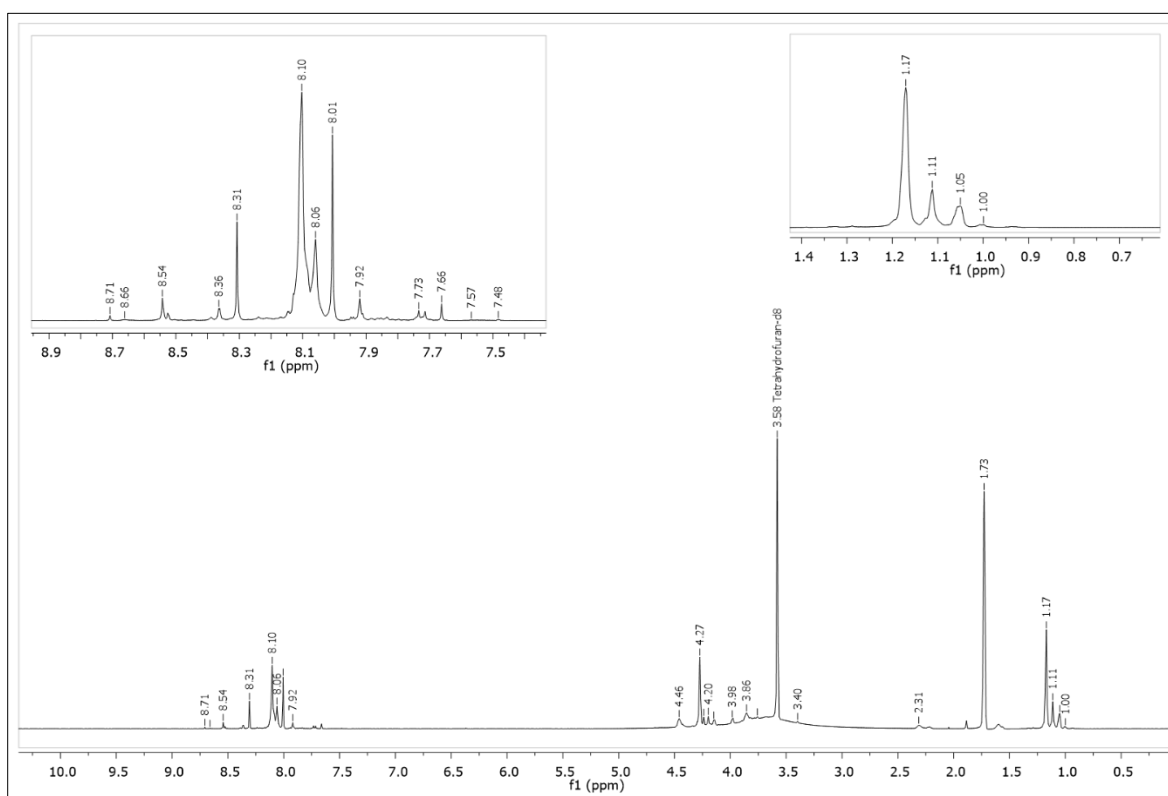


Figure 4.20.  $^1\text{H}$ -NMR analysis of PE2\_PMDA\_2 in  $\text{d}_8$ -THF.

For PE2\_PMDA1/2, GPC analysis of the samples could not be reported due to the high content of PMDA which is harmful to the GPC columns. Also, since GPC is calibrated according to linear polystyrene chains, there would be uncertainty in the analyses of the possibly branched polymers. Although there is a small increase in molecular weight of PE2\_PMDA\_3, no decrease after the anhydride test was observed (Table 4.12).

Table 4.12. The molecular weight of PE2\_PMDA\_3 before and after anhydride test.

Sample Name	$M_n$ (g/mol)	$M_w$ (g/mol)	PDI
PE2	3273	5337	1.64
PE2_PMDA_3	3462	7261	2.10
PE2_PMDA_3A	4040	9941	2.46

The DSC analysis was done with method 3 (Table 4.13). A small increase in  $T_g$  was detected most probably due to crosslinking of four functional PE-2 with PMDA. Two different  $T_g$ 's were observed in samples containing high amount of PMDA.  $T_m$  was observed only in the first heating cycle at 220 °C. There was no crystallization temperature at cooling cycle and no melting temperature in the second heating cycle. Although the PMDA content (0.8 %w) was lower in PE2\_PMDA\_3,  $T_g$  increased to 48°C. Since poly(ester-anhydride) formation was not detected after anhydride test, the increase in  $T_g$  may attributed to crosslinking of PMDA during the DSC run.

Table 4.13. Acid values and thermal properties of second heating cycle of PE2\_PMDA reactions.

Sample Name	PMDA w-%	$T_g$ (°C)	Acid Value (mg KOH/g)
PE2_PMDA_1	35	42 and 53	8.6
PE2_PMDA_2	35	45 and 53	10.7
PE2_PMDA_3	0,8	48	86.0
PE-2	-	44	71

As a result, poly(ester-anhydride) synthesis was not achieved by increasing functionality of polyester and the anhydride monomer. We believe that the limited solubility of PMDA in PE-2 prevents good mixing of reactants and prevent any reaction.

### 4.3. Synthesis of Poly(ester-anhydrides) Using the Synthesized PE-3 and SA

In this study, PE-3 was first synthesized, with an identical monomer composition to PE-1 and then reacted with SA to obtain the corresponding poly(ester-anhydrides).

#### 4.3.1. Synthesis of PE-3 in Melt Polymerization

The aim was to synthesize a polyester that had a similar monomer composition to PE-1. It is well known that, to synthesize an acid terminated polyester, one should set the mol ratio of diacids higher than diols. However, polyester synthesis is a long process and occurs at high temperatures. Alcohols have low boiling points and are partially lost from the reaction medium during the synthesis. Therefore, diols were used in excess. In addition, although the melting point of TPA and IPA were 300 °C and 341 °C respectively, these aromatic acids were soluble in the reaction composition at temperatures around 250 °C.

Aromatic acids have low solubility compared to aliphatic monomers. Therefore, as the mole ratio of TPA increased, for PE3\_3 compared to PE3\_2, reaction proceeded four more hours at high temperatures where an increase in yellowing was observed (in Section 3.3.1, Table 3.5).

DSC analysis were done according to the method 3 (Table 4.15). Depending on molecular weight of synthesized polyesters, different  $T_g$  values were obtained. As seen in Table 4.14, according to the GPC analysis, the  $M_n$  of synthesized polyesters were similar to the commercial PE-1 but  $M_w$  's and thus PDI 's were lower.

Table 4.14. Molecular weights, thermal properties, and acid values of synthesized polyesters.

Sample Name	$M_n$ (g/mol)	$M_w$ (g/mol)	PDI	Acid Value (mg KOH/g)	$T_g$ (°C)
PE3_1	4406	7393	1.68	31.4	48
PE3_2	4184	8074	1.93	30.5	49
PE3_3	3651	6462	1.77	34.1	47
PE3_4	4841	8296	1.71	31.8	45
PE3_5	5224	9163	1.75	21.9	50
PE-1	3831	11643	3.04	31.0	51

The appearances of polyesters were colorless and transparent. Their acid value ranged between 22 mg KOH/g and 34 mg KOH/g. As expected, the higher the acid value, the lower the molecular weight of the polyester was.

Polymers were soluble in  $CDCl_3$ . There was no significant difference in their  $^1H$ -NMR analyses (Figure 4.21). The detailed assignment of the peaks was mentioned in Section

4.1. Thus, the polyester synthesis was achieved successfully. Although excess diol used for polyester synthesis, the integral value of hydroxyl bearing proton peaks were low.

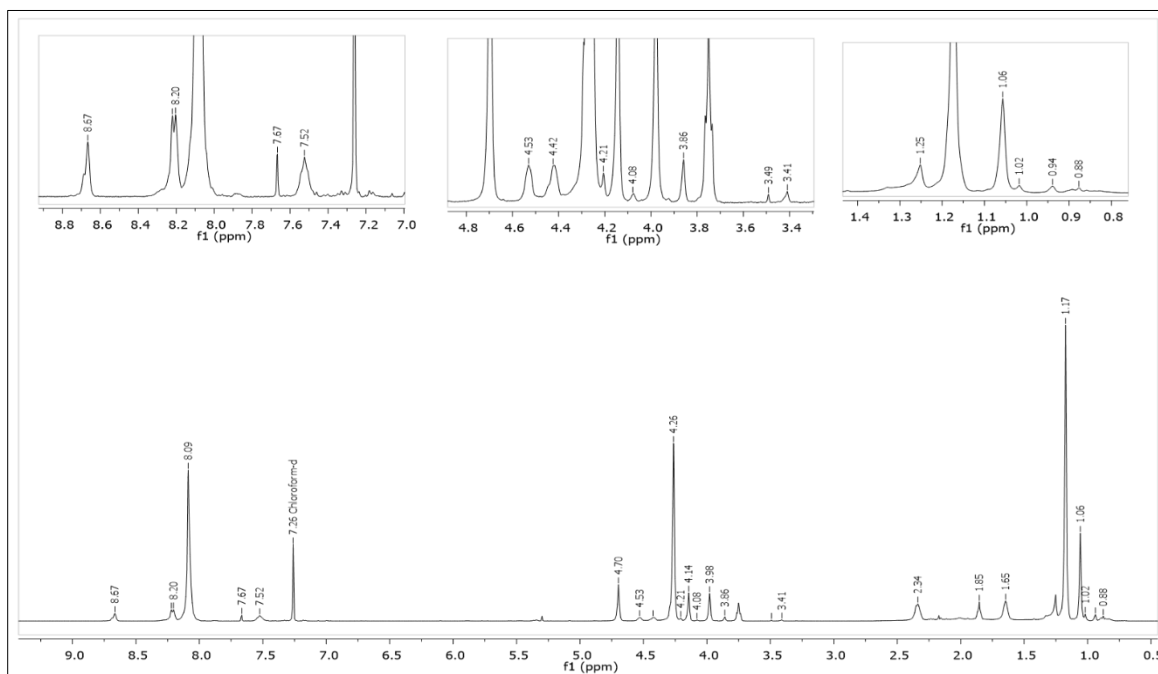


Figure 4.21.  $^1\text{H-NMR}$  analysis of PE<sub>3\_4</sub> in  $\text{CDCl}_3$ .

#### 4.3.2. Synthesis of Poly(ester-anhydrides) based on PE-3 and SA

Among the polyester synthesized above only PE<sub>3\_4</sub> (4.27 g,  $M_n$ : 4841 g/mol,  $M_w$ : 8296 g/mol, PDI: 1.71) was reacted with SA (0.35 g). The polymers were light yellow colored, and transparent. A shifting in the carbonyl stretching was observed at  $1786\text{ cm}^{-1}$  in FT-IR, in Figure 4.22. In addition, there were no residual succinic acid absorption peaks.

The obtained polymers were soluble in  $\text{CDCl}_3$  and there was no significant change in repeating units in  $^1\text{H-NMR}$  analysis as seen in Figure 4.23. Similar to PE-1 and SA reactions, there was unreacted SA remained in polymer composition as evidenced by the peak at 3.0 ppm.

It can be said that the difference between the reaction of PE<sub>3\_SA</sub> and its commercially available counterpart PE<sub>1\_SA</sub> was the polymer compositions and weight percent of SA. In this case, the weight percent of SA (7.5%) was lower than reaction of PE<sub>1\_SA</sub> (10%). This may indicate that as the weight percent of SA decreased in the reaction medium, the possibility of the formation of mixed anhydride linkages also decreased. The

location of these anhydride linkages may be found between polyester chains and in end groups as illustrated in Section 4.2.1, Figure 4.6.

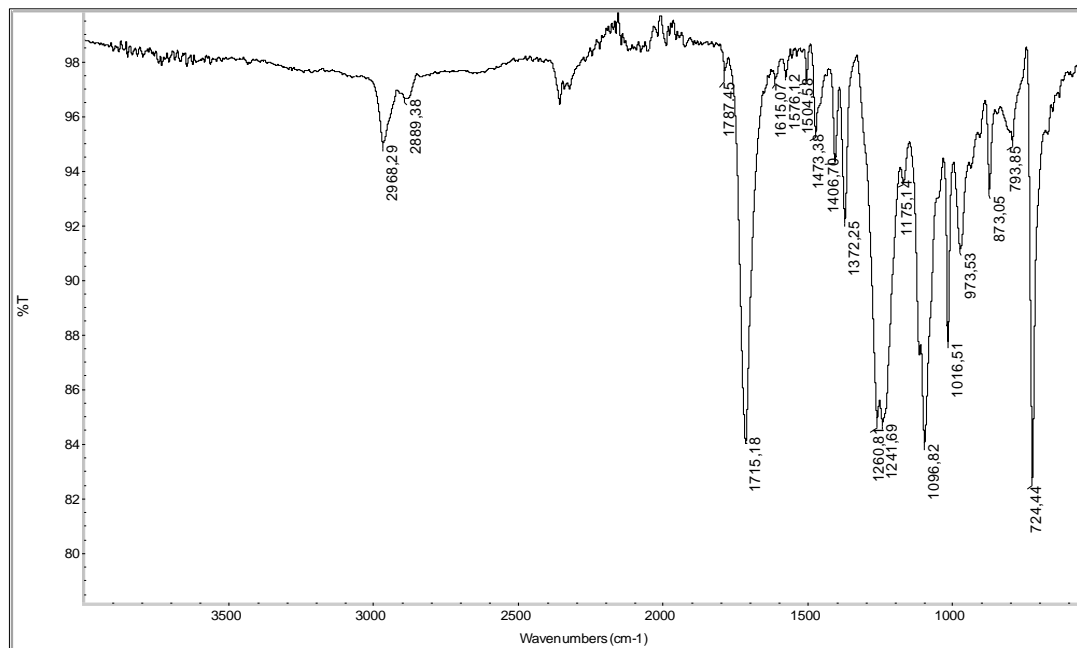


Figure 4.22. FT-IR spectrum of PE3\_4\_SA1.

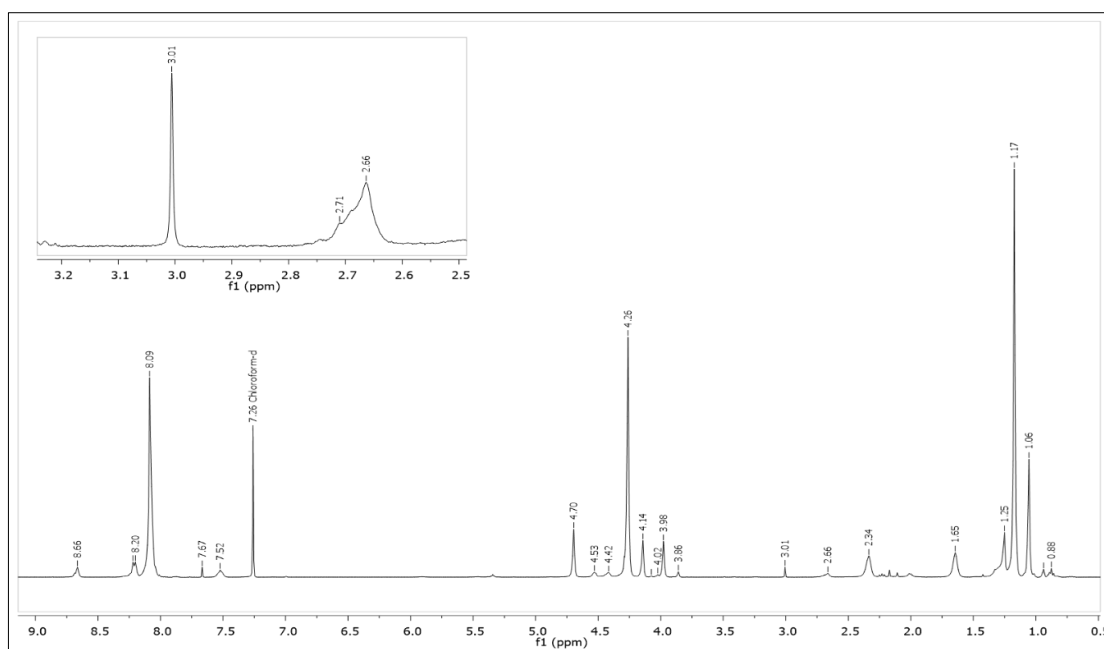


Figure 4.23.  $^1\text{H-NMR}$  analysis of PE3\_4\_SA1 in  $\text{CDCl}_3$ .

The molecular weight of both resins was lowered after the anhydride test (Table 4.15). Thus, accordingly the poly(ester-anhydride) synthesis was achieved. For the experiment PE3\_4\_SA1, although an increase in  $M_n$  was observed the  $M_w$  did not change much. This may indicate a higher reaction between SA and the more mobile shorter chains in the polymer melt.

Table 4.15. The molecular weight obtained from PE3\_SA reactions.

Sample Name	$M_n$ (g/mol)	$M_w$ (g/mol)	PDI	$M_n$ (g/mol) Anhydride Test	$M_n$ (g/mol) Anhydride Test	PDI Anhydride Test
PE3_4	4841	8296	1.71	-	-	-
PE3_4_SA1	5675	8493	1.49	4711	9461	2.00
PE3_4_SA2	4677	6977	1.49	4331	7548	1.74

Both polyesters had  $T_g$  's around 43 °C, which is slightly lower than the  $T_g$  of PE3\_4 (45 °C) but higher than that of the polymers obtained with the commercial PE-1 (Section 4.1). In addition, contrary to the reactions of commercial PE-1 (Section 4.1),  $T_c$  and  $T_m$  were not observed (Table 4.16). These results may indicate that there was no significant succinic acid or free polysuccinic anhydride whose presence can be seen by additional  $T_c/T_m$  peaks and significant lowering of  $T_g$ .

Table 4.16. Thermal properties and acid values of PE3\_4\_SA reactions.

Sample Name	$T_g$ (°C)	Acid Value (mg KOH/g)
PE3_4_SA1	43	53.3
PE3_4_SA2	43	51.1

In addition, PE3\_4\_SA1 was stored at room temperature. A decrease in the molecular weight of PE3\_4\_SA1 was observed after 2-3 weeks (from  $M_n$  5.675 g/mol to  $M_n$  :4.919 g/mol,). This means the stability of anhydride linkages between polyester chains was lower than expected. To conclude, side product formation was not observed after the reaction of PE3\_4 with SA. Poly(ester anhydride) synthesis was achieved where no side product formation was observed. However, initial results indicate low stability of poly(ester-anhydrides).

#### 4.4. Rheological Behaviors of Polymers

Several temperature sweep tests were done to understand the general properties of the polymers. The aim was to compare the rheological behavior of the polymers obtained from the reaction of cyclic anhydrides with commercial polyesters (PE-1 and PE-2) and synthesized polymers (PE-3). Experiments were carried out with unpurified samples, since no purification was envisioned for the industrial scale synthesis. Also, as will be discussed later, the data obtained from such measurements confirmed some of the findings discussed in previous sections. Therefore, it is important to mention that sublimation of both succinic anhydride or pyromellitic dianhydride was observed during the rheological analyses of all samples.

Loss modulus ( $G''$ ) and storage modulus ( $G'$ ) are main rheological parameters of analyses where the former represents the elasticity and the latter viscosity. The difference between loss modulus and storage modulus, informs about the physical state of the materials.

For example, if storage modulus is larger than loss modulus, this means the polymer is solid. For a typical amorphous polymer, as seen in Figure 4.24, the temperature where loss modulus is increasing is accepted as  $T_g$ , in which transition from glassy to rubbery phase occurs. The melting of polymers begins where  $G' = G''$ . As temperature increases above the crossover of loss modulus and storage modulus, both  $G'$  and  $G''$  decreases and transition occurs eventually into the melt state. Crosslink polymers remains in rubbery phase until thermal decomposition temperature is reached.

Temperature sweep test of the synthesized polyesters (Figure 4.24) was similar to PE-1. A comparison can be done between the newly synthesized polyesters. The hardness of resins was lowered in the order of PE3\_5, PE3\_4, and PE3\_3. The viscosity of PE3\_3 was the lowest in the molten state. The higher the molecular weight, the higher the hardness of the polyester was before and after  $T_g$ . As a result, the similarity in thermal and rheological behavior of these polyesters proved again that the targeted polyester synthesis was achieved successfully.

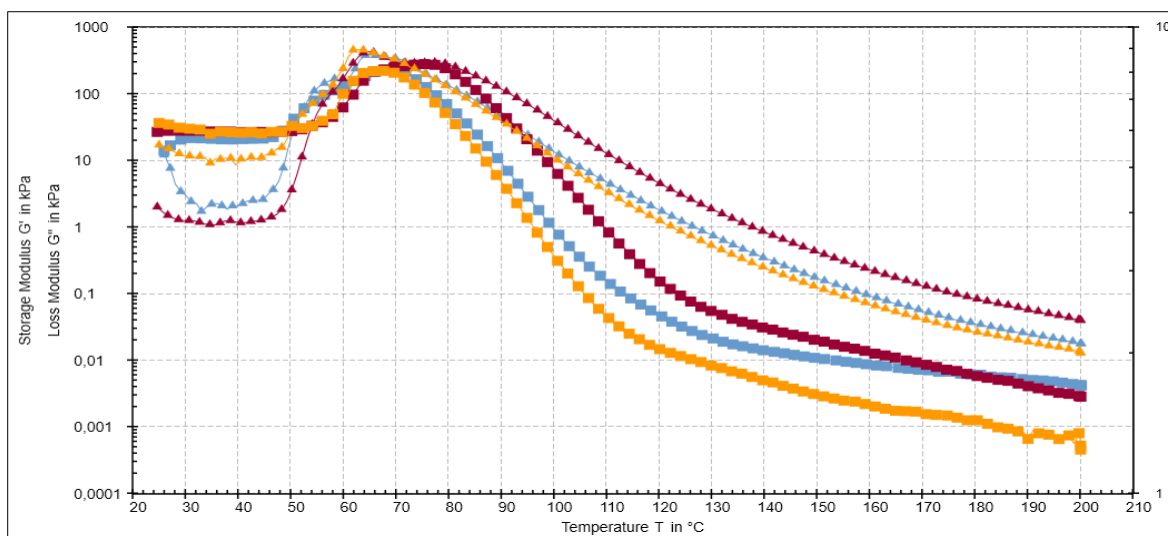


Figure 4.24. Temperature sweep test of PE3\_3 (orange), PE3\_4 (blue), and PE3\_5 (claret red).

As seen in Figure 4.25, in the glassy state the difference between storage modulus and loss modulus, which means hardness, of the polyester (PE3\_4) decreased after reaction with SA. Note that there is a slight decrease in  $T_g$  values in reactions with SA (Section 4.3.2, Table 4.16), which confirms the previous DSC results. After the crossover, polymers in the molten phase. The viscosity of polyester was higher than PE3\_SA resins in the molten state since SA works as plasticizer for the latter.

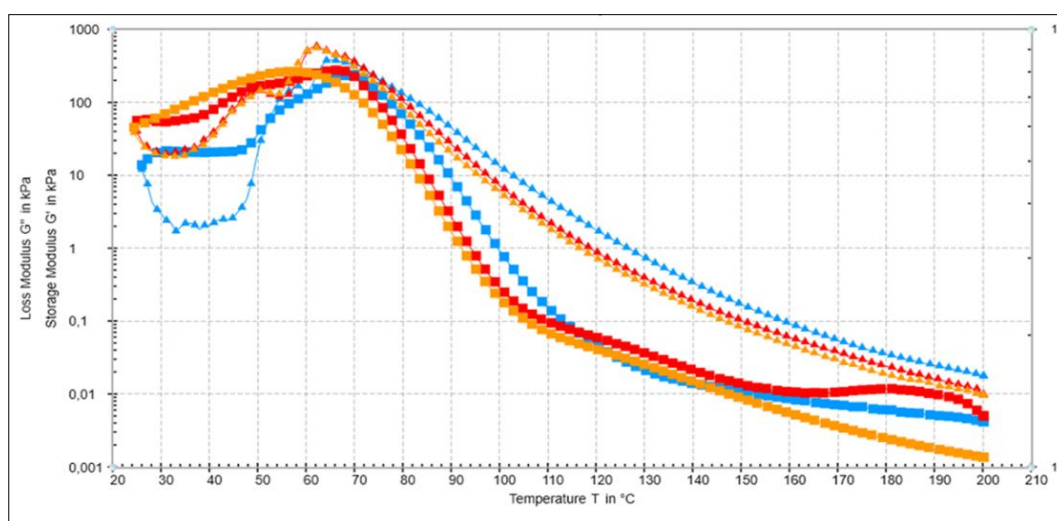


Figure 4.25. Temperature sweep test of PE3\_4 (blue) compared to PE3\_SA1 (red) and PE3\_4\_SA2 (orange).

In Figure 4.26, the temperature sweep test of PE-2 with SA and PMDA are compared. At low temperatures in the glassy state, hardness of PE2\_PMDA\_2 was higher. This result is in accordance with the DSC results where the latter had the highest  $T_g$  (in Section 4.2.4, Table 4.13). After  $T_g$ , as the temperature was increased, PE-2 and PE2\_SA\_6 continued to be in molten state. However, after 110°C, physical state of PE2\_PMDA\_2 was changed from liquid to solid as indicated by the higher storage modulus of PE2\_PMDA\_6 compared to the loss modulus. In other words, crosslinking was observed between unreacted PMDA and PE-2 after a certain temperature. It is most likely that as the functionality increases, the amount of crosslinking between multifunctional polyesters increases. Also, after the analysis, a phase separation was observed in this sample.

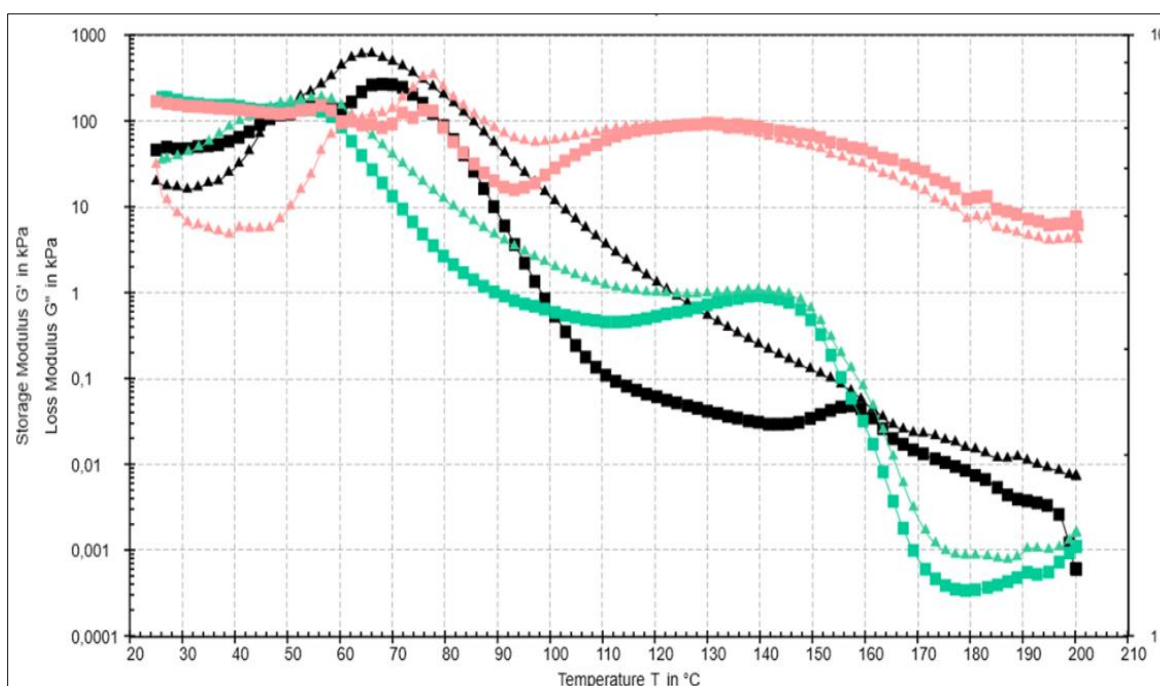


Figure 4.26. Temperature sweep tests of PE-2 (black), PE2\_SA\_6 (green), and PE2\_PMDA\_2 (pink).

The difference between storage modulus and loss modulus was decreased after the reaction with cyclic anhydrides. The storage modulus of PE2\_SA\_6 began to increase at lower temperature than PE-2. Rubbery plateau appeared after melting of both PE2\_SA\_6 and PE2\_PMDA\_2. In this region, the storage modulus is proportional to crosslinks per unit volume.

As a result, the rheological behavior of synthesized and commercial polyesters was compared in 20 °C to 200 °C temperature range. The temperature sweep test of poly(ester-anhydrides), obtained from the reaction of commercial and synthesized polyesters and SA, had similar behaviors in glassy and molten phase. As the functionality of polyester was increased from two (PE-1) to four (PE-2), a rubbery plateau was generated in temperature sweep test. The aromatic units in the polymer chain brings hardness and rigidity to composition by crosslinking. Therefore, as the PMDA content was increased, the viscosity of polymers increased.

## 5. CONCLUSION

The synthesis of polyesters and poly(ester-anhydrides) were carried out by melt polymerization. The effect of functionality of both cyclic anhydrides and carboxyl terminated polyesters on poly(ester-anhydride) synthesis was investigated. The possible connection scenarios of SA and PMDA on both di- and multi-functional polyesters were studied.

Poly(ester-anhydride) synthesis was achieved by the reaction of aliphatic SA with both difunctional commercial and newly synthesized polyesters. However, the stability of the anhydride linkages was lower than expected. If PE-1 and PE-2 are compared, in other words, as the functionality of polyester was increased, it is estimated that anhydride linkage formation and scission occurred simultaneously.

In contrast to the reactions of SA with polyesters,  $T_g$  of final resins was increased by the reaction of PMDA with commercial polyesters. However, poly(ester-anhydride) synthesis was not detected after anhydride test. According to rheology analysis, as the functionality of reactants were increased, crosslinking and thus viscosity increase was observed.

## REFERENCES

1. Rogers, M. E., and E. L. Timothy, *Synthetic Methods in Step-Growth Polymers*, John Wiley & Sons, Inc., New Jersey, NJ, USA, 2003.
2. Jones, F. N., M. E. Nichols, S.P. Pappas, *Organic coatings : Science and Technology, Fourth Edition*, John Wiley & Sons, Inc., New Jersey, NJ, USA, 2017.
3. Edlund, U., A. C. Albertsson, “Polyesters Based on Diacid Monomers”, *Advanced Drug Delivery Reviews*, Vol. 55, pp. 585-609, 2003.
4. Parcheta, P., J. Datta, “Structure-Rheology Relationship of Fully Bio-Based Linear Polyester Polyols for Polyurethanes - Synthesis and Investigation”, *Polym. Test.*, Vol. 67, pp. 110-121, 2018,
5. Edlund, U., A. C. Albertsson, “Degradable Polymer Microspheres for Controlled Drug Delivery”, *Adv. Polym. Sci.*, Vol. 157, pp. 67–112, 2002.
6. Peters, E. N., *Applied Plastics Engineering Handbook*, Second Edition, Elsevier, Amsterdam, The Netherlands, 2016.
7. Wang, L., Y. Wang, F. Zhang, Y. Bai, and L. Ding, “Syntheses and Properties of the PET-co-PEA Copolyester”, *J. Appl. Polym. Sci.*, Vol. 134, No. 36, pp. 1–9, 2017.
8. Lukey, C.A., *Encyclopedia of Materials: Science and Technology*, Elsevier, 2001.
9. Ni, H., J. L. Daum, and M. D. Soucek, “Cycloaliphatic polyester based high solids polyurethane coatings: I. The effect of difunctional alcohols”, *Journal of Coatings Technology*, Vol. 74, pp. 49–56, 2002.
10. Li, Y., L. Liu, Y. Gu, J. Xie, J. Zhang, and, J. Qu, “Improve Surface Levelling of Powder Coating with Semi-Crystalline Polyester Resin”, *Prog. Org. Coatings*, Vol. 99, pp. 191–196, 2016.
11. Ding, L., L. Xie, J. Cao, and Y. Bai, “Crystallization Behavior of Poly(ethylene terephthalate-co-neopentyl terephthalate-co-ethylene isophthalate-co-neopentyl

- isophthalate) Copolyester and Its Application in Laminated Tin-Free Steel”, *J. Appl. Polym. Sci.*, Vol. 132, No. 31, pp. 1–8, 2015.
12. Scott, G., *Degradable Polymers: Principles and Applications*, Springer, New York, NY, USA, 2002.
  13. Korhonen, H., R. A. Hakala, A. O. Helminen, and J. V. Seppälä, “Synthesis and Hydrolysis Behaviour of Poly(ester anhydrides) from Polylactone Precursors Containing Alkenyl Moieties”, *Macromol. Biosci.*, Vol. 6, No. 7, pp. 496–505, 2006.
  14. Jiang, H. L., G. P. Tang, L. H. Weng, and K. J. Zhu, “In vivo Degradation and Biocompatibility of A New Class of Alternate Poly(ester-anhydrides) Based on Aliphatic and Aromatic Diacids”, *J. Biomater. Sci. Polym. Ed.*, Vol. 12, No. 12, pp. 1281–1292, 2001.
  15. Ramis, X., A. Cadenato, J. M. Morancho, and J. M. Salla, “Curing of A Thermosetting Powder Coating by Means of DMTA, TMA and DSC”, *Polymer (Guildf.)*, Vol. 44, No. 7, pp. 2067–2079, 2003.
  16. Rudin, A. and P. Choi, *The Elements of Polymer Science & Engineering*, Elsevier, 2013.
  17. Ebewele, R. O., *Polymer Science and Technology*, CRC Press., New York, NY, USA, 2000.
  18. Spyrou, E., *Powder Coatings Chemistry and Technology*, Vincentz Network, Hanover, Germany, 2012.
  19. Odian, G., *Principles of Polymerization*, John Wiley&Sons, Inc., New Jersey, NJ, USA, 2004.
  20. Mafi, R., S. M. Mirabedini, M. M. Attar, and S. Moradian, “Cure Characterization of Epoxy and Polyester Clear Powder Coatings Using Differential Scanning Calorimetry (DSC) and Dynamic Mechanical Thermal Analysis (DMTA)”, *Prog. Org. Coatings*, Vol. 54, No. 3, pp. 164–169, 2005.
  21. Shrivastava, A., *Introduction to Plastics Engineering*, Elsevier, 2018.

22. Umoren, S. A. and M. M. Solomon, "Polymer Molecular Weight Determination", *Polym. Sci. Res. Adv. Pract. Appl. Educ. Asp.*, Vol. 1, pp. 412–419, 2016.
23. Rudin, A., *The Elements of Polymer Science & Engineering*, Elsevier, 1999.
24. Minko, S., and D. Hall, *Introduction to Polymer Science and Chemistry A Problem Solving Approach*, CRC Press, 2011.
25. Izunobi, J. U. and C. L. Higginbotham, "Polymer Molecular Weight Analysis by <sup>1</sup>H NMR Spectroscopy", *J. Chem. Educ.*, Vol. 88, No. 8, pp. 1098–1104, 2011.
26. Antheunis, H., J. C. Van Der Meer, M. De Geus, , A. Heise, and C. E. Koning, "Autocatalytic Equation Describing the Change in Molecular Weight During Hydrolytic Degradation of Aliphatic Polyesters", *Biomacromolecules*, Vol. 11, No. 4, pp. 1118–1124, 2010.
27. Dogan, E. and A. E. Acar, "The Use of Anhydride Linkages to Increase The Glass Transition Temperatures of Polymers Containing Carboxyl End Groups: A Perspective in Powder Coatings", *Prog. Org. Coatings*, Vol. 76, No. 2–3, pp. 513–518, 2013.
28. Mitra, T., G. Sailakshmi, A. Gnanamani, and A. B. Mandal, "Studies on Cross-Linking of Succinic Acid with Chitosan/Collagen", *Mater. Res.*, Vol. 16, No. 4, pp. 755–765, 2013.

## **APENDIX A: SPECTROSCOPY DATA**

FT-IR, DSC, <sup>1</sup>H-NMR, and rheological analyses of polymers.

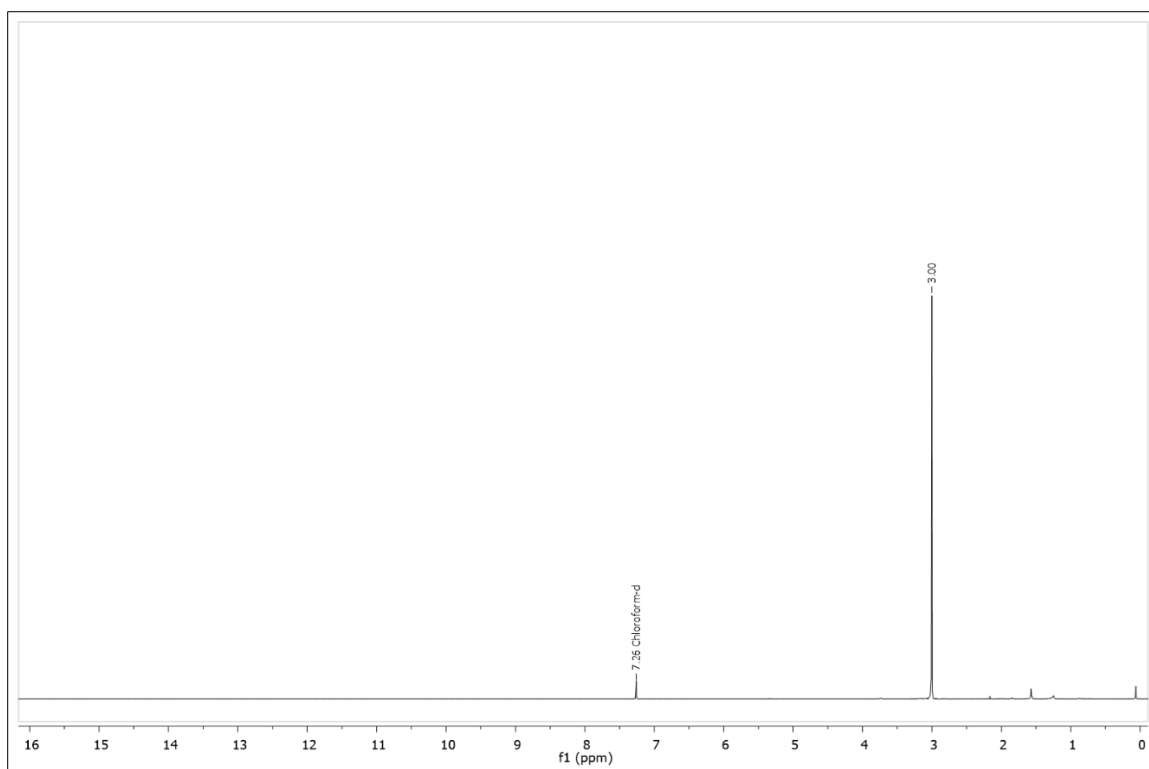


Figure A.1. <sup>1</sup>H-NMR Analysis of SA in CDCl<sub>3</sub>.

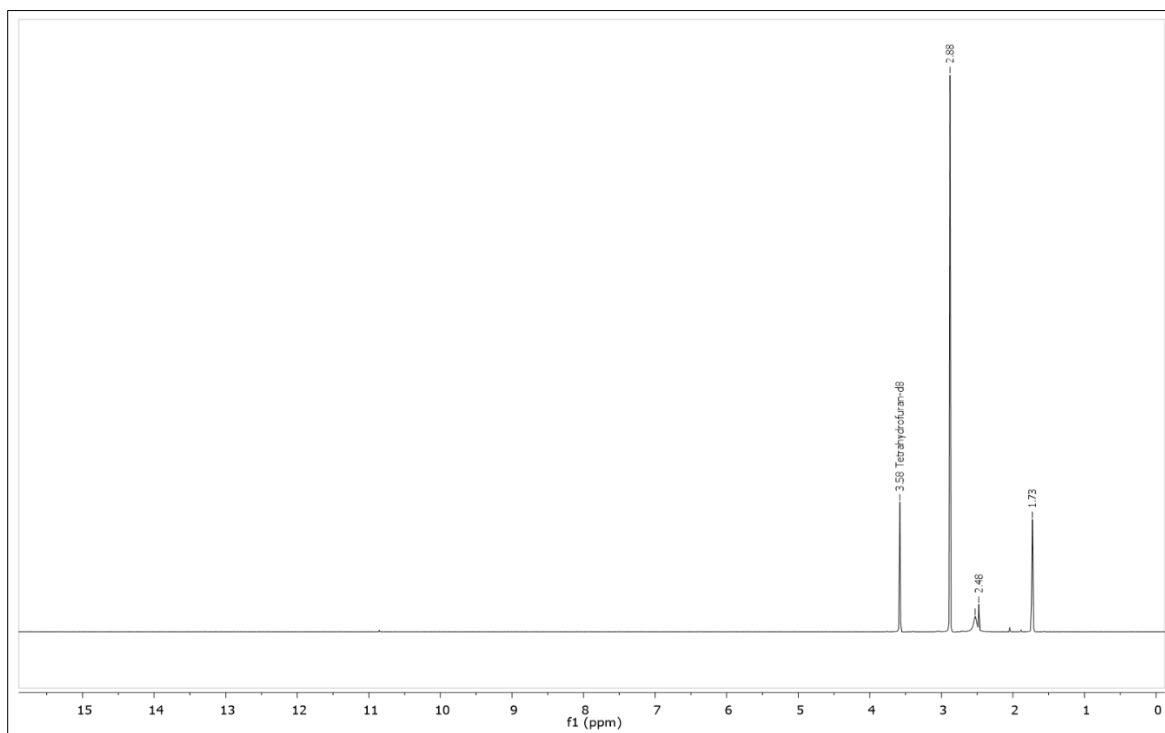


Figure A.2. <sup>1</sup>H-NMR Analysis of SA in d<sub>8</sub>-THF.

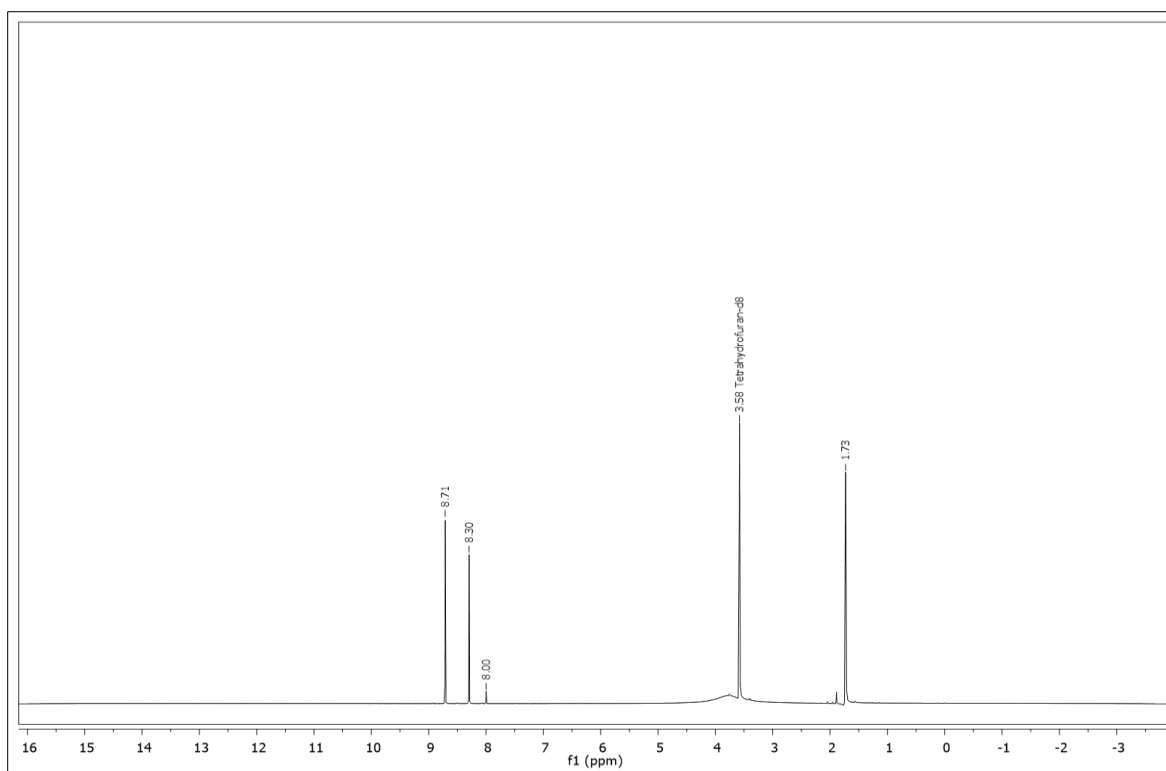


Figure A.3.  $^1\text{H-NMR}$  Analysis of PMDA in  $d_8\text{-THF}$ .

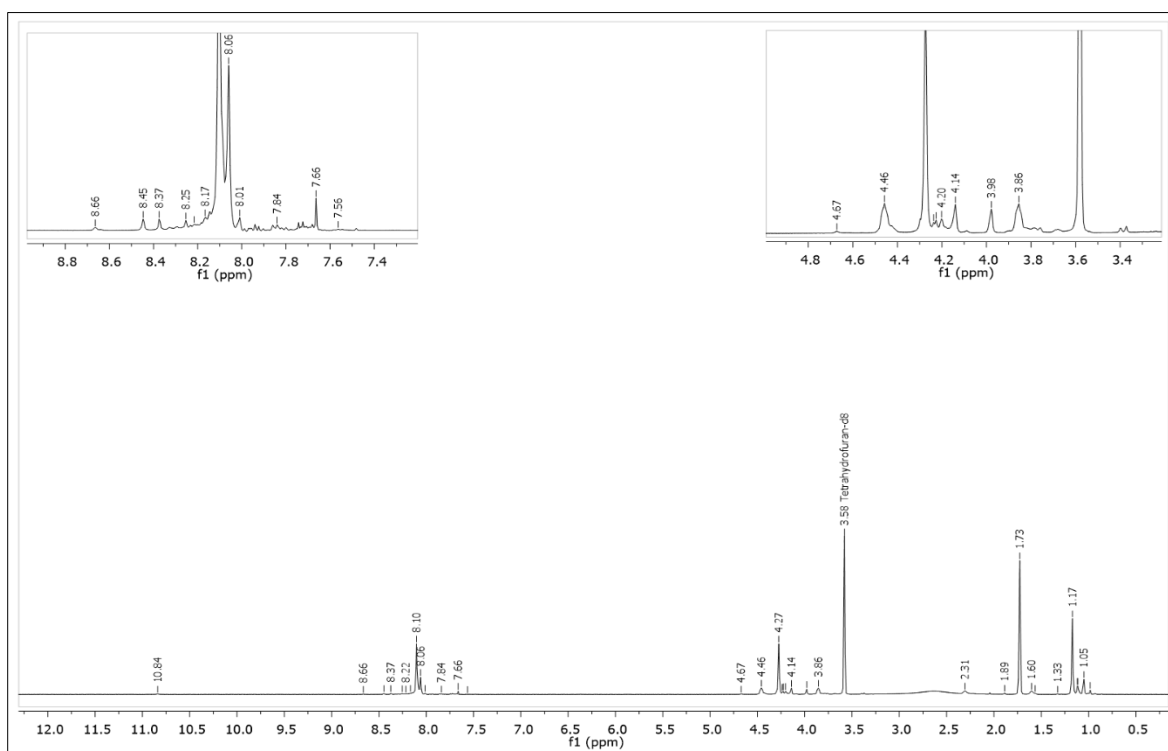
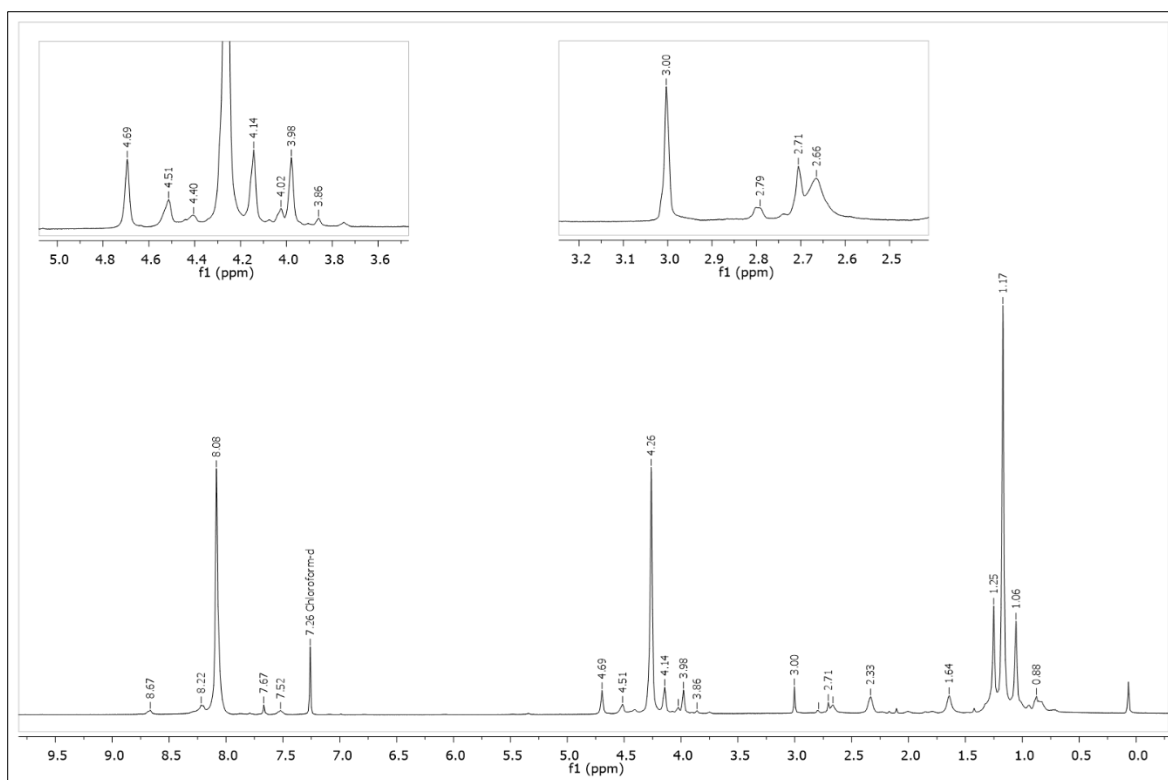
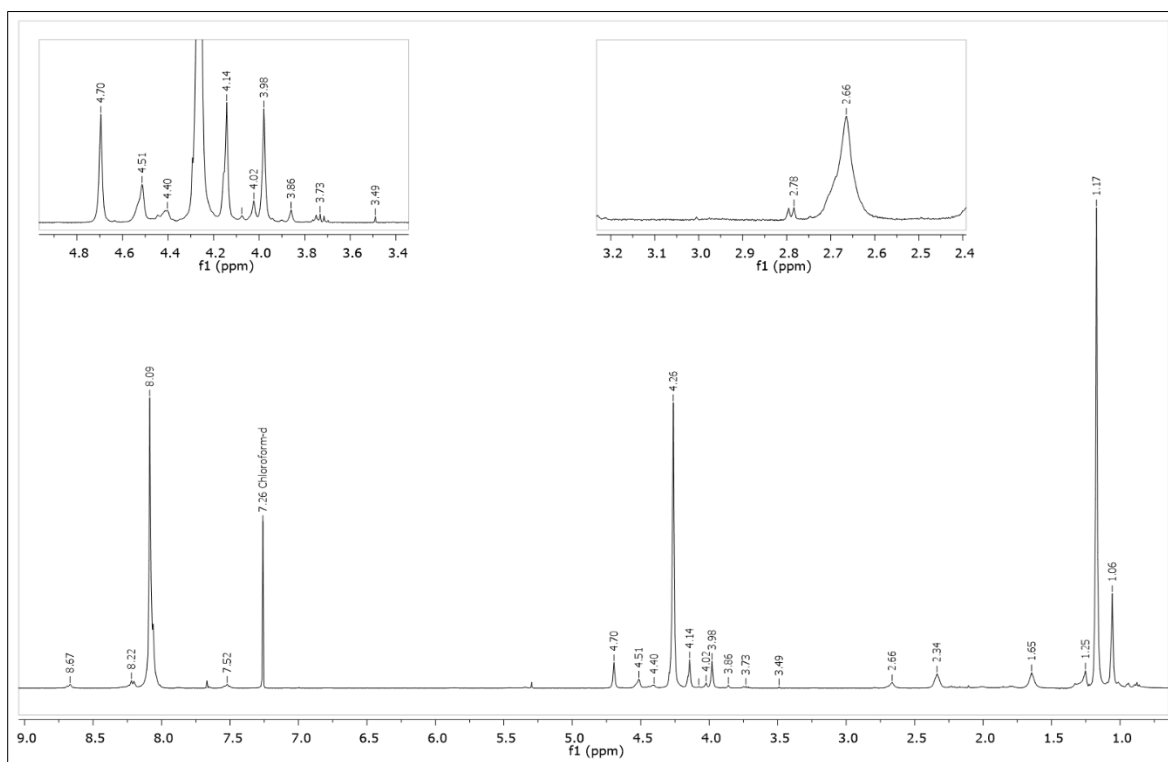
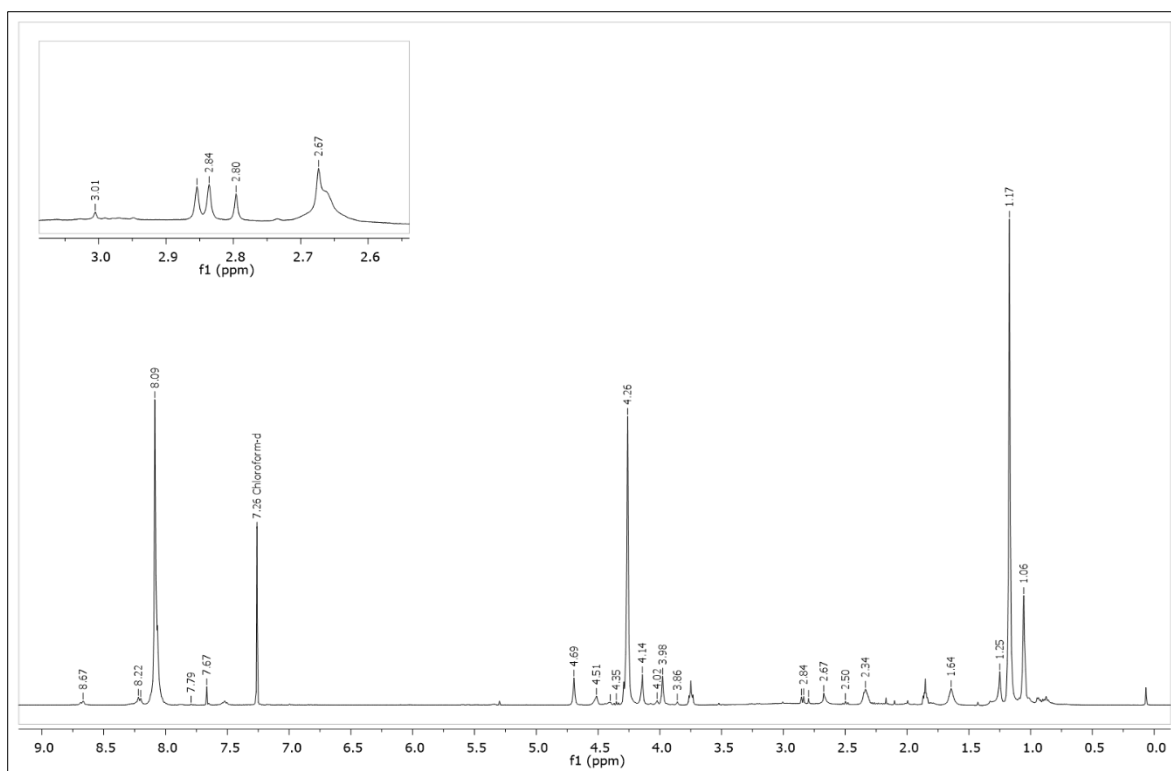
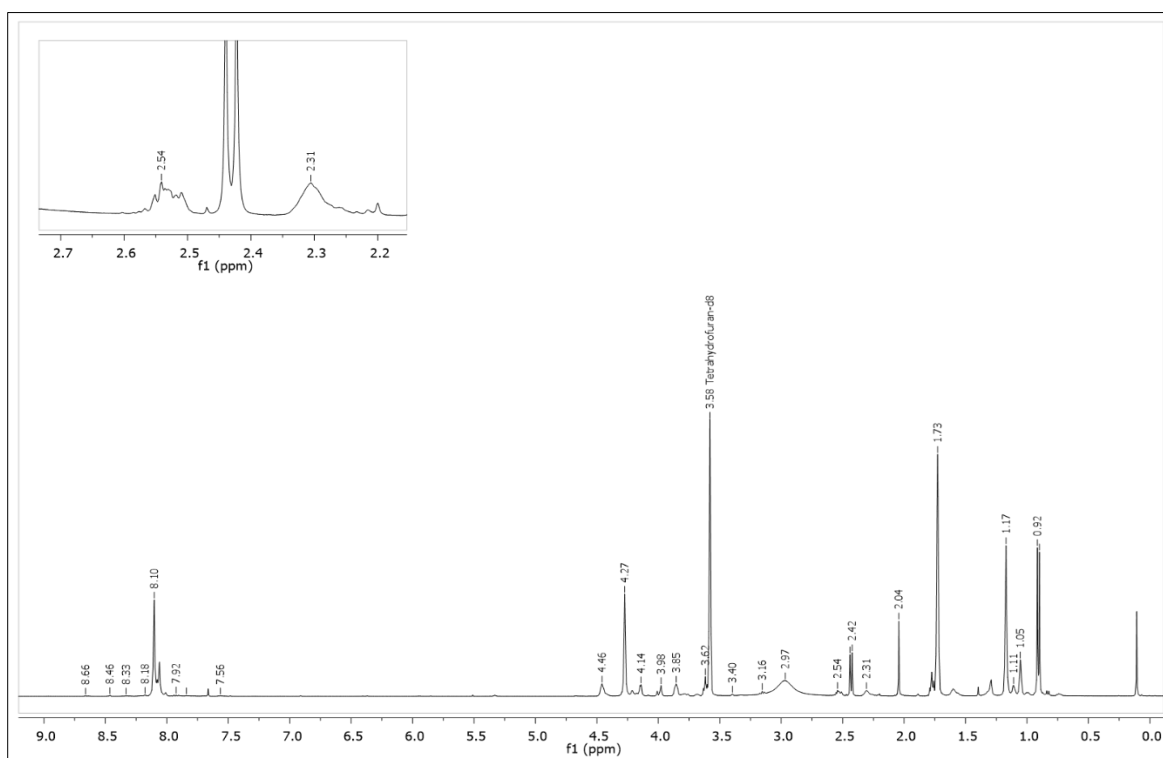


Figure A.4.  $^1\text{H-NMR}$  Analysis of PE-2 in  $\text{CDCl}_3$ .

Figure A.5.  $^1\text{H-NMR}$  Analysis of PE1\_SA\_5 in  $\text{CDCl}_3$ .Figure A.6.  $^1\text{H-NMR}$  Analysis of PE1\_SA\_5pnt in  $\text{CDCl}_3$ .

Figure A.7. <sup>1</sup>H-NMR Analysis of PE1\_SA\_3\_A in CDCl<sub>3</sub>.Figure A.8. <sup>1</sup>H-NMR Analysis of PE2\_SA\_3\_A in d<sub>8</sub>-THF.

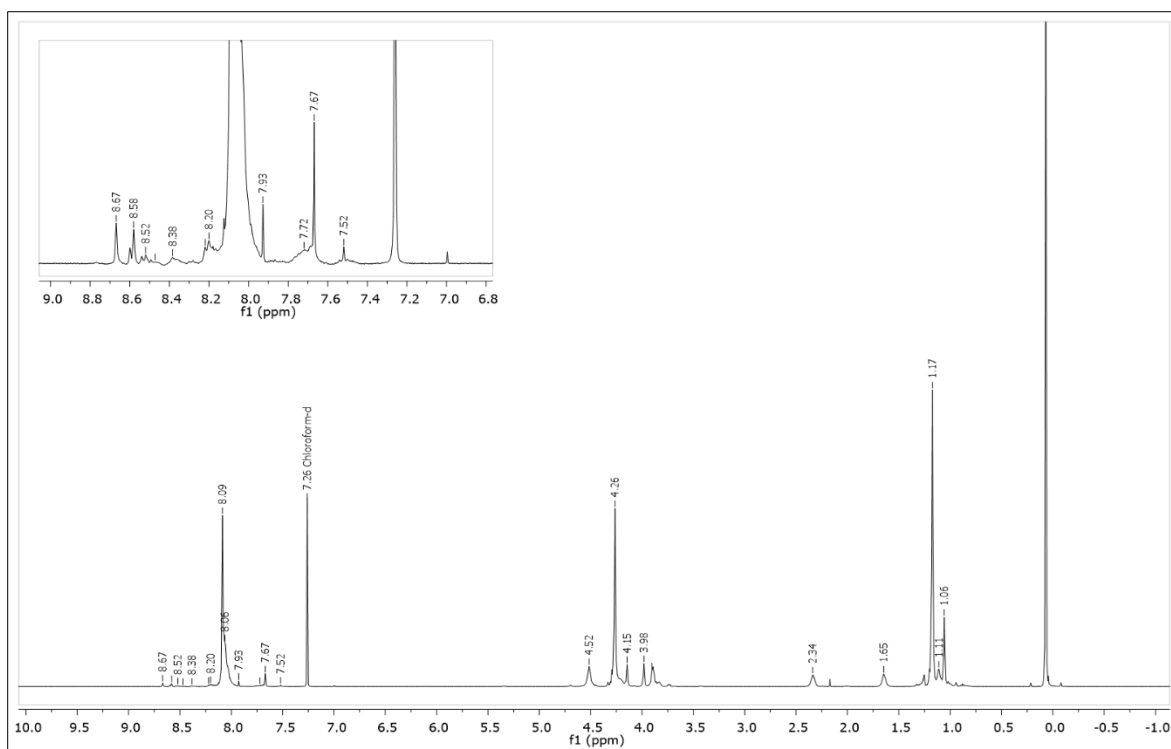


Figure A.9.  $^1\text{H-NMR}$  Analysis of PE2\_Pv in  $\text{CDCl}_3$ .

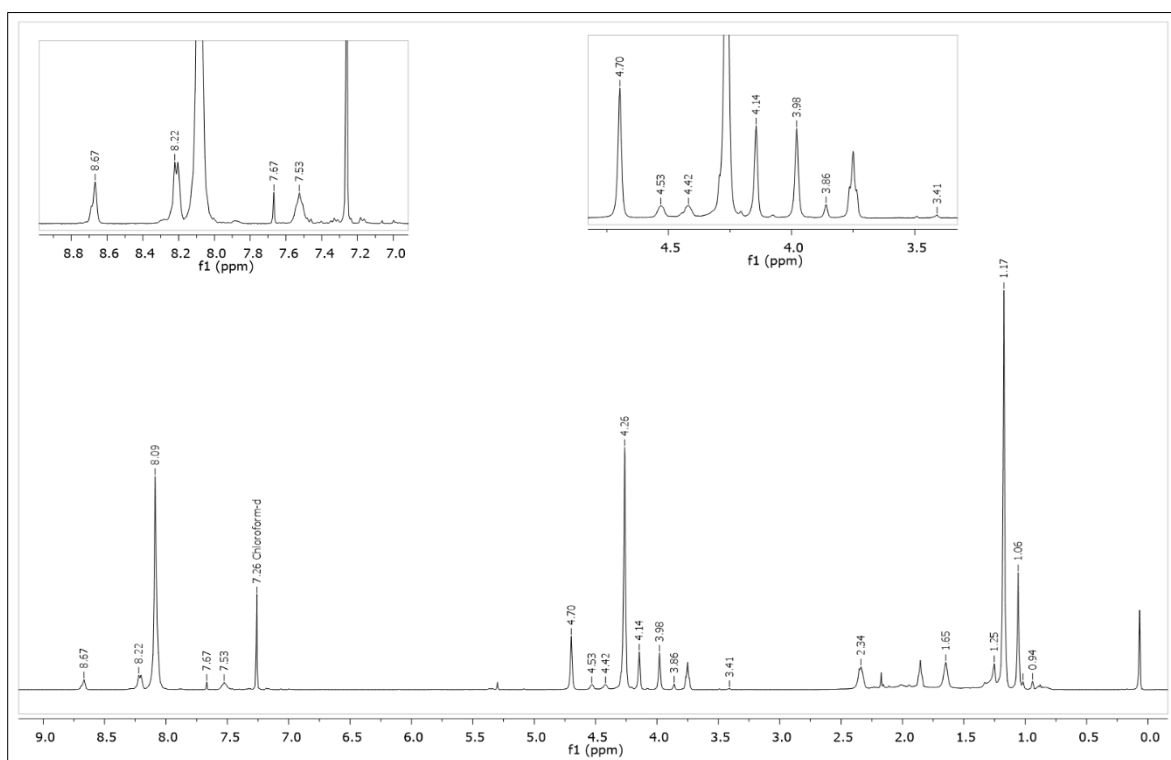


Figure A.10.  $^1\text{H-NMR}$  Analysis of PE3\_5 in  $\text{CDCl}_3$ .

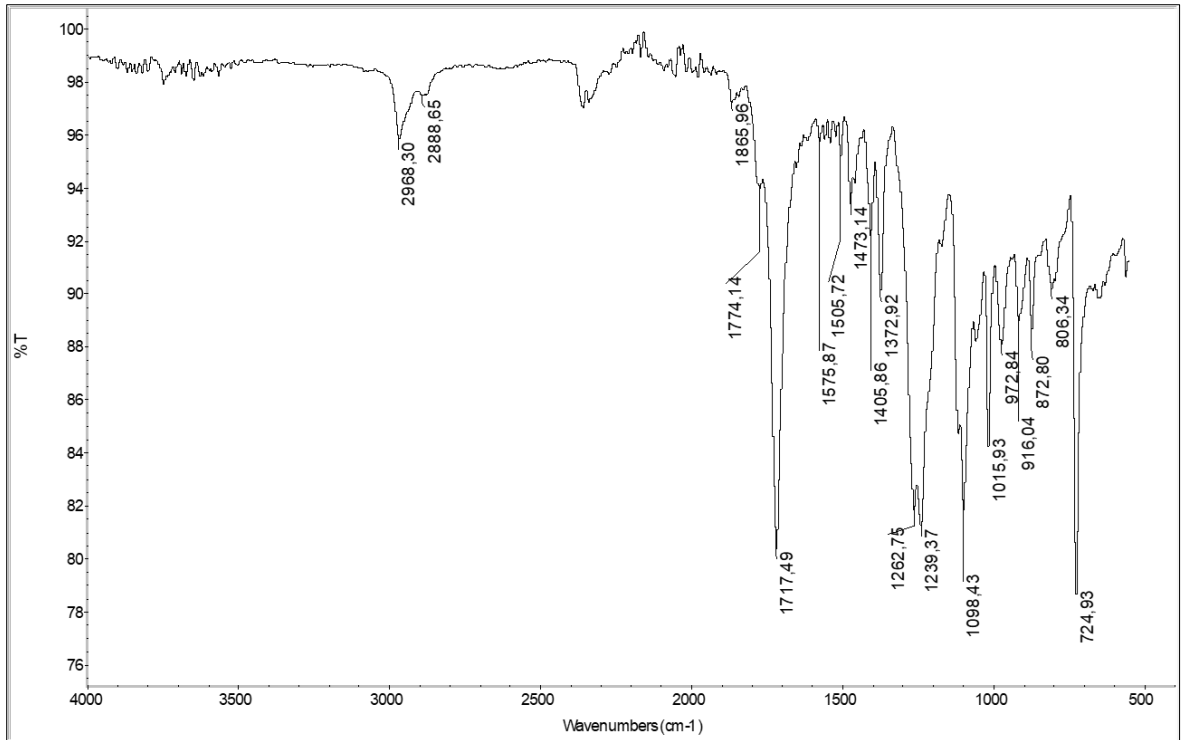


Figure A.11. FT-IR spectrum of physical mixing of PE-1 and SA.

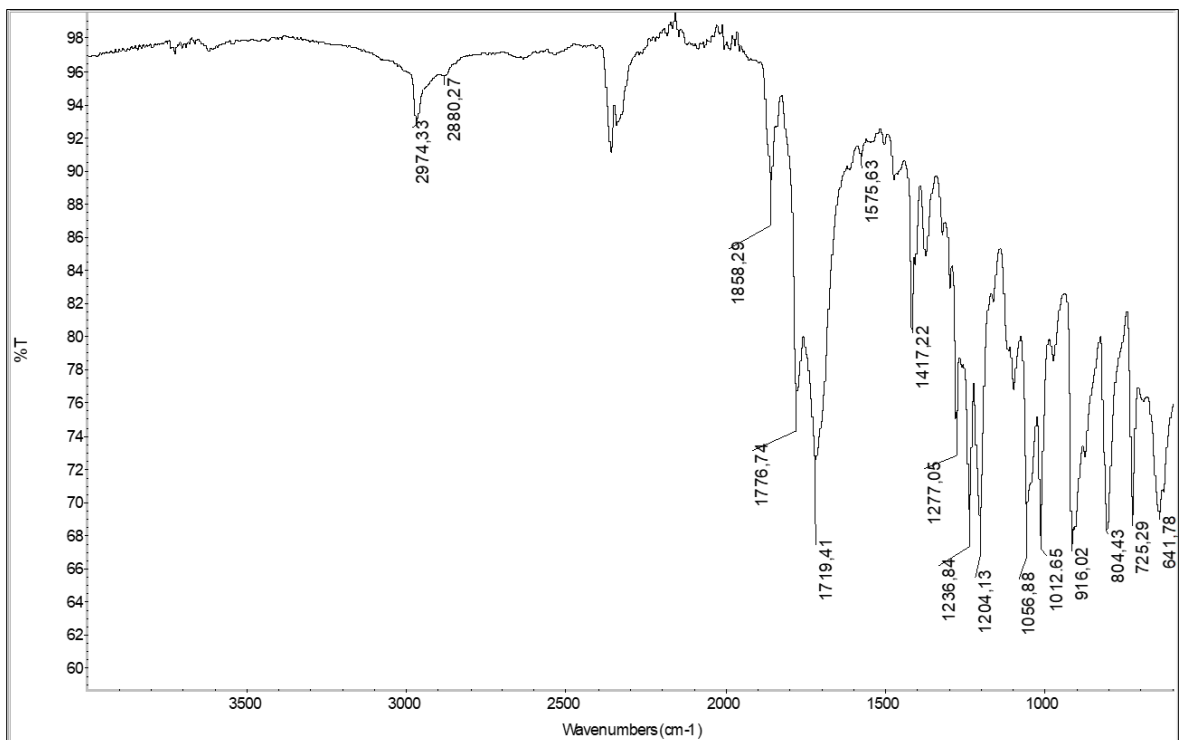


Figure A.12.. FT-IR spectrum of physical mixing of PE-2 and SA.

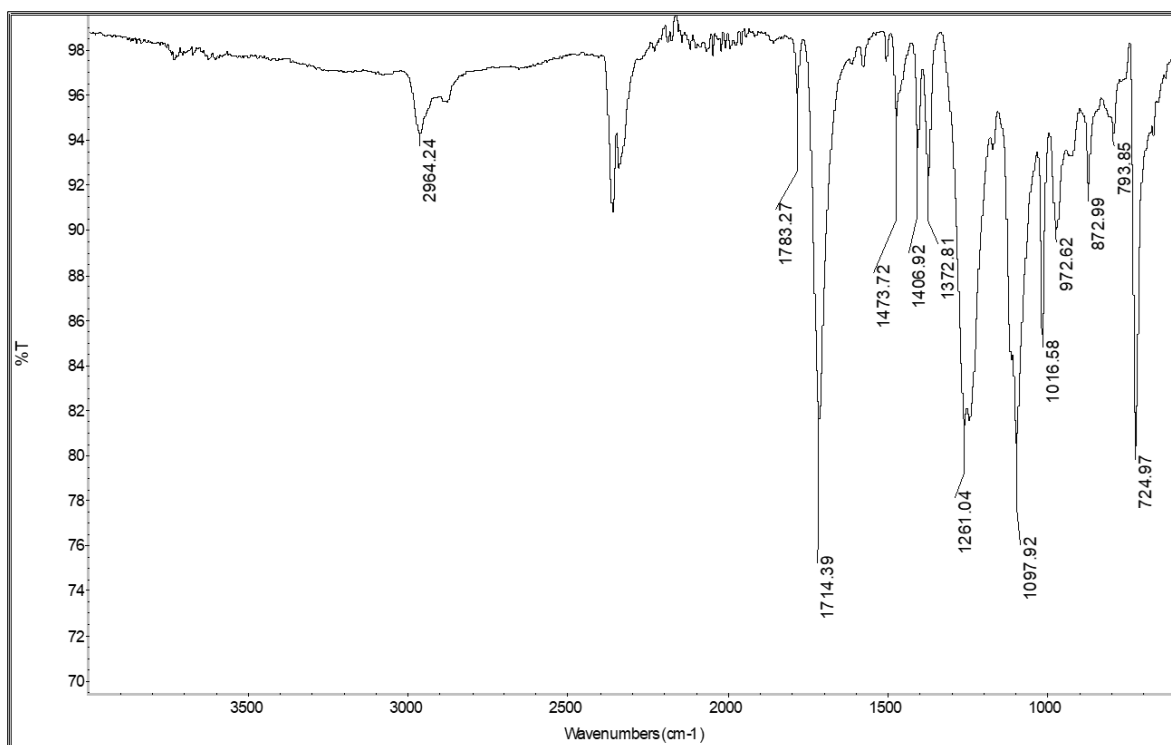


Figure A.13. FT-IR spectrum of PE2\_Pv.

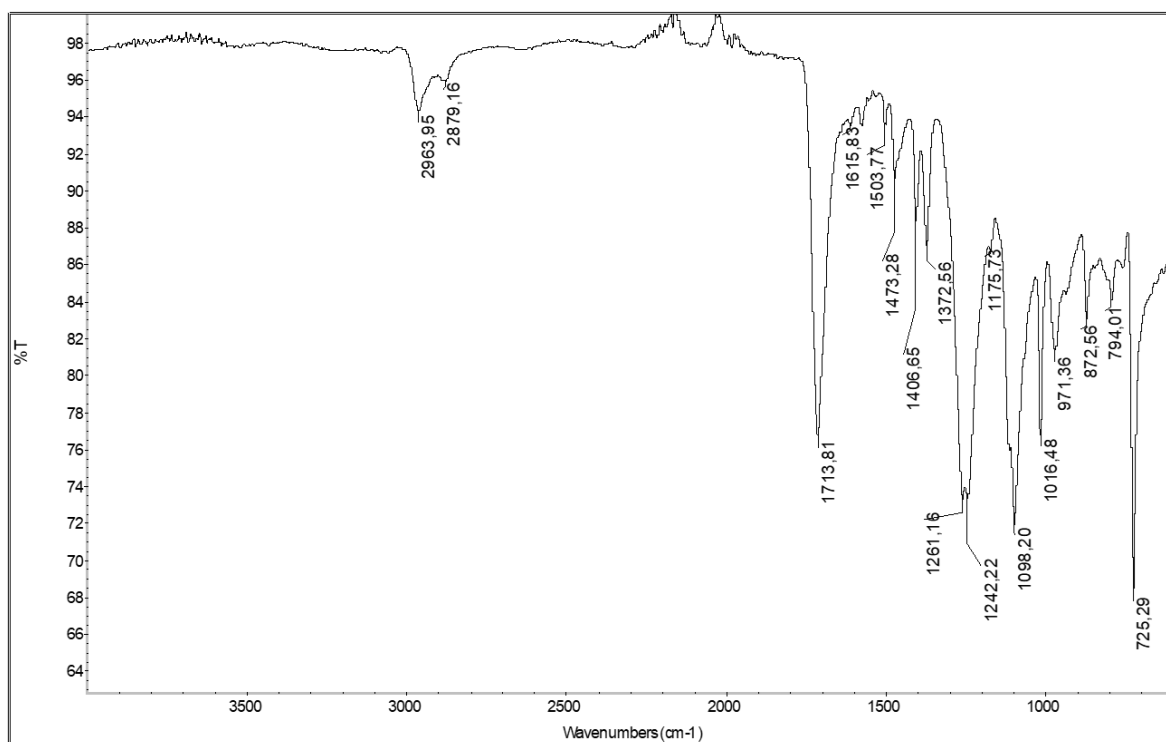


Figure A.14. FT-IR spectrum of PE2\_Pv.

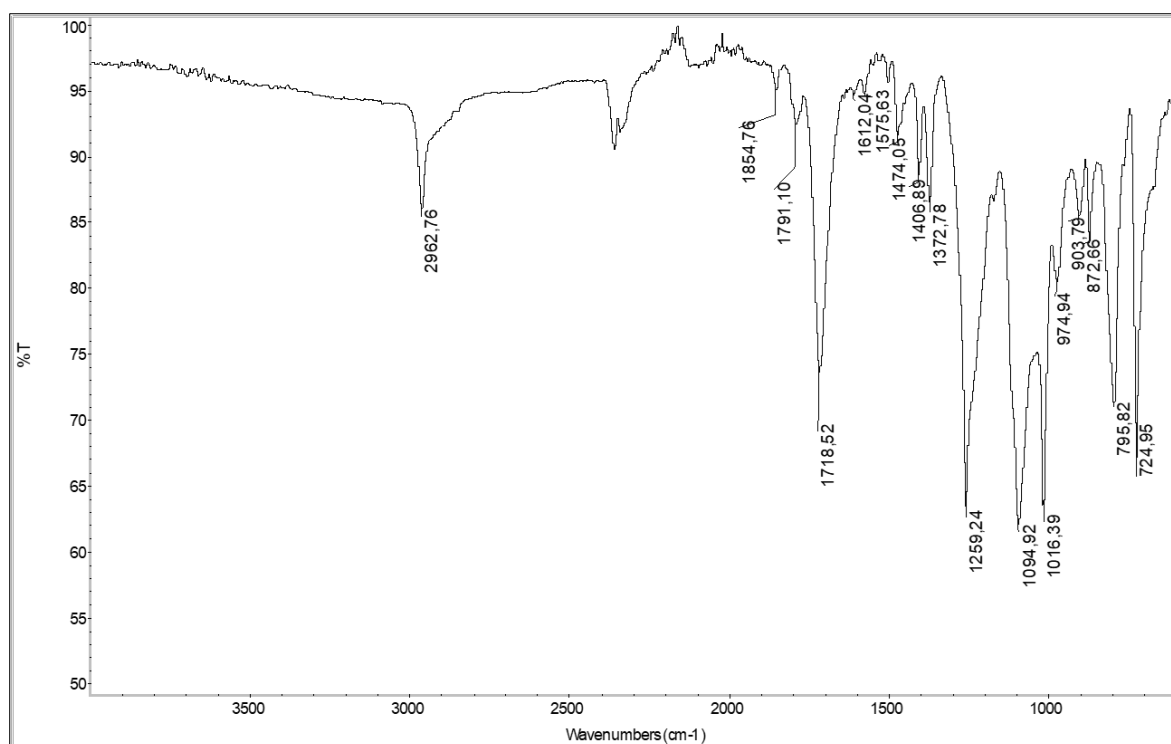


Figure A.15. FT-IR spectrum of PE2\_PMDA1.

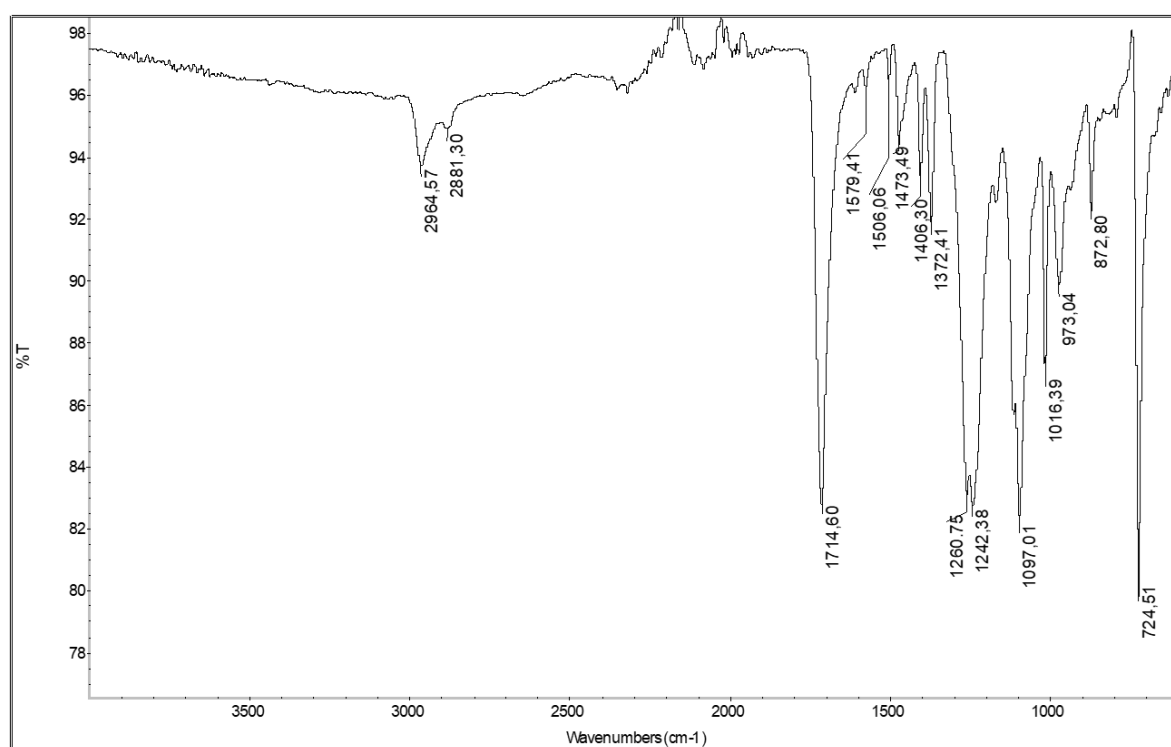


Figure A.16. FT-IR spectrum of PE3\_4.

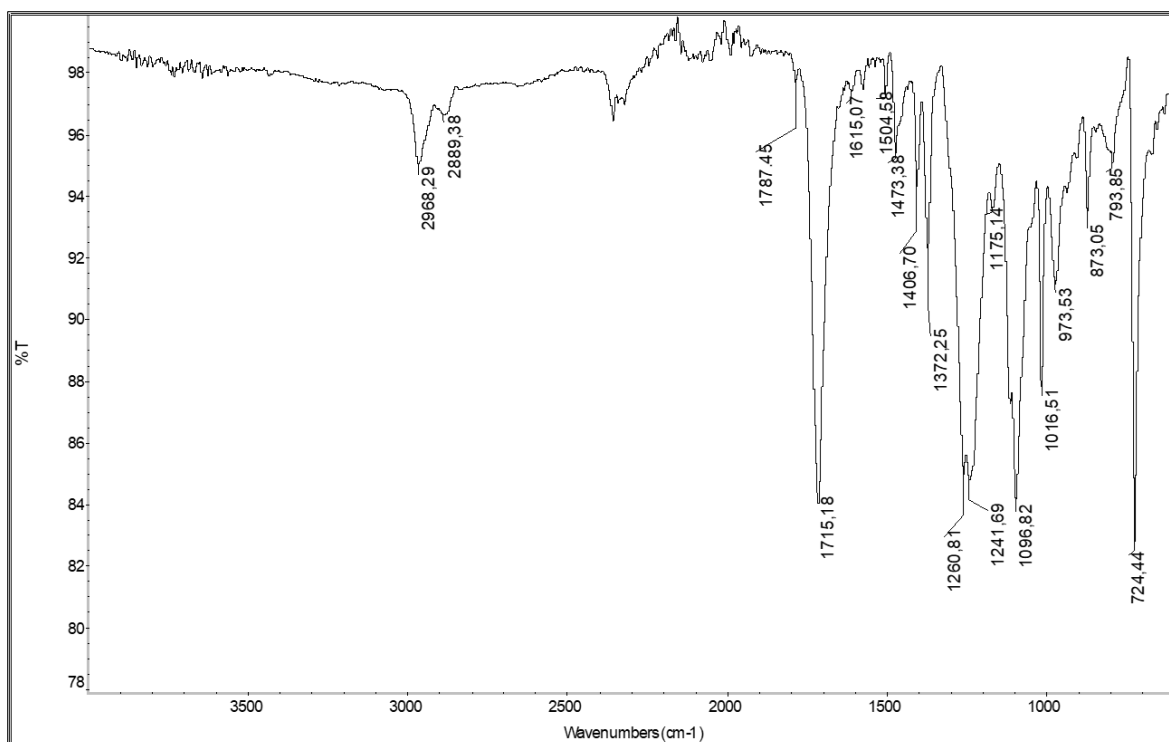


Figure A.17. FT-IR spectrum of PE3\_4\_SA\_1.

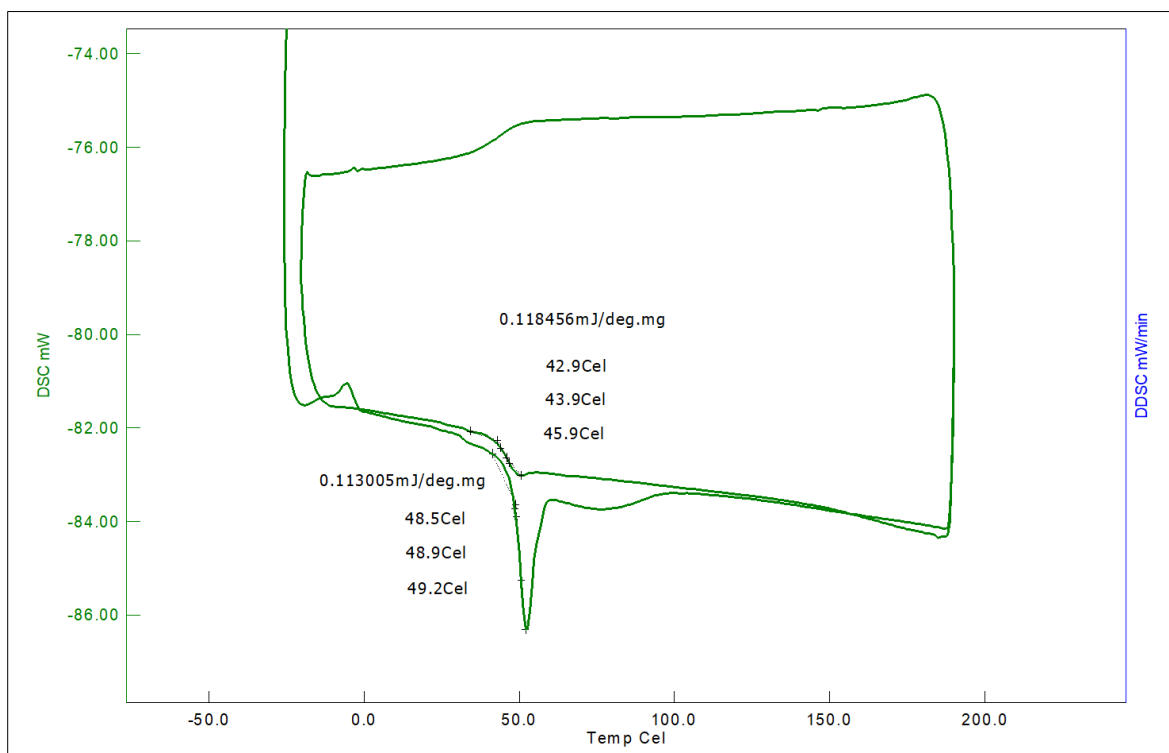


Figure A.18. DSC analysis of PE-2.

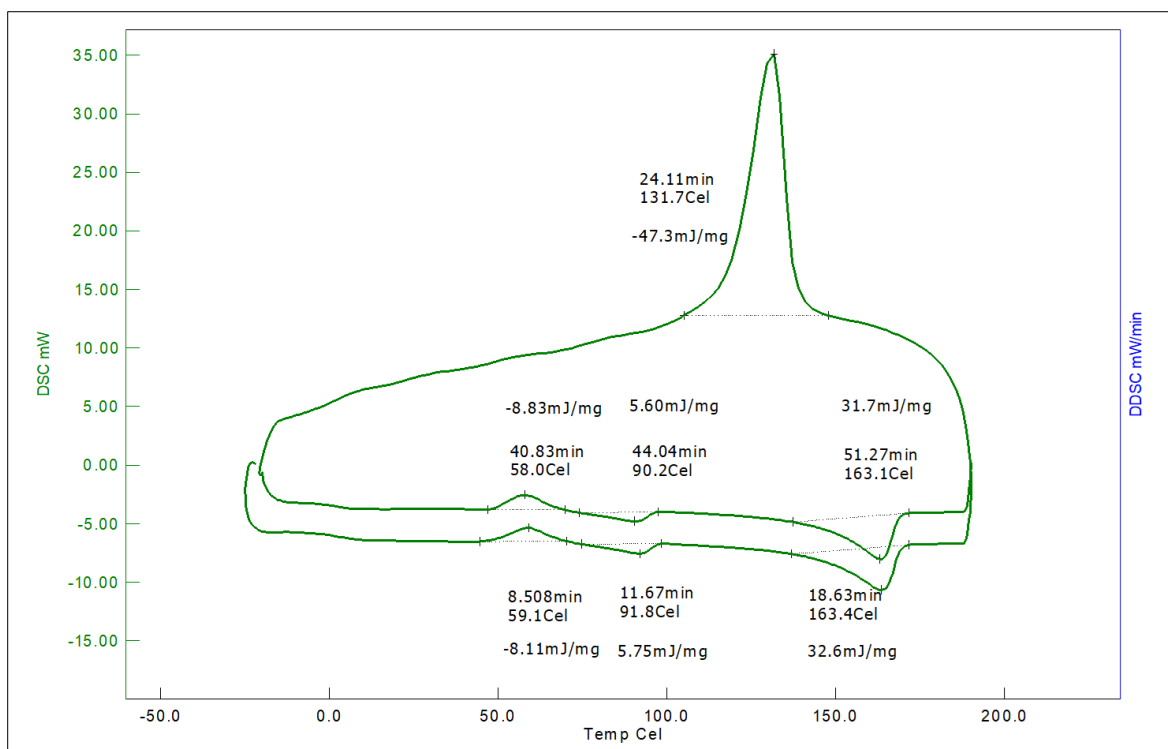


Figure A.19. DSC analysis of PE2\_SA\_1.

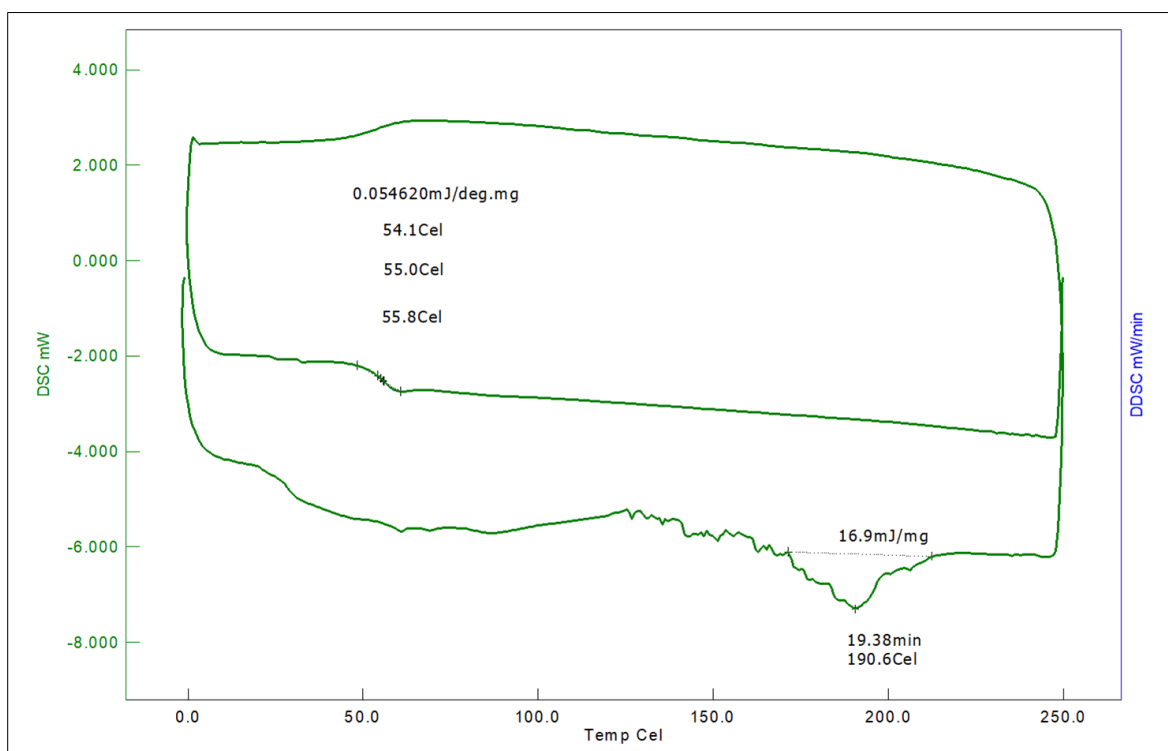


Figure A.20. DSC analysis of PE1\_PMDA\_1.

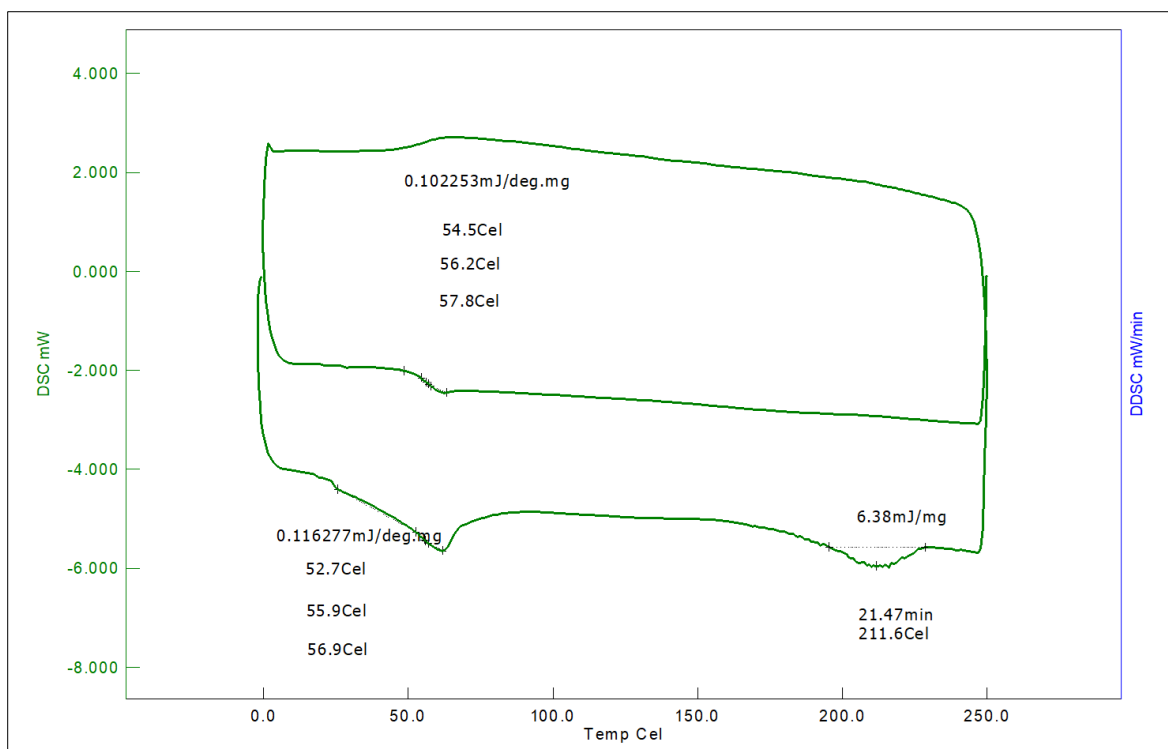


Figure A.21. DSC analysis of PE1\_PMDA\_1\_A.

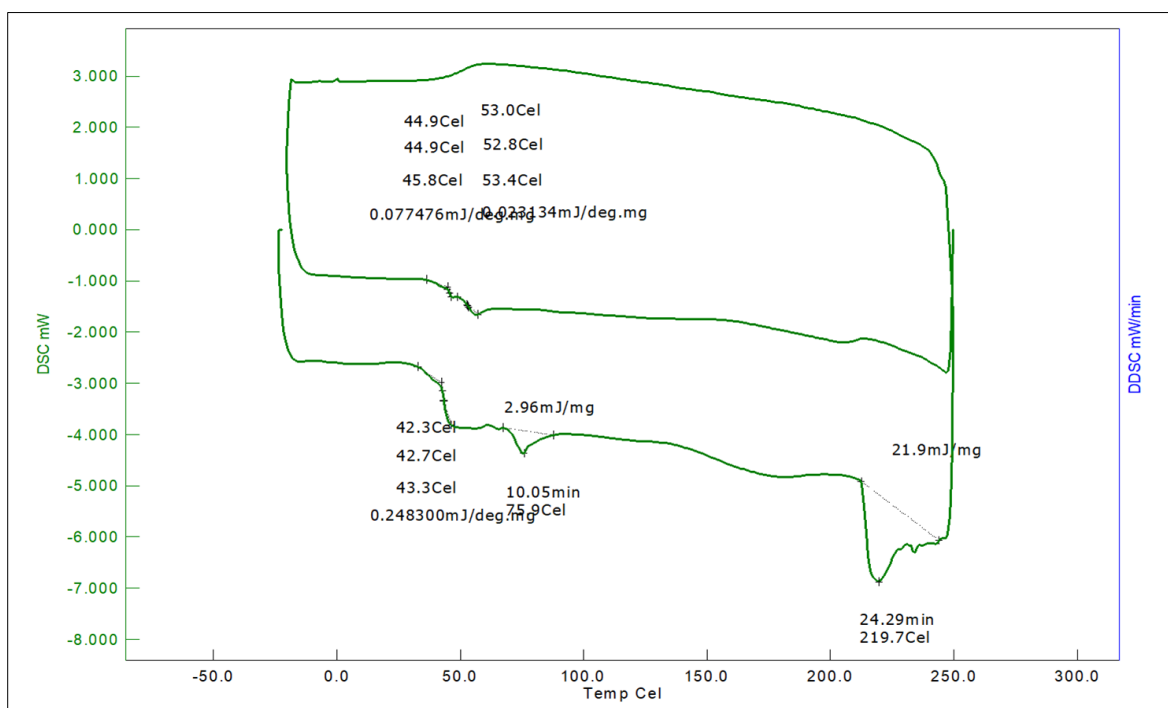


Figure A.22. DSC analysis of PE2\_PMDA\_2.

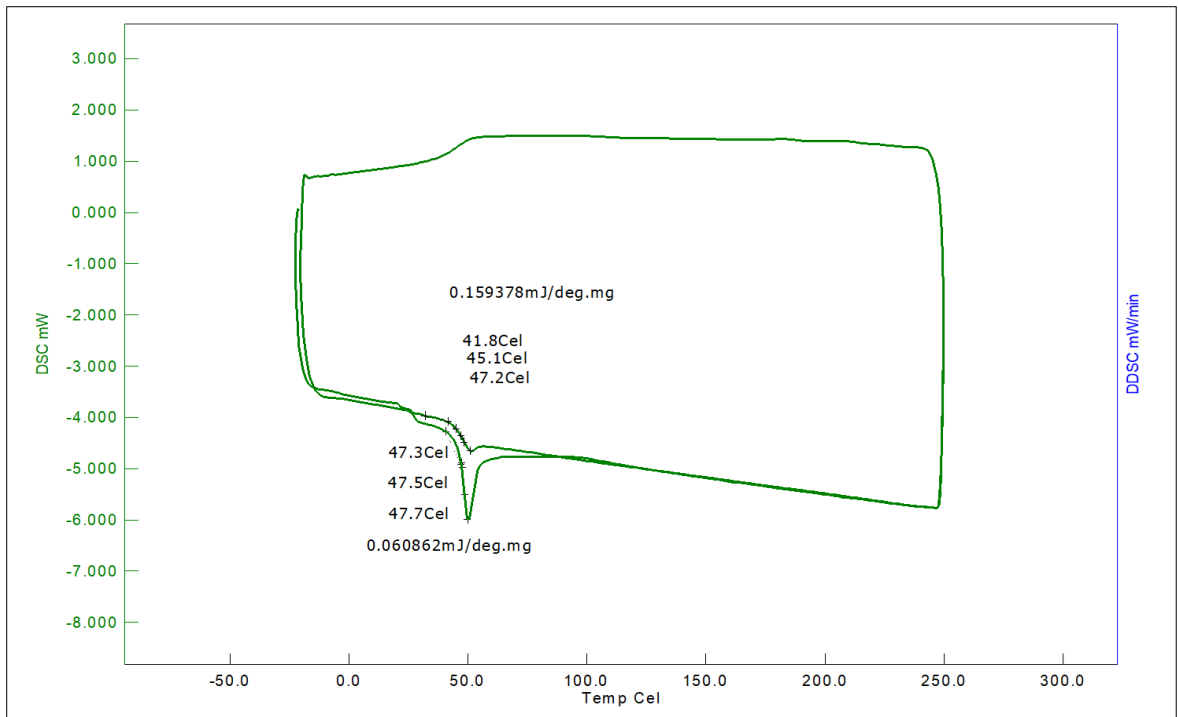


Figure A. 23. DSC analysis of PE3\_SA\_4.

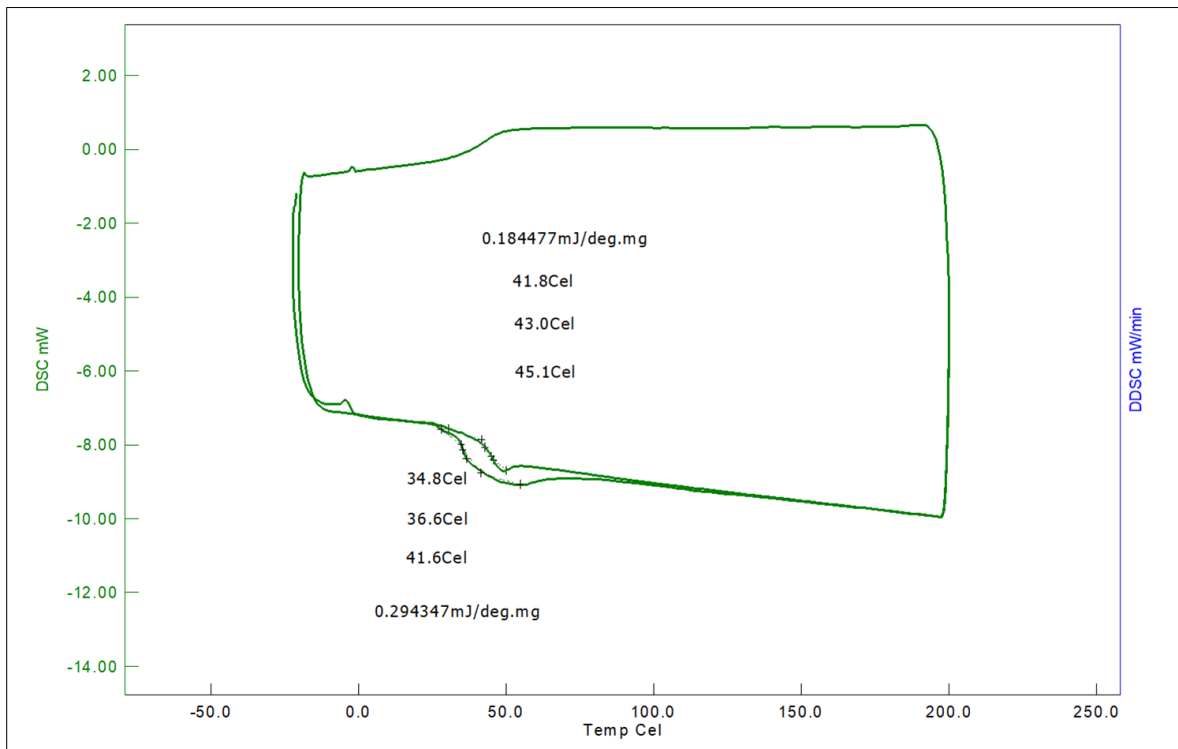


Figure A.24. DSC analysis of PE3\_4\_SA\_1.

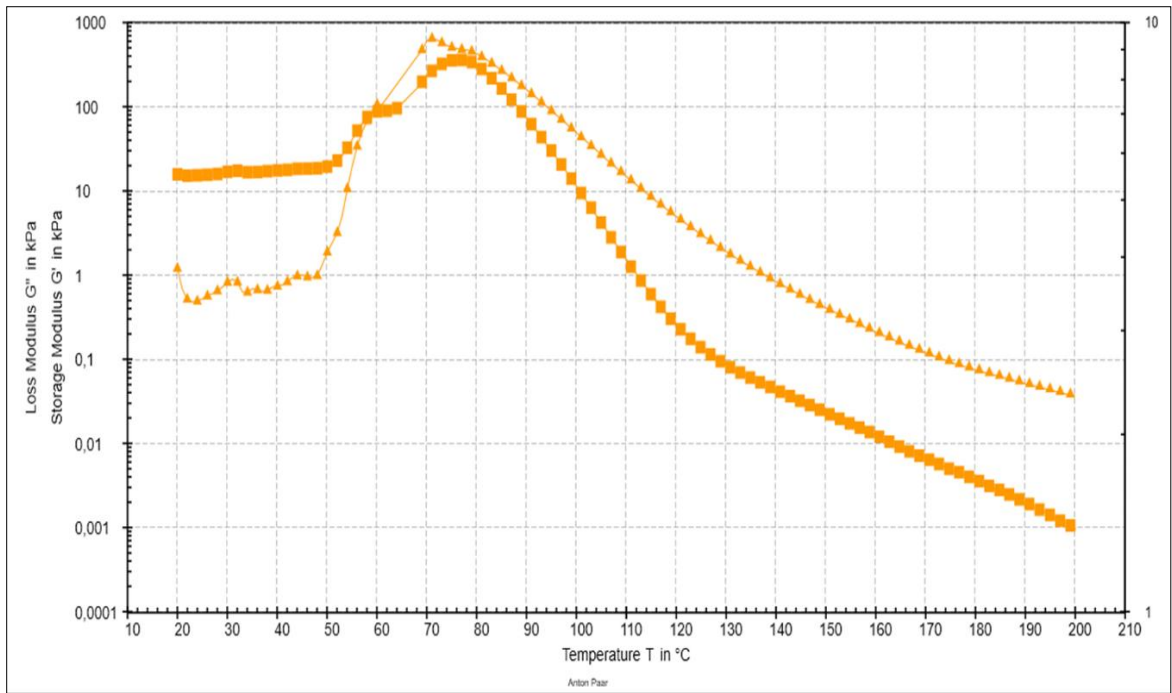


Figure A.25. Temperature sweep test of PE-1.

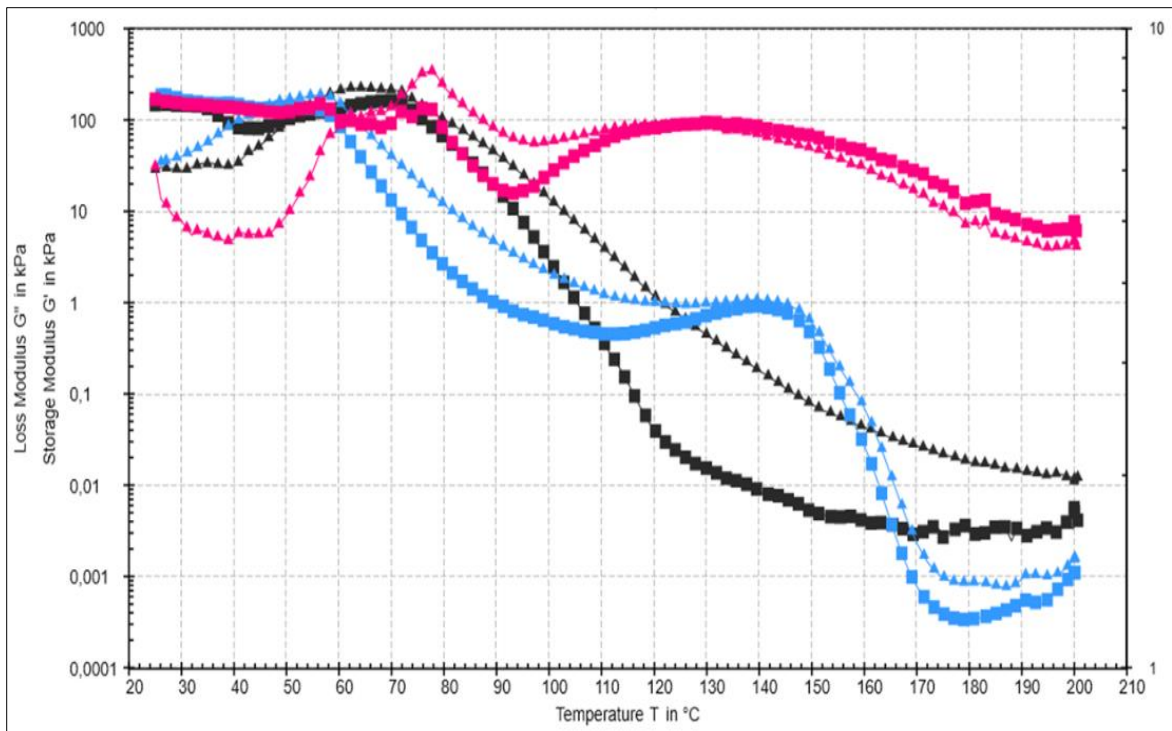


Figure A.26. The temperature sweep test of PE1\_SA\_8, PE2\_SA6, and PE2\_PMDA\_2.

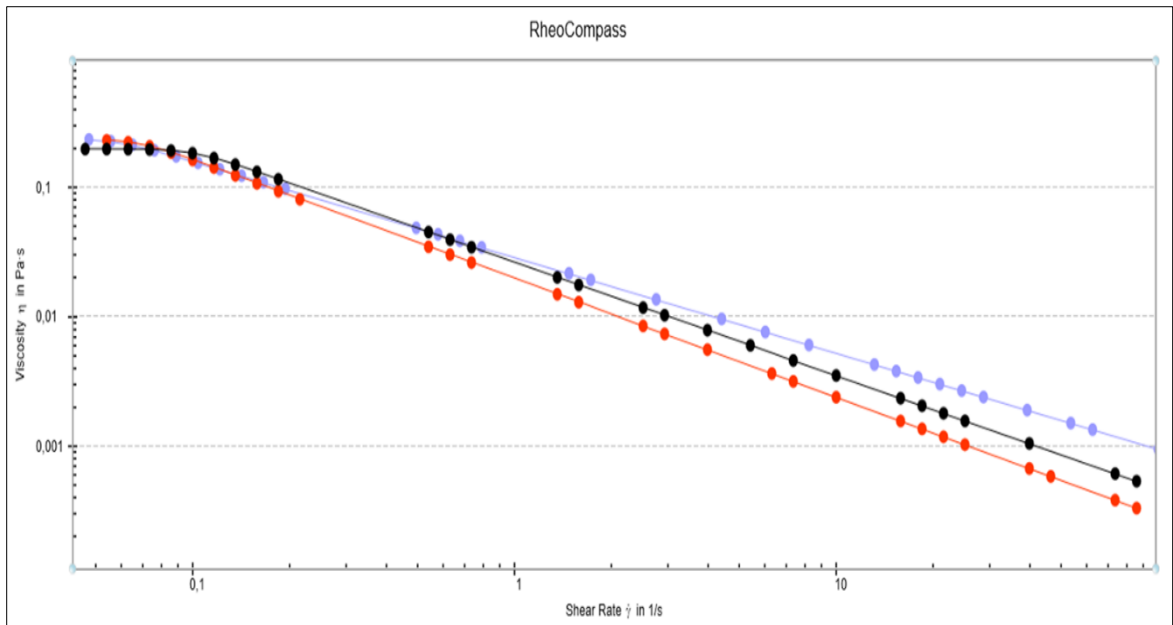


Figure A.27. The flow curves of PE3\_4 (purple), PE3\_4\_SA1 (red), and PE-1 (black).

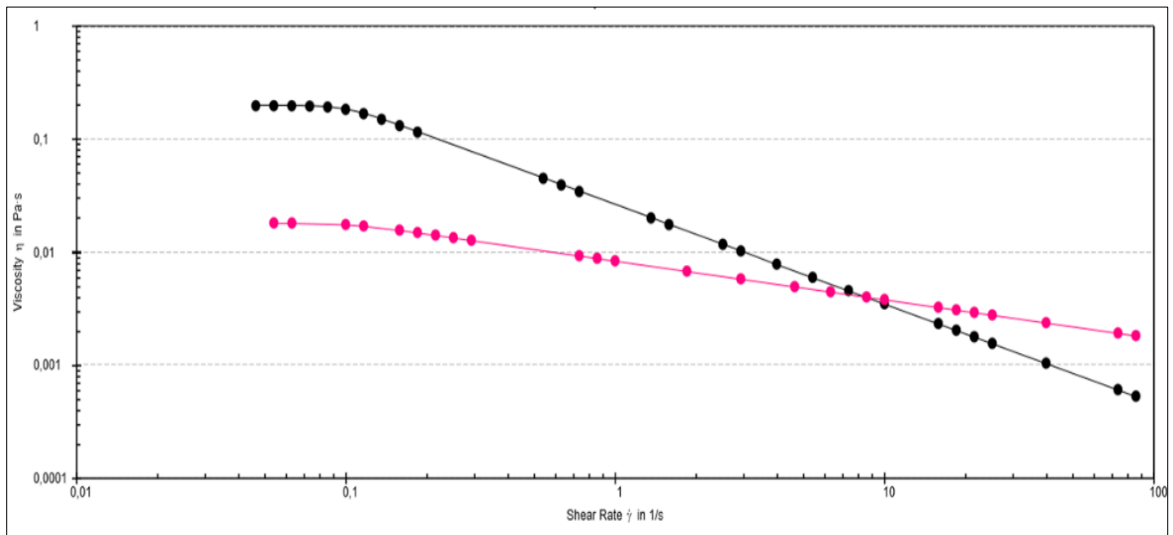


Figure A.28. The flow curves of PE-1 (black) and PE1\_PMDA\_8 (pink).

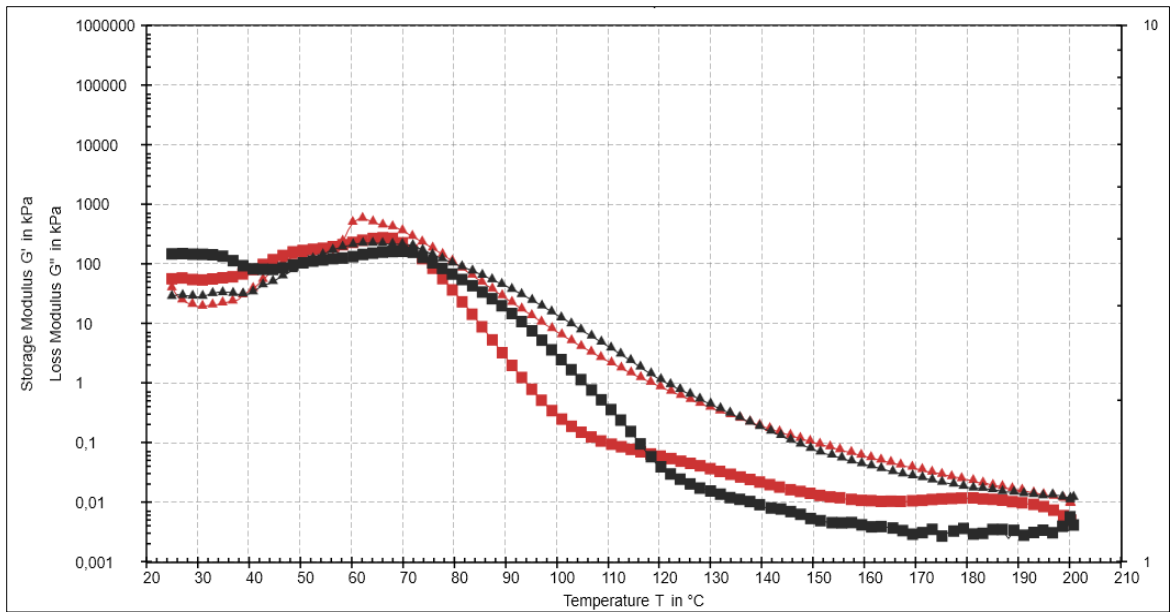


Figure A.29. Temperature sweep test of PE3\_4\_SA1 (red) and PE1\_SA\_8 (black).

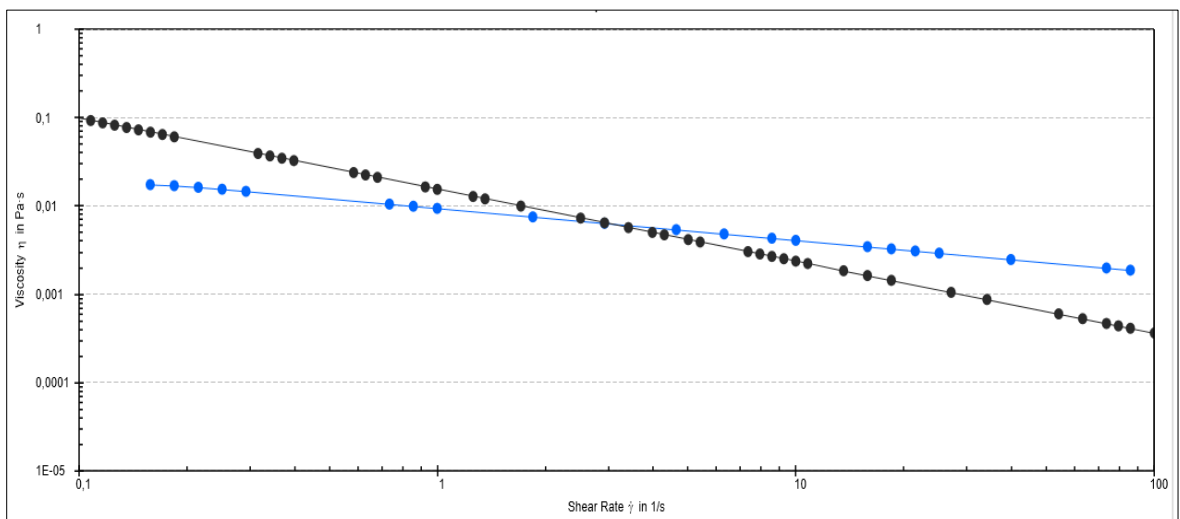


Figure A.30. The flow curves of PE-2 (black) and PE2\_PMDA\_3 (blue).

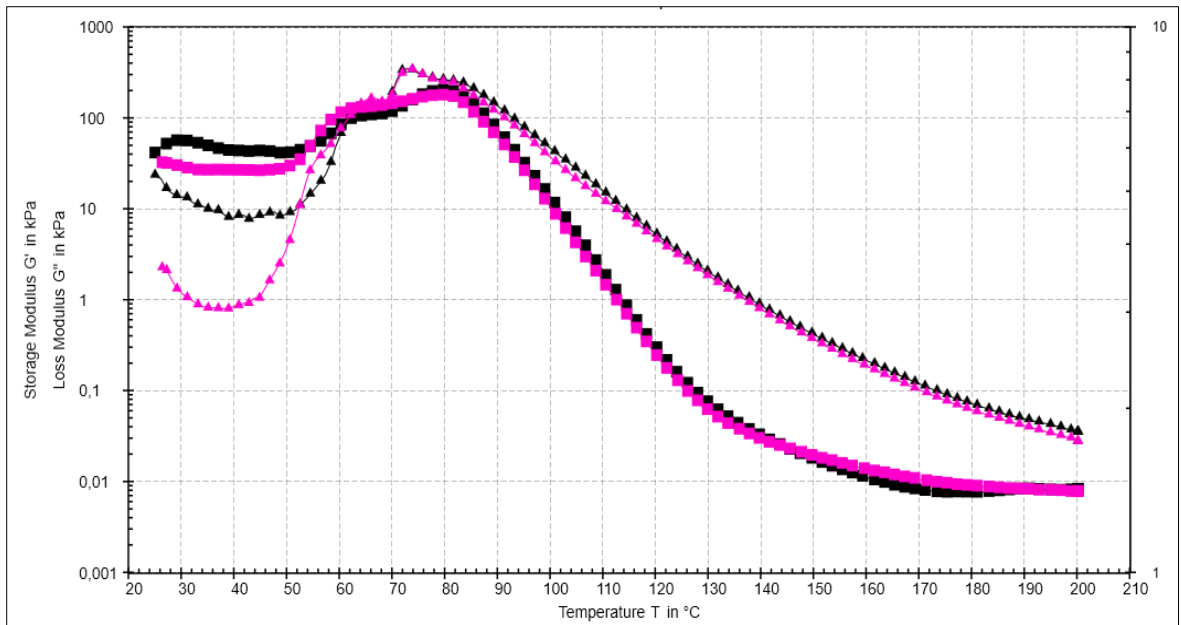


Figure A.31. Temperature sweep tests of PE-1 (black) and PE1\_PMDA\_8 (pink).

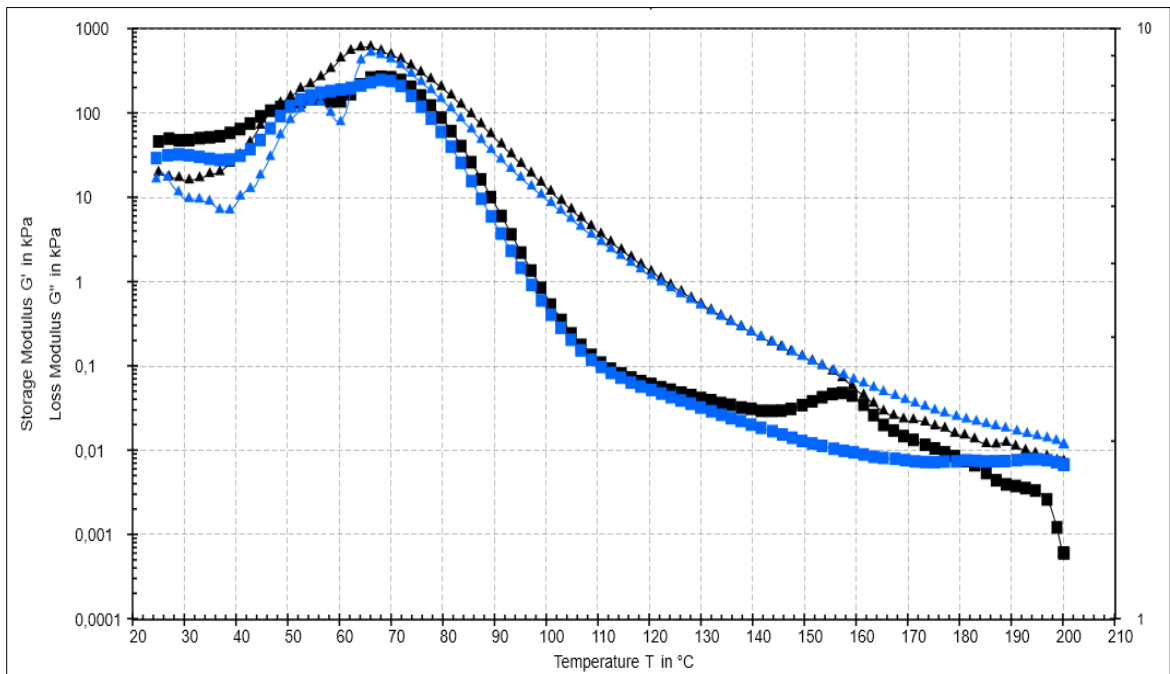


Figure A.32. Temperature sweep tests of PE-2 (black) and PE2\_PMDA\_3 (blue).

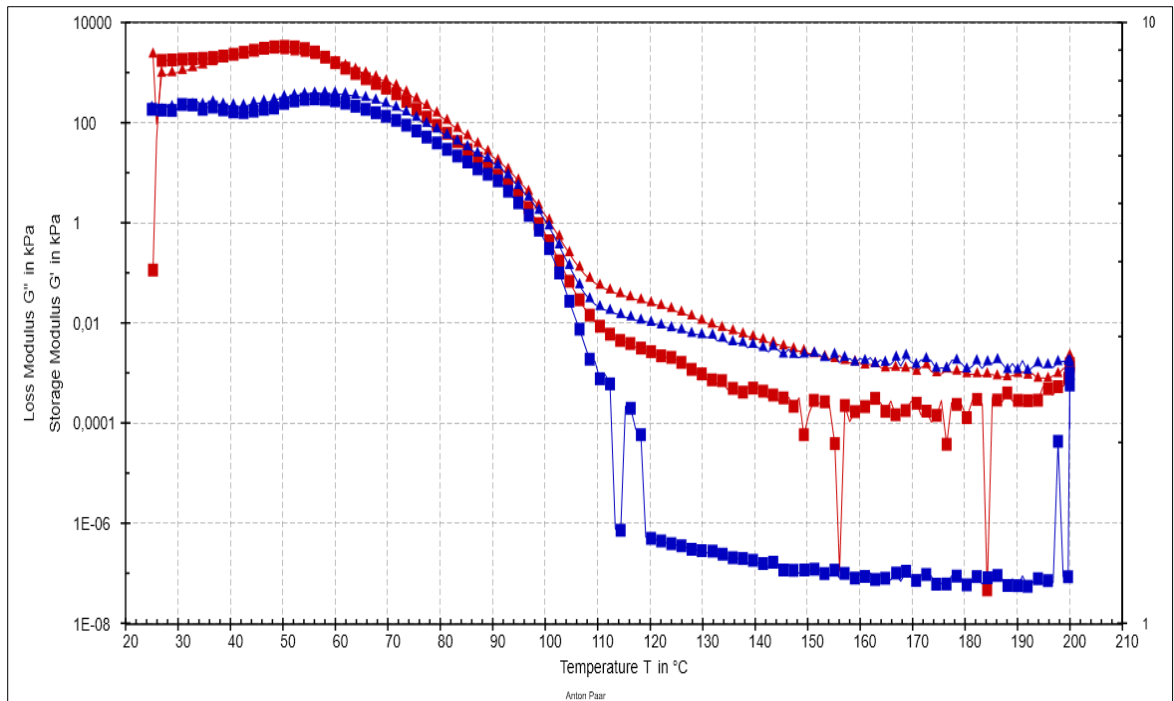


Figure A.33. Temperature sweep tests of PE2\_SA\_1 (red) and PE2\_SA\_1 (blue).